

UCLA

UCLA Electronic Theses and Dissertations

Title

Role of PACAP/PAC1 Signaling in Neuromodulation of the Immune System and Neuroprotection

Permalink

<https://escholarship.org/uc/item/8tq2c67p>

Author

Van, Christina

Publication Date

2018

Peer reviewed|Thesis/dissertation

UNIVERSITY OF CALIFORNIA

Los Angeles

Role of PACAP/PAC1 Signaling in Neuromodulation of the Immune System
and Neuroprotection

A dissertation submitted in partial satisfaction of the requirements for the degree

Doctor of Philosophy in Molecular Biology

by

Christina Van

2018

© Copyright by

Christina Van

2018

ABSTRACT OF THE DISSERTATION

Role of PACAP/PAC1 Signaling in Neuromodulation of the Immune System and Neuroprotection

by

Christina Van

Doctor of Philosophy in Molecular Biology

University of California, Los Angeles, 2018

Professor James A. Waschek, Chair

Pathological inflammation and neurodegeneration in the central nervous system (CNS) in diseases such as multiple sclerosis (MS), Alzheimer's Disease, stroke, and traumatic brain injury can lead to cognitive and motor impairment which have devastating effects on quality of life for patients. In addition, these diseases lead to overwhelming financial costs and increased societal burden. Currently available drugs can partially restrict inflammation, but chronic low-level inflammation contributes to accumulative neurodegeneration. There is an unmet need for a therapeutic which can both target inflammation as well as protect against neuron loss and axonopathy in the CNS. A protein called pituitary adenylate cyclase-activating polypeptide (PACAP) has reported neuroprotective and anti-inflammatory properties in several models of neurodegenerative diseases. However, the mechanisms for these actions are not clear.

In these studies, we investigated two possible mechanisms through which PACAP may act to regulate inflammation and neurodegeneration in the experimental autoimmune encephalomyelitis (EAE) model of MS. Using a conditional knockout approach, we deleted PACAP's PAC1 receptor from catecholaminergic neurons and demonstrate that PAC1 signaling through these neurons regulates helper T cell polarization, regulatory T cell proliferation, and inflammatory cytokine secretion during disease development. This study indicates that PACAP can modulate inflammation in part by acting through catecholaminergic neurons, such as those of the sympathetic nervous system, which regulate the immune response. Furthermore, we also conditionally deleted PAC1 receptors in the retina and found that even in the absence of disease, PAC1 is important for maintaining neurons as well as their dendrites and axons in the eye. In addition, in the optic nerve, PAC1 plays a role in protecting axonal integrity as well as regulating the numbers of immune cells during optic neuritis. Finally, using a CNS-tropic adeno-associated virus viral vector, we demonstrated as a proof-of-principle that PACAP overexpression can protect against EAE. PACAP overexpression in the CNS led to delayed onset of EAE symptoms and reduced numbers of immune cells in the optic nerve. These studies further strengthen evidence implicating PACAP and its PAC1 receptor as promising targets for developing therapeutics to manipulate the inflammatory response and to protect against neuron loss and axonopathy in MS as well as other inflammatory neurodegenerative diseases.

The dissertation of Christina Van is approved.

Harley I. Kornblum

Melissa J. Spencer

Rhonda Renee Voskuhl

David S. Williams

James A. Waschek, Committee Chair

University of California, Los Angeles

2018

Dedication

I dedicate this work to my family and to my friends who I consider my extended family. I am grateful to have each and every one of you in my life. As the saying goes: “Friends make the bad times good and the good times unforgettable.” Thank you for all the support, love, laughter, and memories through these years. Cheers to many more years together.

To my mom, Linh Van, who shoulders all of life’s burdens and devotes every ounce of energy to giving her daughters better lives. I could not have asked for a better mother.

To my sister, Jennifer Van, who has been unwaveringly by my side through it all. You have been my champion and my lifeline in the roughest patches.

To my husband, Khang Huynh, who patiently supported me through hundreds of hours of weeknights, weekends, and holidays disrupted in the name of science. I am lucky to have you.

Table of Contents

ABSTRACT OF THE DISSERTATION	ii
Dedication	v
Table of Contents	vi
List of Figures	vii
Acknowledgements	ix
Curriculum vitae	xiii
Chapter 1 – Introduction	1
Chapter 2 – PACAP/PAC1 regulation of inflammation via catecholaminergic neurons in a model of multiple sclerosis	
Abstract	18
Introduction	19
Materials and Methods	24
Results	32
Discussion	37
Acknowledgements	39
Tables	41
Figures	42
Chapter 3 – Roles of PACAP/PAC1 signaling on neuroprotection and modulating optic neuritis in a model of multiple sclerosis	
Abstract	51
Introduction	51
Materials and Methods	63
Results	63
Discussion	65
Acknowledgements	67
Figures	68
Chapter 4 – Test ability of AAV-mediated PACAP overexpression to ameliorate EAE	
Abstract	81
Introduction	81
Materials and Methods	85
Results	95
Discussion	97
Acknowledgements	98
Figures	99
Chapter 5 – Conclusions	99
References	112

List of Figures

Chapter 1 – Introduction

Figure 1-1. Multiple Sclerosis.....	14
Figure 1-2. Experimental Autoimmune Encephalomyelitis (EAE).....	16
Figure 1-3. Hypothesized mechanisms of PACAP.....	17

Chapter 2 – PACAP/PAC1 regulation of inflammation via catecholaminergic neurons in a model of multiple sclerosis

Figure 2-1. Experimental approach.....	42
Figure 2-2. PAC1 receptor gene expression is specifically knocked down in catecholaminergic cells	44
Figure 2-3. Conditional knockdown of PAC1 receptors in catecholaminergic cell led to early inhibition of, then enhanced, EAE severity	46
Figure 2-4. Conditional knockdown of PAC1 in sympathetic ganglia alters CD4 ⁺ helper T-cell polarization during EAE	47
Figure 2-5. Conditional knockdown of PAC1 in catecholaminergic neurons led to decreased production of IFN γ from spleen and lymph node cells cultured with MOG ₃₅₋₅₅	49
.....	
Figure 2-6. Flow cytometry analysis of T _{regs} in thymus	50

Chapter 3 –Roles of PACAP/PAC1 signaling on neuroprotection and modulating optic neuritis in a model of multiple sclerosis

Figure 3-1. Approach for conditional knockout of PAC1 and induction of experimental autoimmune encephalomyelitis	68
Figure 3-2. AAV2 infects retinal ganglion neurons.....	69
Figure 3-3. Viral reporter in brain	
Figure 3-4. Retinal ganglion cell quantification	71
Figure 3-5. In naïve animals, AAV2 Cre GFP administration into the eye leads to loss of SMI-32 neurons and decreased number of dendrites per cell	73
Figure 3-6 Eyes injected with AAV2 Cre GFP have fewer SMI-32 immunoreactive axons radiating from the optic nerve than eyes injected with AAV2 GFP	74
Figure 3-7. Astrocytes in the retina.....	75
Figure 3-8. Microglia/macrophage characterization	76
Figure 3-9. Loss of PAC1 in the eye leads to axonopathy in both naïve and EAE optic nerves...77	

Figure 3-10. PAC1 deletion leads to increased CD45+ immunopositivity in the optic nerve during EAE	79
Figure 3-11. Microglia/macrophage presence	80

Chapter 4 – Test Ability of AAV Delivered PACAP to the Eye to Ameliorate EAE-Induced Retinopathy

Figure 4-1. Construct to express PACAP and a red fluorescent reporter protein under the human synapsin promoter.	99
Figure 4-2. Experimental approach for systemic administration of PACAP overexpressing virus and subsequent induction of EAE	100
Figure 4-3. Using PHP.B AAV to express a transgene under the human synapsin promoter results highly specific expression of the viral reporter in the CNS	101
Figure 4-4. PACAP expressed is increased in the brains of animals systemically injected with the PACAP overexpressing virus while the levels of PAC1 receptor expression does not change	102
Figure 4-5. Clinical scores for animals systemically injected with PBS, AAV tDimer, and AAV PACAP, and induced with chronic EAE	103
Figure 4-6. Virus reporter expression reporter in retina of animals systemically injected with PHP.B AAV tDimer	104
Figure 4-7. Effect of systemic administration of PHP.B AAV PACAP P2A tDimer or control virus on numbers of CD45 immunopositive cells in the optic nerve	105
Figure 4-8. Viral reporter of intraocularly injected PHP.B AAV tDimer in retina	106
Figure 4-9. Viral reporter of intraocularly injected PHP.B AAV tDimer in brain	107

List of Tables

Chapter 2 – PACAP/PAC1 regulation of inflammation via catecholaminergic neurons in a model of multiple sclerosis

Table 2-1. List of primers used in qPCR assays	41
--	----

Acknowledgements

I would like to thank my advisor, Dr. James Waschek, for his support, guidance, and understanding through the years, as well as the other members of my thesis committee: Dr. Harley Kornblum, Dr. Melissa Spencer, Dr. Rhoda Voskuhl, and Dr. David Williams, for all their guidance and advice.

I would also like to thank the current and former members of the Waschek lab for their help and company: Dr. Michael Condro, Dr. Abha Rajbhandari, Dr. Yukio Ago, Dr. Bhavaani Jayaram, Youtong Huang, Viren Makhijani, Ivan Garcia, Navjot Singh, Miku Tsubosaka, Dr. Guillermina Calo, and Dr. Lingli Lu. I particularly wish to thank Dr. Condro for taking me under his wing. His mentorship has been invaluable through the turbulent waters of both grad school and life. Special thanks to the undergraduate and high school students who assisted me in my work (in chronological order): Anna Diep, Henly Ko, Anh Hoang, Kenny Lov, Ruoyan Zhu, Nhat Nguyen, and Patrick Ricaflanca. Your dedication, enthusiasm, and intellect frequently left me in awe. Wherever you go in life, people will be lucky to have you.

Thanks to all our collaborators and expert consultants: Dr. Gerald Lipshutz, Dr. Prashant Rajbhandari, Dr. Benjamin Deverman, Dr. Allan Mackenzie-Graham, Dr. Mei Jiang, and Dr. Alessia Tassoni, some of whom helped with projects described in this dissertation and others who helped on projects not described here.

I am also grateful for other members of the UCLA community who have supported me outside of the lab. Special thanks to Dr. Peter Bradley, Dr. Jerome Zack, and Dr. Sherie Morrison for their mentorship.

I would also like to thank the staff, particularly Andrea Knipe, Martha Maxwell, and Mary Loutzenhiser, of the UCLA Department of Laboratory Animal Medicine for their assistance in the care of our animals or for technical training, Drs. Dorwin Birt and Michael Condro for their assistance with microscopy at the UCLA Intellectual and Developmental Disabilities Research Center Microscopy Core, and Jeff Calimlim for technical assistance at the UCLA Janis V. Giorgi Flow Cytometry Core.

Furthermore, I am exceptionally grateful for the wonderful mentors I have had over the years: Paul Yang, Dr. Fernando Aleman Guillen, and Dr. Miller Tran, Dr. Emily Lowe and Dr. Allan Chen. These generous, compassionate, and dedicated mentors were fundamental to my growth as a scientist. I particularly want to thank Dr. Tran who very early on in my career fostered critical thinking and independent learning, as well as encouraged me to challenge myself with higher goals.

Chapter 2 is a version of **Van, C.**, Condro, M.C., Lov, K., Zhu, R., Ricaflanca, P.T., Ko, H.H., Diep, A.L., Hoang, A.Q., Pisegna, J., Rohrer, H., and Waschek, J.A. (2018). PACAP/PAC1 Regulation of Inflammation via Catecholaminergic Neurons in a Model of Multiple Sclerosis. *Journal of Molecular Neuroscience*. doi: 10.1007/s12031-018-1137-8. It is reprinted here with permission by Springer Nature. Funding was provided by The National Multiple Sclerosis Society (RG3928A2, RG-1501-02646). JAW devised the model. CV oversaw the experiments. CV, MCC, KL, RZ, PTR, HHK, ALD, and AQH performed the experiments. CV, KL, RZ, and PTR analyzed data. CV wrote the original manuscript. CV and JAW edited the manuscript. We would like to thank Dr. Joseph Pisegna, for helping to generate the PAC1 floxed mouse line, Dr. Hermann Rohrer for the D β H-CreER mouse line, and Dr. Anton Maximov for the Ai9 reporter mouse line.

This project received support from the National Multiple Sclerosis Society (RG 1501-02646), the Cousins Center for Psychoneuroimmunology, UCLA Semel Institute, and the NIH/NCATS UCLA CTSI Grant Number UL1TR000124). The latter award helped fund the generation of the PAC1^{loxP/loxP} D β H-CreER mice. The research was made possible by the equipment made available at the following cores: UCLA Intellectual and Developmental Disabilities Research Center (IDDRC) Core which is supported by a grant from the Eunice Kennedy Shriver National Institute of Child Health (5U54HD087101-03) and is an Organized Research Unit supported by the Jane and Terry Semel Institute for Neuroscience and Human Behavior, and the UCLA Jonsson Comprehensive Cancer Center (JCCC) and Center for AIDS Research Flow Cytometry Core Facility which is supported by National Institutes of Health awards P30 CA016042 and 5P30 AI028697, and by the JCCC, the UCLA AIDS Institute, the David Geffen School of Medicine at UCLA, the UCLA Chancellor's Office, and the UCLA Vice Chancellor's Office of Research.

Chapter 3 is adapted from a manuscript in preparation. Dr. James Waschek conceived of the idea. Christina Van supervised the project. Christina Van, Dr. Michael Condro, Patrick Ricaflanca, Anh Hoang, Nhat Nguyen, Henly Ko, Ruoyan Zhu, and Anna Diep performed experiments. Dr. Mei Jiang provided technical assistance. Christina Van, Patrick Ricaflanca, and Nhat Nguyen analyzed data. Christina Van wrote the manuscript. Christina Van and Dr. James Waschek edited the manuscript. We thank the National Multiple Sclerosis Society for funding this study (RG3928A2, RG-1501-02646). We also thank the UCLA Intellectual and Developmental Disabilities Research Center (IDDRC) Core for use of their microscopes and cryostat. The IDDRC is supported by a grant from the Eunice Kennedy Shriver National Institute of Child Health

(5U54HD087101-03) and is an Organized Research Unit supported by the Jane and Terry Semel Institute for Neuroscience and Human Behavior.

Chapter 4 is adapted from a manuscript in preparation. Dr. James Waschek conceived of the idea. Christina Van designed the experiments and supervised the project. Christina Van, Patrick Ricaflanca, Ruoyan Zhu, and Kenny Lov performed the experiments. Christina Van and Patrick Ricaflanca analyzed the data. Christina Van wrote the original manuscript. Christina Van and Dr. James Waschek edited the manuscript. The PHP.B AAV PACAP P2A tDimer and PHP.B AAV tDimer viruses were packaged by Dr. Benjamin Deverman. Thank you to Dr. Benjamin Deverman and Dr. Gerald Lipshutz for technical assistance. We thank the National Multiple Sclerosis Society for funding this study (RG3928A2, RG-1501-02646). We also thank the UCLA Intellectual and Developmental Disabilities Research Center (IDDRC) Core for use of their equipment. The IDDRC is supported by a grant from the Eunice Kennedy Shriver National Institute of Child Health (5U54HD087101-03) and is an Organized Research Unit supported by the Jane and Terry Semel Institute for Neuroscience and Human Behavior.

Vitae

EDUCATION

- University of California, Los Angeles (UCLA) Expected Dec 2018
Ph.D., Molecular Biology
- University of California, San Diego (UCSD) 2012
B.S., Biochemistry and Cell Biology, Minor: Psychology

RESEARCH / WORK EXPERIENCE

Graduate Student, UCLA Molecular Biology Interdepartmental Program 2013 - present

- Investigate the role of a protein in modulating inflammation using targeted genetic manipulations, *in vivo* modeling, cell culture, flow cytometry, RNA *in situ* hybridization, and ELISA, resulting in a first author publication
- Test ability of a novel viral vector made in collaboration with an AVV expert to target a therapeutic protein to the central nervous system *in vivo*, using histology and fluorescent microscopy imaging. Presented work at international symposium
- Mentor 2 rotation/visiting doctoral students, 8 undergraduate/high school students

Teaching Assistant, UCLA Dept. Microbio., Immunology, and Molec. Genetics 2014 - 2015

- Lead interactive discussion sections; created weekly illustrated handouts
- Rated “Very High” or “Always” by 26 out of 26 students in evaluation in all categories including: knowledge, concern for student learning, organization, and communication
- Honored with 2015 departmental teaching award

Production Chemist, BioLegend, San Diego 2013

- Completed 30% more work orders than expected output
- Selected to perform custom, re-work, and product development work orders
- Trained new personnel on SOPs for antibody conjugation, protein column purification
- Maintained organized production records using Microsoft Dynamics NAV & Filemaker

Research Assistant, UCSD Department of Biological Sciences 2011 –2012

- Performed protein engineering, transformations, genetic screening, mid-scale protein production, and protein purification to demonstrate the use of algae as an expression platform for engineered full-length, dimeric drug-conjugated antibodies, resulting in a publication with over 100 citations
- In collaboration with an oncology lab, tested the function of immunotoxins to target cancer cells through *in vitro* cytotoxicity cell culture assays and *in vivo* tumor model, leading to a publication

Teaching Assistant, UCSD Department of Biological Sciences 2010 – 2012

- Lead interactive discussion sections; strived to maintain inclusive environment
- Nominated for 2012 departmental teaching award

PUBLICATIONS

Van, C., Condro, M.C., Lov, K., Zhu, R., Ricaflanca, P.T., Ko, H.H., Diep, A.L., Hoang, A.Q., Pisegna, J., Rohrer, H., et al. (2018). PACAP/PAC1 Regulation of Inflammation via Catecholaminergic Neurons in a Model of Multiple Sclerosis. *Journal of Molecular Neuroscience*. doi: 10.1007/s12031-018-1137-8.

Ago Y., Condro M.C., Rajbhandari A.K., **Van C.**, Jayaram B., May V., Waschek J.A. (2016) PACAP modulation of CNS and peripheral inflammation, in *Pituitary Adenylate Cyclase Activating Polypeptide – PACAP*; Current Topics in Neurotoxicity, Springer. ISBN:978-3-319-35133-9.

Condro, M.C., Matynia, A., Foster, N.N., Ago, Y., Rajbhandari, A.K., **Van, C.**, Jayaram, B., Parikh, S., Diep, A.L., Nguyen, E., May, V., Dong H.W. and Waschek, J.A. (2016). High-resolution characterization of a PACAP-EGFP transgenic mouse model for mapping PACAP-expressing neurons. *J. Comp. Neurol.* doi: 10.1002/cne.24035.

Chen, A.L., Kim, E.W., Toh, J.Y., Vashisht, A.A., Rashoff, A.Q., **Van, C.**, Huang, A.S., Moon, A.S., Bell, H.N., Bentolila, L.A., et al. (2015). Novel Components of the Toxoplasma Inner Membrane Complex Revealed by BioID. *mBio* 6, e02357–14. doi: 10.1128/mBio.02357-14.

Tran, M., Henry, R.E., Siefker, D., **Van, C.**, Newkirk, G., Kim, J., Bui, J., and Mayfield, S.P. (2013). Production of anti-cancer immunotoxins in algae: Ribosome inactivating proteins as fusion partners. *Biotechnol. Bioeng.* 110, 2826–2835. doi 10.1002/bit.24966.

Tran, M., **Van, C.**, Barrera, D.J., Pettersson, P.L., Peinado, C.D., Bui, J., and Mayfield, S.P. (2012). Production of unique immunotoxin cancer therapeutics in algal chloroplasts. *PNAS* 110, 14–14. doi: 10.1073/pnas.1214638110.

TALKS/POSTER PRESENTATIONS (2 of 17)

- **Van, C.**, Rajbhandari, P., Pisegna, J., Germano, P., Condro, M.C., Lov, K., Zhu, R., Ricaflanca, P. T., Ko, Henly H., Hoang, A.Q., Diep, A.L., Tontonoz, P. and Waschek, J.A. PACAP/PAC1 modulation of thermogenesis, metabolism, and inflammation via catecholaminergic neurons in the sympathetic nervous system. Oral presentation delivered at 22nd International Symposium on Regulatory Peptides, Acapulco, Mexico. September 24, 2018.
- **Van, C.** Role of PACAP/PAC1 in protecting neurons and modulating inflammation in a model of multiple sclerosis and optic neuritis. Oral presentation delivered at the 13th International Symposium on PACAP, VIP, and Related Peptides at the University of Hong Kong, Hong Kong. December 5, 2017.

HONORS / CERTIFICATION

- **22nd International Symposium on Regulatory Peptides**, Travel award 2018
- **Brain Research Institute**, Society for Neuroscience travel award 2018
- **UCLA Institute of the Environment and Sustainability**, Leaders in Sustainability certificate 2018
- **UCLA Anderson School of Management Entrepreneurship for Science Medicine, and Technology**, Certificate of completion 2018
- **13th International Symposium on VIP, PACAP and Related Peptides**, Young Investigation Award 2017
- **UCLA Entering Mentoring Training Program**, Certificate of completion 2017
- **Moving Targets Symposium (USC) 22nd International Symposium on Regulatory Peptides**, Graduate division poster prize 2017
- **Society of Asian Scientists and Engineers**, Travel award 2016
- **Department of Microbiology, Immunology, and Molecular Genetics**, Teaching assistant award 2015
- **UCLA Grad Slam Competition**, Semi-finalist 2015

EXTRACURRICULAR / VOLUNTEER

- **Data Management & Electronic Laboratory Notebook Workshop**, *Organizer* 2017
- **California Nanosystems Institute (CNSI) High School Nanoscience Program**, *Workshop Instructor, Nanovation competition team mentor* 2014–present
- **Exploring Your Universe at UCLA**, *Event Coordinator* 2014–present
- **White House Initiative at UCLA**, *Event Coordinator* 2015
- **Society of Asian Scientists & Engineers**, *Outreach Director* 2013–2016

Chapter 1 – Introduction

Inflammation in the central nervous system

Neurodegenerative disease is a term used to describe a range of diseases which primarily involve atrophy and loss of neurons and/or their processes. More recently, it became clear that inflammation plays a major role in the pathology of most neurodegenerative diseases ¹. Neurodegenerative diseases of the central nervous system (CNS) include Alzheimer's disease, Parkinson's disease, Huntington's disease, and multiple sclerosis. These diseases are chronic and often progressive, leading to cognitive and motor impairment which can have severe effects on daily quality of life ². In adult humans, neural stem cells proliferation appears quite limited, and thus when neurons are damaged or lost, they are generally not replaced. With great medical advances in the past century, the average human lifespan has been prolonged. However, with the advent of longer life spans comes the increased risk for developing neurodegenerative diseases. The rising prevalence of neurodegenerative diseases will not only impact the quality of life for a growing number of people, it will also increase societal burden and financial costs. As there is currently no available treatment to halt neurodegeneration, there is a clear unmet need to understand more about how to protect the CNS against neuron atrophy and loss, as well as against inflammation. For these studies, we focus on studying neuroprotection and inflammation in the context of multiple sclerosis (MS), a chronic autoimmune and neurodegenerative disease which affects 2.5 million people worldwide and is the leading cause of non-trauma related disability in young adults.

Multiple sclerosis

MS is characterized by autoreactive T cells which target myelin wrapped around the axons of neurons. This myelin sheath provides insulation to enhance the propagation of neuronal electrical impulses signals down an axon. Long-term autoreactivity of immune cells to myelin leads to repeated demyelination and eventual loss of neurons and their axons in the CNS (**Figure 1-1**), which includes the brain, spinal cord, eye, and optic nerve. This results in neurological disability. Symptoms include vision loss, numbness, tingling sensations, pain, and paralysis, with bladder, bowel, and sexual dysfunction, fatigue, and cognitive impairment contributing to reduced quality of life ^{3,4}. Approximately 20% of patients diagnosed with MS initially present with symptoms of vision loss and ocular pain. Diagnosis of MS typically involves magnetic resonance imaging (MRI) which can reveal characteristic lesions in the brain and spinal cord and may also include lumbar puncture to test for the presence of autoreactive antibodies.

There are four recognized forms of multiple sclerosis (**Figure 1-1**). Most patients present with the relapsing remitting form of the disease. Patients with relapsing remitting MS experience relapses during which they experience MS symptoms, punctuated by periods of remission in which their symptoms are absent or noticeably milder. Primary-progressive MS is not common and is characterized by the steady and increasingly severe occurrence of symptoms without periods of relapses or remissions. An even less common form of MS is progressive-relapsing, which is similar to primary-progressive, except there are periods of relapses in which symptoms temporarily intensify beyond the steady increase in disease severity. With time, patients who originally presented with the relapsing-remitting form of the disease may enter the progressive form of the disease. This is called secondary-progressive MS, and in this stage, patients experience increasing severity of symptoms without periods of remission.

Most available drugs only provide relief to patients in the relapsing remitting stage. Although various genetic, epigenetic, and environmental factors have been linked to MS, there does not appear to be a single cause or trigger of MS. Rather it seems disease arises from the combination of multiple factors. The lack of a clear cause of disease makes the development of treatments for MS particularly challenging. Furthermore, MS varies greatly from patient to patient and the disease progression in each patient is unpredictable. This further complicates the task of treatment development.

Currently available MS treatments

Current United States Food and Drug Administration (FDA) approved drugs for MS are listed below.

Drug (Year US FDA approved) References	Form of MS treated	Identity & Presumed mechanism of action	Treatment Effect
glatiramer acetate (1996) 5-7	Relapsing- remitting	<i>Identity:</i> Mixture of polymers composed of the four amino acids found in myelin basic protein—alanine, glutamic acid, lysine, and tyrosine <i>Mechanism:</i> The peptides serve as decoy for autoreactive immune cells	Reduces relapse rate, reduced brain lesions
Mitoxantrone (2000) 8-10	Worsening relapsing- remitting, secondary progressive, progressive- relapsing	<i>Identity:</i> Type II topoisomerase inhibitor <i>Mechanism:</i> Disrupts DNA synthesis in cells by intercalating within DNA strand leading to cell death. Also causes defect in antigen presentation and thus reduces secretion of	Reduced relapse rate, disability progression, and fewer patients with active lesions

		proinflammatory cytokines from immune cells	
interferon beta 1a/1b (2002) 11–17	Relapsing-remitting	<i>Identity:</i> Cytokine produced in mammalian cells (1 α) or E. coli (1 β) <i>Mechanism:</i> Binds to interferon beta receptor and leads to reduced antigen presentation and T cell proliferation, reduces inflammatory cytokine expression, promotes secretion of anti-inflammatory cytokines, and reduces migration of leukocytes over the blood-brain barrier	Reduced relapse rate, reduced brain lesions (MRI)
Natalizumab (2004) 18–22	Relapsing-remitting, secondary progressive	<i>Identity:</i> Humanized monoclonal antibody against alpha-4 integrin adhesion molecule <i>Mechanism:</i> Binds to an adhesion molecule on the surface of white blood cells and prevents immune cells from adhering to vascular endothelium and trafficking into target tissues	Reduced relapse rate, number and volume of persistent and new active lesions, and improved quality of life
Fingolimod (2010) 23–26	Relapsing-remitting	<i>Identity:</i> A structural analogue of sphingosine, it modulates sphingosine-1-phosphate receptor activity <i>Mechanism:</i> In lymphocytes, fingolimod is phosphorylated and binds to S1P receptors in an antagonistic manner and leads to internalization of S1P receptors. Down regulation of S1P1 reduces lymphocyte egress from lymphatic tissue. The result is the sequestration lymphocytes in the lymphatic tissue to prevent lymphocytes from migrating to the CNS	Reduces relapse rate, brain lesions, and disability progression as well as protect against brain volume loss
Teriflunomide (2012)	Relapsing-remitting	<i>Identity:</i> Active metabolite of leflunomide <i>Mechanism:</i>	Reduces relapse rate, brain lesions, and disability

27–30		Inhibits the mitochondrial enzyme dihydroorotate dehydrogenase required to synthesize pyrimidines <i>de novo</i> , therefore inhibits reproduction of rapidly dividing cells such as lymphocytes	progression as well as protect against brain volume loss
dimethyl fumarate (2013) 31,32	Relapsing-remitting	Identity: methyl ester of fumaric acid Mechanism: Mechanism not clear but reduces lymphocyte numbers, promotes Th2 helper T cell and dendritic response and anti-oxidative responses	Reduced relapse rate, brain lesions, and disability
Alemtuzumab (2014) 33–37	Relapsing-remitting	Identity: Recombinant human monoclonal antibody with hypervariable regions derived from rat antibodies which target CD52 Mechanism: Binds to CD22 on B lymphocytes and leads to antibody-dependent cell-mediated cytotoxicity and complement-dependent cytotoxicity	Reduced relapse rate and prevent worsening disability
Daclizumab (2016) 38,39	Relapsing-remitting	Identity: Humanized monoclonal antibody targeting CD25 Mechanism: Blocks IL-2 binding to its receptor, prevents activation of T cells, and enhances CD56-high natural killer cells	Reduced relapse rate, fewer new lesions
Ocrelizumab (2017) 3,34	Relapsing-remitting, primary progressive	Identity: Humanized monoclonal antibody which targets CD20 Mechanism: Binds mature B-cells and leads to antibody-dependent cell-mediated cytotoxicity and complement-dependent cytotoxicity	Reduced relapse rate, worsening disability, fewer brain lesions

These drugs are termed disease-modifying drugs because they help relieve symptoms but do not target the root cause of disease. The goal of these drugs is to reduce the occurrences of relapse, stent the progression of disease, and prevent or minimize disability. Relapses may also be treated with corticosteroids such as methylprednisolone ⁴⁰, prednisone, and adrenocorticotropic hormone. Treatment with corticosteroids can facilitate recover from a relapse but do not prevent relapses from occurring ⁴¹. There is also evidence corticosteroids can reduce brain atrophy ⁴². However, use of corticosteroids as a disease modifying treatment has been greatly reduced because of severe side effects associated with chronic long-term use. Moreover, there are few drugs which are effective in patients with the progression form of MS ^{43,44}. In fact, ocrelizumab is the only FDA approved drug for the aggressive primary-progressive form of MS, and it has only a mild clinical benefit ^{45,46}. As is the case in many diseases, patients are advised to manage their lifestyle to include a healthy diet, exercise, and mental health. There are also drugs to treat specific symptoms of MS ⁴⁷ but these are not disease modifying drugs. Most drugs can reduce inflammation in MS patients, but thus far, there is not yet an FDA approved drug capable of reducing inflammation and independently protecting neurons undergoing inflammatory attack. Consequently, treatments can help reduce pathological inflammation, but chronic low-level inflammation leads to accumulated neuronal damage.

Treatments under development

There are other treatments for MS are under clinical trial testing. One treatment, estriol, was conceived from the observation that pregnant women with MS had fewer relapses during the trimester of their pregnancy. This led to the discovery of the connection between elevated estrogen levels and reduced relapses. A recent clinical trial in women found that patients treated with estriol

had less cortical grey matter atrophy⁴⁸. More research needs to be done to understand the effects and mechanisms of estriol treatment, and to determine whether estriol would be safe treatment for men.

More recently, stem-cell based treatments have been offered in clinical trials. These include autologous hematopoietic stem cell therapy⁴⁹⁻⁵², intravenous injection of mesenchymal stem cells⁵³⁻⁵⁵, and use of human fetal-derived neural stem cells⁵⁶. These studies generally demonstrate the safety in administering stem cell therapy but significant neuroprotection and/or reduction in inflammation is not consistently observed through assessments of cognition, ambulation, visual function, and effect on lesion size as shown by MRI. Stem cell therapies for MS appear promising but are still under development.

Cognitive therapies such as mindfulness based therapies^{57,58} and behavior modifying therapy are effective at reducing perceived stress, anxiety, depression, and pain but there is not yet evidence to show that these therapies are able to prevent relapse, slow disease progression, or reduce objectively quantifiable disease measures.

Experimental autoimmune encephalomyelitis (EAE) model of multiple sclerosis

To identify and investigate potential pathological processes in MS and to test the efficacy of new therapies, the paralytic symptoms of MS can be recapitulated *in vivo* with artificially induced autoimmunity against myelin. The myelin oligodendrocyte glycoprotein (MOG₃₅₋₅₅) C57BL/6 experimental autoimmune encephalomyelitis (EAE) model is commonly used in MS research⁵⁹⁻⁶¹. To induce EAE, mice are subjected to a well-characterized protocol in which MOG₃₅₋₅₅, a fragment of a protein in myelin, is administered peripherally with adjuvant (see

Methods sections in Chapters 2 or 3). This generates an autoimmune response, producing T cells autoreactive to myelin⁶². Additionally, the animals are administered *Bordetella pertussis toxin* which causes permeability of the blood brain barrier, thus allowing the autoreactive T cells to infiltrate into the CNS to target the myelin sheaths of neurons. To capture both the acute inflammatory and the chronic neurodegenerative aspects of MS, two different models of EAE were used: acute and chronic (**Figure 1-2**). To study active inflammation, the acute model is used. In this model, the animals develop an acute autoimmune attack on myelin and clinical symptoms for a short period and eventually recover in many cases. To study long term neurodegeneration, the chronic model is used. In this model, the animals develop symptoms and continue experiencing symptoms for the remainder of the experiment, typically up to 60 days. The severity of disease is scored on a standard scale of 0 through 5, based on the degree of paralysis observed. Of course, there are limitations to this model. Importantly, 1) there are differences between human and mouse immune systems and anatomy, 2) autoreactive T cells are expanded against a particular antigen in a controlled manner in EAE, whereas in MS patients, the cause is not known, and 3) B cells play an key role in the pathology of MS⁶³ whereas the role of these cells in EAE seems to differ^{64,65}. Therefore, the EAE model is only a rough capitulation of MS. Nonetheless, the major disease manifestations are captured and several drugs have been developed based on original testing in the EAE model^{66,67}. Some other shortcomings of the EAE model include the lack of genetic variability as only particular strains of inbred mice are used, the short timeframe of the experiments may not demonstrate real long-term disease course, as well as the failure to predict infectious, metabolic and immunological complications^{68,69}. Despite these limitations, EAE remains a key proof-of-concept model for development of MS therapies.

PACAP and its receptors

In the 30 years since its discovery, there has been increasing interest in the neuroprotective and anti-inflammatory properties of a protein called pituitary adenylate cyclase-activating polypeptide (PACAP). PACAP was originally discovered as a 38-amino acid hypothalamic peptide that potently induced cyclic adenosine monophosphate (cAMP) levels in cultured pituitary cells ⁷⁰. PACAP is an endogenous, evolutionarily highly conserved protein, and is known to be involved in many biological processes, including: regulation of circadian rhythm, stress responses, brain development, glucose levels, angiogenesis, and immune cell activity ⁷¹. Additionally, PACAP is upregulated in response to injury, ischemia, and inflammation and has been shown to provide neuroprotection in animal models of neurodegenerative diseases such as Alzheimer's, Parkinson's Disease, and stroke ⁷²⁻⁷⁹.

PACAP binds three different receptors: PAC1 (gene *ADCYAP1R1*), VPAC1 (gene *VIPR1*), and VPAC2 (gene *VIPR2*) which are heterotrimeric G-protein-coupled receptors which generally signal through activation of cyclic AMP ^{80,81}. While the latter two also bind a homologous ligand called vasoactive intestinal peptide (VIP) ⁸², PAC1 is highly selective for PACAP. VPAC1 and VPAC2 mediate some of the immunomodulatory actions of PACAP ^{83,84}, whereas primarily PAC1 mediates its growth and neuroprotective actions ^{76,78,79}. Furthermore, PAC1 is more highly and widely expressed throughout the CNS as compared to VPAC1 or VPAC2 ⁸⁵.

Three independent studies found no correlation between single nucleotide polymorphisms in PACAP between MS patients versus controls subjects ⁸⁶⁻⁸⁸. There have yet to be any studies on the correlation between SNPs in the PAC1 receptor gene and MS. Moreover, there have not been any reports on differential expression of either PACAP or PAC1 in MS patients as compared to

healthy controls. There is, however, a reported defect in expression of another PACAP receptor, VPAC2, in MS patients. VPAC2 is lowly expressed in resting CD4 helper T cells but upon *in vitro* activation with antibodies against CD3 and CD28, the increase in VPAC2 expression in MS patient cells was significantly less than cells from healthy controls ⁸⁹.

Role of PACAP in EAE

An earlier study found that PACAP administration to mice with EAE resulted in ameliorating disease symptoms ⁹⁰. In addition, cell cultures from mice treated with PACAP had reduced population of proinflammatory helper T cells, less secretion inflammatory cytokines, and reduced costimulatory factors on the surface of antigen-presenting cells.

Subsequently, the Waschek lab described effects of PACAP and PACAP receptors on the immune response in EAE using knockout (KO) models. For example, the Waschek lab previously demonstrated that PACAP KO mice exhibited enhanced, prolonged EAE compared to wild type (WT) mice ^{91,92}. During EAE, WT and PACAP KO mice upregulated expression of both pro-inflammatory cytokines and anti-inflammatory cytokines, however, PACAP KO mice had significantly higher expression of some pro-inflammatory cytokines and significantly lower expression of anti-inflammatory cytokines than WT mice ⁹³. Furthermore, PACAP also promotes the skewing of helper T cells away from the more inflammatory Th1 and Th17 phenotype and towards a less inflammatory Th2 phenotype, as well as the expansion of regulatory T cells during EAE which helps control pathological inflammation ^{92,93}. Therefore, it is known that PACAP can promote a less inflammatory state during EAE. However, little is known about the mechanisms of PACAP.

Which receptors mediate the neuroprotective and anti-inflammatory properties of PACAP? Mice deficient in VPAC2⁹⁴ or PAC1 (unpublished) mimicked the more severe and prolonged EA, similar to that observed in PACAP KO mice. Paradoxically, VIP KO and VPAC1 KO mice were found to be resistant to EAE^{95,96}. These results indicate that PACAP protection against EAE is likely mediated primarily through the VPAC2 and/or PAC1 receptors and not through VPAC1. Studies have shown that VIP and PACAP can act directly on lymphocytes and macrophages to inhibit the production of inflammatory cytokines^{97,98}. That the *in vitro* actions of VIP and PACAP on inflammatory cells exhibit nearly identical pharmacology suggests that main receptors mediating the response is VPAC1 and/or VPAC2, and probably not PAC1. Furthermore, VPAC1 and VPAC2 were found to be expressed in human dendritic cells, and dendritic cells incubated with VIP promoted T cell proliferation and promoted IL-4 expressing (Th2 type) T cells⁹⁹. Similarly, VPAC1 and VPAC2 are both expressed on human T cells. VPAC1 expression highest in resting T cells and downregulated with T cell activation while VPAC2 expression is lower in resting T cells and upregulated with T cell activation¹⁰⁰. However, little is known about PAC1 receptor activity in immune cells.

PAC1 Mechanisms of action

Need to first show our unpublished figure on EAE in PAC1 KO mice., we proposed that PACAP might regulate immune function by way of its action as a neuromodulator. PACAP receptors are also found on neurons. Could PACAP's anti-inflammatory and neuroprotective properties act through neurons? Of particular interest, is the PAC1 receptor. PACAP is expressed in the intermediolateral cell column preganglionic neurons of the sympathetic nervous system¹⁰¹.

The sympathetic nervous system is a known regulator of the immune system. Moreover, PAC1 is expressed on 90% of the postganglionic neurons which innervate the peripheral immune organs^{102,103}. We hypothesize PACAP can act through PAC1 receptors in the sympathetic nervous system to regulate inflammation.

Furthermore, it has been shown that PACAP interaction on neurons has been shown to inhibit apoptosis¹⁰⁴ and protect against ROS-mediated neuronal death *in vitro*¹⁰⁵. PACAP has also been shown to prevent neurodegeneration in a model of diabetic retinopathy^{106,107}. It is thought that PAC1 mediates these neuroprotective effects. It has not yet been tested *in vivo* if PACAP's neuroprotective properties are mediated through the PAC1 receptor.

Significance

Inflammation of the central nervous system characterizes many neurodegenerative diseases such as MS, stroke, Parkinson's Disease, Alzheimer's Disease, and traumatic brain injury. Some of these diseases are chronic and can have devastating effects on the patient's quality of life. Current FDA approved drugs can reduce inflammation in the periphery but do not target inflammation in the CNS. Nor do they protect against further neurodegeneration and neuron loss. There is a clear unmet need for additional therapeutic options. It is known that PACAP has anti-inflammatory and neuroprotective properties in various model of neurodegenerative diseases⁷²⁻⁷⁹. However, there is little known about the mechanisms through which PACAP acts. Here we use a model of multiple sclerosis to investigate the ability of PACAP and PAC1 signaling to modulate inflammation and protect neurons. In these studies, we investigate two potential mechanisms by which PACAP/PAC1 modules inflammation during EAE: 1) whether PACAP it can act on the

neural circuitry which regulates inflammation, and if 2) PACAP can act directly on PAC1 receptors on neural cells to protect them against inflammatory insult. Finally, using CNS-trophic recombinant adeno-associated virus, we target a PACAP-overexpressing construct to the CNS to test whether it can protect against EAE and optic neuritis. These studies identify targets of interest for manipulating neuron-mediated modulation of inflammation and for developing treatments for inflammatory neurodegenerative diseases.

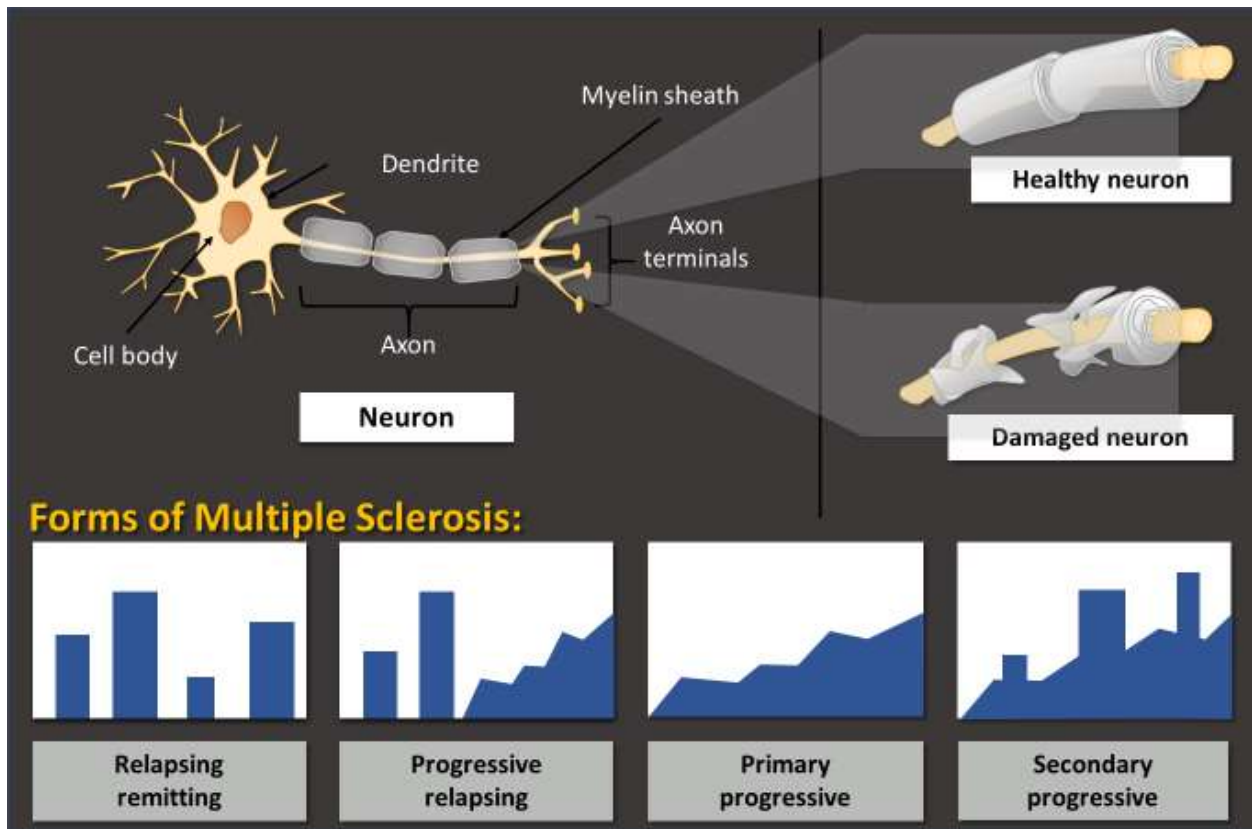
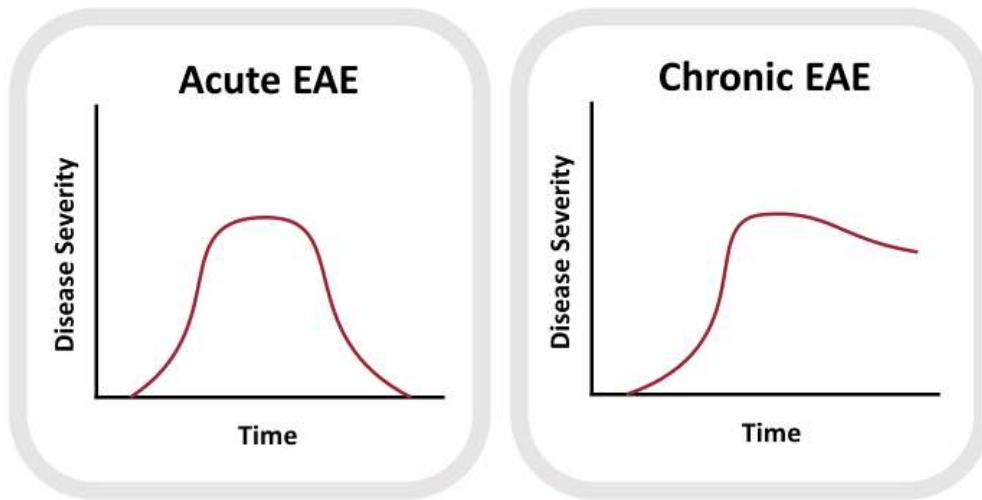
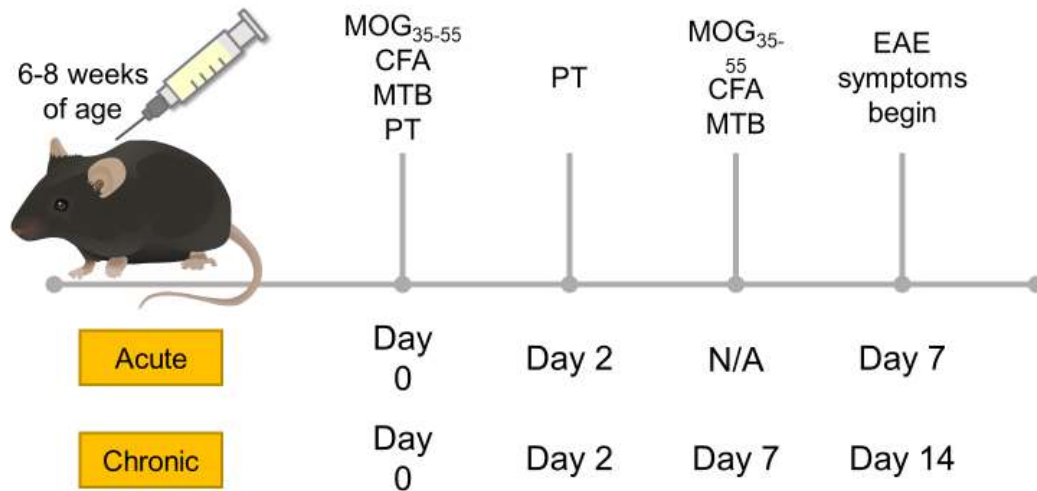


Figure 1-1. Multiple sclerosis. Multiple sclerosis is an autoimmune neurodegenerative disease in which chronic autoreactivity of T cells targeting myelin eventually leads to neurodegeneration and neuron loss. There are four forms of multiple sclerosis.

(a)



(b)



CLINICAL SCORING	
Score	Symptoms
0	Unaffected
1	Limp tail
2	Partial paralysis or failure to resist inversion
3	Complete paralysis of one hindlimb
4	Complete paralysis of both hindlimbs
5	Moribund or death

Figure 1-2. Experimental Autoimmune Encephalomyelitis (EAE). (a) Acute and chronic EAE. The acute model of EAE is used to model active inflammation. In the acute model of EAE, the animals develop paralysis symptoms, peak in disease severity, and subsequently recover. The chronic model of EAE is used to model long-term neurodegeneration. In the chronic model of EAE, the animals develop paralysis symptoms, peak in disease severity and subsequently show very mild recovery but otherwise continue to maintain approximately the same level of disease severity over time. **(b) EAE acute induction protocol.** EAE acute induction protocol. On Day 0, the mice are injected subcutaneously with an emulsion containing Complete Freund's Adjuvant (CFA) supplemented with additional Mycobacterium tuberculosis (MTB) and mixed with myelin oligodendrocyte glycoprotein (MOG) 35-55. This concoction induces an autoimmune response against myelin and leads to destruction of neurons. In addition, the mice are also injected peritoneally with Pertussis toxin which permeates the blood brain barrier and allows inflammatory Immune cells to traffic across the blood brain barrier to access the central nervous system. The mice are given a booster injection of Pertussis toxin on Day 2 to keep the blood brain barrier permeable. For acute EAE, this is sufficient to induce paralysis symptoms that typically begin around Day 7 and peak in severity around Day 14. For chronic EAE, a second dose of MOG₃₅₋₅₅, CFA, and MTB is required to induce long-term EAE symptoms. With chronic EAE, initial symptoms typically begin around Day 10 and peak in severity around Day 17.

Possible mechanisms of action:

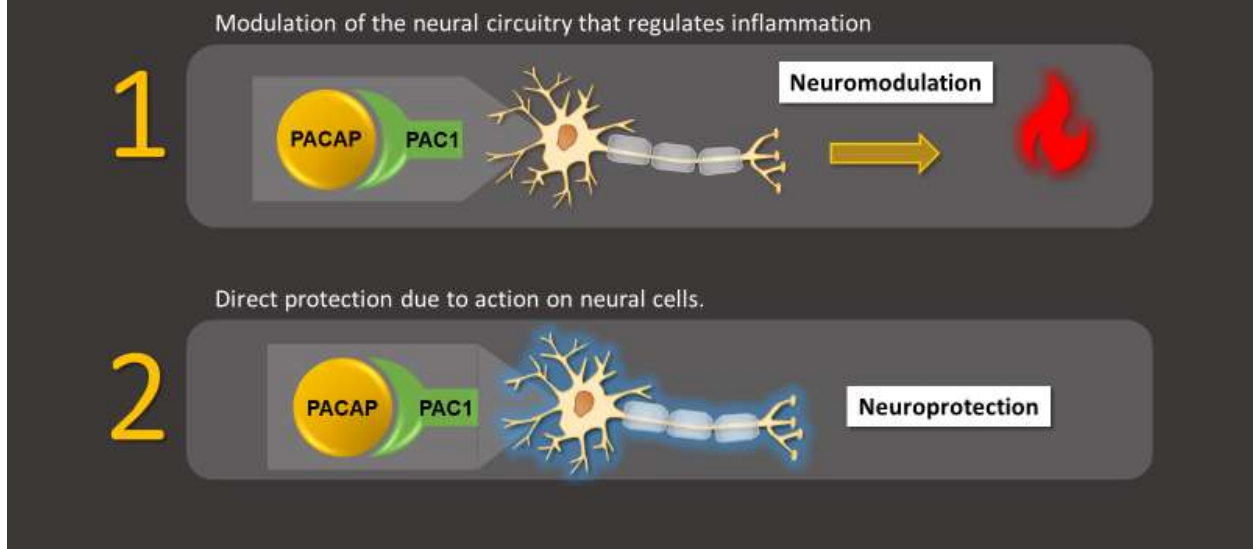


Figure 1-3. Hypothesized mechanisms of PACAP. PACAP may be 1) binding to PAC1 receptors on neurons with immunomodulatory properties, or 2) binding to PAC1 receptors on neural cells to directly protect them from insult.

Chapter 2 – PACAP/PAC1 Regulation of Inflammation via Catecholaminergic Neurons in a Model of Multiple Sclerosis

Christina Van^{1,2}, Michael C. Condro¹, Kenny Lov¹, Ruoyan Zhu¹, Patrick T. Ricaflanca¹, Henly H. Ko¹, Anna L. Diep¹, Anh Q. Hoang¹, Joseph Pisegna³, Hermann Rohrer^{4,5}, James A. Waschek¹

1. Semel Institute for Neuroscience and Human Behavior/Neuropsychiatric Institute, Intellectual and Developmental Disabilities Research Center, University of California, Los Angeles, Los Angeles, CA, USA
2. Molecular Biology Interdepartmental Program at University of California, Los Angeles, Los Angeles, CA, USA
3. Center for Ulcer Research and Education (CURE): Digestive Diseases Research Center at University of California, Los Angeles, Los Angeles, CA, USA
4. Max Planck Institute for Brain Research, Frankfurt, Germany
5. Institute for Clinical Neuroanatomy, Goethe University, Frankfurt, Germany

ABSTRACT

The sympathetic nervous system (SNS) serves to maintain homeostasis of vital organ systems throughout the body, and its dysfunction plays a major role in human disease. The SNS also links the central nervous system to the immune system during different types of stress via innervation of the lymph nodes, spleen, thymus and bone marrow. Previous studies have shown that pituitary adenylate cyclase-activating polypeptide (PACAP, gene name *adcyap1*) exhibits anti-inflammatory properties in the experimental autoimmune encephalomyelitis (EAE) model of multiple sclerosis. Because PACAP is known to regulate SNS function, we hypothesized that part of the immunoprotective action of PACAP is due to its neuromodulatory effects on sympathetic neurons. To examine this, we used an inducible, targeted approach to conditionally disrupt the PACAP-preferring PAC1 receptor gene (*adcyap1r1*) in dopamine β -hydroxylase-expressing cells, which includes postganglionic sympathetic neurons, but also catecholaminergic neurons in the brain and adrenomedullary chromaffin cells. In contrast to our previous EAE studies using PACAP

global knockout mice which developed severe and prolonged EAE, we found that mice with conditional loss of PAC1 receptors in catecholaminergic cells developed a delayed time course of EAE with reduced helper T-cell type 1 (Th1) and Th17 and enhanced Th2 cell polarization. At later time points, similar to mice with global PACAP loss, mice with conditional loss of PAC1 exhibited more severe clinical disease than controls. The latter was associated with a reduction in the abundance of thymic regulatory T cells (T_{regs}). These studies indicate that PAC1 receptor signaling acts in catecholaminergic cells in a time-dependent manner. At early stages of disease development, it enhances the ability of the SNS to polarize the Th response towards a more inflammatory state. Then, after disease is established, it enhances the ability of the SNS to dampen the inflammatory response via T_{regs} . The lack of concordance in results between global PACAP KO mice and mice with the PAC1 deletion targeted to catecholaminergic cells during early EAE may be explained by the fact that PACAP acts to regulate inflammation via multiple receptor subtypes and multiple targets, including inflammatory cells.

INTRODUCTION

Multiple sclerosis (MS) affects about 2.5 million people worldwide and is a leading cause of disability in young adults. In this disease, auto-reactive immune cells target oligodendrocytes and neurons in the central nervous system (CNS). Chronic inflammation leads to neurodegeneration and causes symptoms including vision loss, paralysis, and cognitive decline, which can severely interfere with quality of life. Most commonly prescribed drugs target inflammation, and thereby reduce flare-ups and slow progression of the disease, but do not lead to repair or restoration of neuronal function. Additionally, these drugs can cause mild side effects such as aches, fever, fatigue, diarrhea, hair loss, and nausea, as well as more severe effects such as

liver damage, infertility, birth defects, depression, and a suppressed immune system. Thus, there is a need to investigate alternative treatment options to modulate inflammation in MS.

Most available FDA treatments target inflammation in the periphery. A more effective strategy would be to simultaneously treat the central nervous system as well as the periphery ¹⁰⁸. The sympathetic nervous system (SNS) is the arm of the autonomic nervous system that is commonly known as the regulator of fight or flight responses to stress. The SNS links the central nervous system and the immune system, regulates the immune response when injury or inflammation is detected by the CNS ^{109–111}, and has tremendous importance in human disease. The SNS regulates processes which underlie cardiovascular and metabolic disorders, obesity, psychiatric disorders associated with stress, autoimmune and other inflammatory diseases. It is well known that there are positive correlations between stress and development of autoimmune diseases including MS, rheumatoid arthritis, Lupus, and Sjögren's Syndrome ^{112–120}. Drugs that modify sympathetic function currently include those that target catecholamine synthesis, metabolism, uptake, or receptor activity. Strategies to modify symptoms of MS and progression of disease by regulating sympathetic activity have undergone testing in preclinical models ¹²¹.

It is well documented that peripheral lymphoid organs, including the spleen, lymph nodes, thymus, and probably bone marrow, receive abundant innervation from sympathetic ganglia, with nerve terminals projecting to immune and stromal cells. Through these connections, the SNS regulates peripheral inflammatory responses such as T cell polarization and regulator T-cell (T_{reg}) proliferation ^{122,123}. The role of this innervation has been examined primarily by peripheral administration of 6-hydroxydopamine (6-OHDA), which does not appreciably penetrate the blood-brain barrier, and thus selectively ablates sympathetic neurons in the periphery ¹²⁴. Most of these studies, as well as studies in which immune cells were treated with norepinephrine (NE) receptor

analogs *in vitro*, suggested that NE acts primarily via β -2 adrenergic receptors (β -2AR), and mainly inhibits innate inflammatory responses, and either promotes or inhibits adaptive immunity^{109,125}. The advent of gene targeting has provided a new approach to examine the role of the SNS on various functions at a molecular level. Unfortunately, limited illuminating data are available so far which address how the SNS regulates inflammation using this approach. For example, a comprehensive analysis of the immune phenotype of β -2AR-deficient mice reported essentially normal immune responses¹²⁵. On the other hand, dopamine β -hydroxylase deficient mice were found to exhibit diminished Th1-responses to pathogen challenge¹²⁶, providing evidence that SNS actions on adaptive immune cells might support inflammation. Overall, the studies using sympathectomy, and genetically-engineered mice have generally not examined the immunomodulatory of other signaling molecules, such as pituitary adenylyl cyclase activating peptide (PACAP), vasoactive intestinal peptide (VIP), galanin, and neuropeptide Y, that are released by sympathetic neurons or their presynaptic innervation in naïve or stressed rodents^{101,127}. Thus, one potential approach to modify inflammation is through modulation of sympathetic function.

One of the major immune players in MS and EAE are helper T cells. There are several categories of CD4⁺ T cells, including Th1, Th2, Th17, and T_{reg} cells with distinct features and functions¹²⁸. Although some groups have found that both helper T cells and cytotoxic T cells contribute to the development of EAE^{129,130}, the majority of research has focused on the role of helper T cells. There are particular helper T cell subsets and cytokines associated with autoimmunity^{131–133}. In MS patients, Th1 and Th17 are associated with disease onset, progression, and relapse while Th2 is associated with remission. Gain of function and loss of function experiments in animal models support this^{134–138}. Helper T cells can be generally categorized as

having a more Th1/Th17 or Th2 phenotype characterized by their cytokine expression profiles. Th1 T cells secrete IFN- γ , IL-2, and TNF- α while Th2 T cells secrete IL-4, IL-5, and IL-10. Skewing towards one dominant phenotype seems to antagonize secretion of cytokines of the other phenotype¹³⁹. Adoptive transfer of MOG-specific Th1 or Th17 T cells into Rag2 KO mice which do not develop T cells led to development of EAE in mice, while adoptive transfer of Th2 T cells did not induce EAE^{137,140}. Therefore, Th1 and Th17 T cells facilitate EAE disease while Th2 T cells do not. Although both Th1 and Th17 share many features, the actions of Th1 and Th17 differ in function¹⁴⁰. Some MS population studies have found an inverse relationship between having Th2-driven health problems—such as allergies or asthma—and risk of MS^{141,142}. Th2 T cells may help reduce Th1 activity by the secretion of IL-10¹⁴³. Exploiting mechanisms to skew the pro-inflammatory Th1 or Th17 responses towards an anti-inflammatory Th2 response may reduce pathological inflammation.

Another key T cell type relevant to MS and EAE are regulatory T cells (T_{regs}). T_{regs} are activated following inflammation in response to disease or injury. They act to suppress the inflammatory response to prevent an overreactive inflammatory response. In addition, they play a key role in maintaining self-tolerance and have been found to be crucial for protecting against autoimmunity^{144–151}. Therefore, promoting the expansion and regulatory activity of T_{regs} can also be a method to combat inflammation in EAE and MS.

Our laboratory has been investigating immunomodulatory actions of PACAP, VIP, and their receptors in the EAE model using mice globally deficient in these proteins^{92,94,95,152,153}. PACAP was originally isolated and shown to induce adenylyl cyclase to produce cyclic AMP in rat pituitary cell cultures¹⁵⁴. Its receptors include VPAC1, VPAC2, and PAC1. While VPAC1 and VPAC2 also bind the homologous protein VIP with equal high affinity, the PAC1 receptor binds

PACAP with 100-fold greater affinity than it binds VIP. PACAP is highly conserved through evolution, with the human PACAP sequence sharing 90% homolog with cnidarians, the earliest phyla to develop tissue layers. PACAP is upregulated in response to injury and inflammation and has been shown to protect neurons and reduce inflammation in the CNS in animal models of neurodegenerative diseases such as multiple sclerosis, Alzheimer's Disease, Parkinson's Disease, and stroke ^{72,73,75,78,79,155}. Using the EAE model, our lab previously demonstrated that PACAP-deficient mice have more severe clinical disease, greater inflammation, and higher mortality compared to wild type mice ^{92,153}. Moreover, PACAP deficient mice had impaired T_{reg} responses during EAE, along with a skewing of T_{effectors} towards more inflammatory phenotypes (Th1 and Th17), and a reduction of anti-inflammatory Th2 cells. The results imply that PACAP primarily plays an anti-inflammatory role during EAE. However, the relevant anatomical sites of PACAP action cannot be ascertained in these global KO mice studies.

One potential site of PACAP action during EAE is the SNS. PACAP is expressed in neurons in the intermediolateral column of the thoracic spinal cord that provide the presynaptic innervation of sympathetic ganglia ^{101,156}. PACAP in these projections appear to modulate SNS function via action on PAC1 receptors expressed on sympathetic neurons ^{102,103}. We hypothesized that immunoprotective actions of PACAP in EAE are in part mediated through modulation of the SNS (**Figure 2-1a**). More specifically, we hypothesized that mice with conditional elimination of PAC1 receptors from postganglionic sympathetic neurons would mimic PACAP KO mice with respect to EAE, and thus result in more severe clinical disease and increased inflammation.

MATERIALS AND METHODS

Animals

Mice were housed under environmentally controlled conditions in a 12-hour light/dark cycle with access to food and water *ad libitum*. All animal studies were approved by the UCLA institutional animal care and use committee (IACUC) and Animal Research Committee (ARC).

Conditional knockout of PAC1 on catecholaminergic neurons

We used tamoxifen-inducible CreER-Lox recombination to delete PAC1 receptors from dopamine- β -hydroxylase-expressing neurons, including postganglionic SNS neurons (**Figure 2-1b**). The tamoxifen-regulated approach was selected so that we could induce gene deletion in adult mice, thereby avoiding disrupting known effects of PACAP on developing sympathetic neurons^{157,158}. We commissioned the National Institutes of Health Knockout Mouse Project (KOMP) to generate mice with loxP sites flanking the PAC1 gene. Such mice (PAC1^{flx/flx} mice), appeared healthy and showed no obvious behavioral abnormalities. PAC1^{flx/flx} mice were bred with mice obtained from Dr. Hermann Rohrer (Max Planck Institute for Brain Research, Frankfurt, Germany) which express Cre fused to the ligand binding domain of the estrogen receptor (ER) driven by the dopamine β -hydroxylase promoter¹⁵⁹, resulting in PAC1^{flx/flx} D β H-CreER double transgenic mice (**Figure 2-1b**). For all experiments, PAC1^{flx/flx} D β H-CreER mice were bred with PAC1^{flx/flx} mice, so that litters would include both PAC1^{flx/flx} D β H-CreER and PAC1^{flx/flx} control mice. Tamoxifen treatment of PAC1^{flx/flx} D β H-CreER mice results in translocation of Cre recombinase into the nucleus where it targets loxP sites and mediates excision of the PAC1 gene in catecholaminergic neurons. From here onwards, the tamoxifen-treated PAC1^{flx/flx} D β H-CreER mice will be referred to as PAC1 receptor conditional knockdown (cKD) mice, whereas

PAC1^{flox/flox} littermates, which do not express Cre, will be referred to as control mice. In some cases, PAC1^{flox/flox} DβH-CreER mice were bred to an Ai9 reporter mouse line obtained from Dr. Anton Maximov (Scripps Research Institute, La Jolla, CA, USA) which expresses the red fluorescent reporter TdTomato under a CAG promoter downstream of a loxP flanked STOP cassette. Resulting mice (PAC1^{flox/flox} DβH-CreER Ai9) only express the TdTomato reporter when active Cre targets the loxP sites and excises the STOP cassette.

We used a conditional, rather than a global knockout approach to focus relatively specifically on the effects of PAC1 signaling in the SNS, i.e., to avoid confounding effects from lack of PAC1 on other PAC1 receptor-expressing cell types, which include multiple populations of CNS neurons, astrocytes, and macrophages. Additionally, it is known that C57BL/6 mice deficient in PAC1 receptor exhibit high neonatal mortality^{160,161}. Although PAC1 deficient mice appear normal at birth, within the first two postnatal weeks, pups develop pulmonary hypertension and right ventricle heart failure¹⁶¹. It is not feasible to induce EAE in these mice.

Experimental autoimmune encephalomyelitis (EAE)

To induce the acute form of EAE, mice are subjected to a well-characterized protocol in which MOG₃₅₋₅₅, a fragment of myelin oligodendrocyte glycoprotein, is administered peripherally in adjuvant⁶⁶. 100 μg of MOG₃₅₋₅₅ in phosphate-buffered saline (PBS) is emulsified 1:1 with Difco Complete Freund's Adjuvant (BD, Franklin Lakes, NJ, USA) supplemented with an additional 100 mg of Difco Mycobacterium tuberculosis H37RA (BD, Franklin Lakes, NJ, USA). The emulsion is split and subcutaneously injected in the left and right flanks posterior to the forelimbs. This was specified as day 0 of EAE (**Figure 2-1c**). This results in the expansion of T-cells autoreactive to myelin⁶⁶. Additionally, the mice receive an intraperitoneal injection of 200

ng of pertussis toxin (List Biological Laboratories, Campbell, CA, USA) dissolved in PBS. Pertussis toxin causes permeabilization of the blood brain barrier, thus allowing the T-cells targeting MOG to enter the CNS. After two days, the mice are given an additional 200 ng booster injection of pertussis toxin. Mice reproducibly begin to develop demyelination and paralysis within 7-10 days. Clinical scores of EAE severity were given based on a 5-point scale where 0=asymptomatic, 1=limp tail, 2=partial paralysis or failure to resist inversion, 3=complete paralysis of one hind limb, 4=complete paralysis of both hind limbs, and 5=moribund or death. EAE was monitored for 21 days. In cases where mice reached the moribund state, they were euthanized as dictated by federal and university policy.

Lymph node, spleen, and thymus cell suspension preparation

On days 11 and 12 post-MOG₃₅₋₅₅ immunization lymph nodes (auxiliary, brachial, and inguinal), spleens, and thymi were collected into Complete Medium (2% fetal bovine serum, 10,000 I.U./mL Penicillin, 10,000 µg/mL Streptomycin in Roswell Park Memorial Institute (RPMI) 1640 medium) on ice. The tissues were mechanically dissociated into a single cell suspension using the plunger from a 5 mL syringe to gently grind the tissues through a 40 µm cell strainer basket. The cell suspension was centrifuged at 400 rpm at 4°C for 7 min using a Sorvall RT7 (Thermo Scientific, Canoga Park, CA, USA) refrigerated centrifuge. The supernatant was aspirated, and the cell pellet was resuspended in 2% fetal bovine serum, 10,000 I.U./mL Penicillin, 10,000 µg/mL Streptomycin in RPMI 1640.

Flow cytometry

Cells were incubated in 2% fetal bovine serum, 10,000 I.U./mL Penicillin, 10,000 µg/mL Streptomycin in RPMI 1640 containing 50 ng/ml phorbol 12-myristate 13-acetate (PMA) (Sigma Aldrich, St. Louis, MO, USA), 1 µg/ml ionomycin (Sigma Aldrich, St. Louis, MO, USA), 1X brefeldin A (BioLegend, San Diego, CA, USA), 1x monesin (BioLegend, San Diego, CA, USA) for 4 hours at 37°C. The cell cultures were centrifuged at 400 rpm at 4°C for 7 min, and then washed with phosphate-buffered saline (PBS). To distinguish live/dead cells, cell were stained with Zombie UV™ dye (BioLegend, San Diego, CA, USA) diluted in 1xPBS, and incubated at room temperature (RT) in the dark for 30 min. The cells were washed with 1% bovine serum albumin (BSA) in 1xPBS to quench the reaction and then centrifuged at 400 rpm at 4°C for 7 min. The supernatant was aspirated, and the cells were washed with 1xPBS. The cells were centrifuged again at 400 rpm at 4°C for 7 min, and the supernatant aspirated. For extracellular staining, the cell pellet was resuspended in 1% BSA 1xPBS containing an extracellular antibody cocktail (anti-CD4 VioBlue, anti-CD8a FITC, Miltenyi Biotec, Bergisch Gladbach, Germany). The cells were incubated at 4°C for 15 min shielded from light. The cells were washed with 1xPBS, then centrifuged at 400 rpm at 4°C for 7 min. The supernatant was aspirated and the cells were fixed with 2% paraformaldehyde (PFA) in 1xPBS at 37°C for 10min. Then, the cells were washed with 0.2% Tween-20 in 1xPBS. Following centrifugation at 400 rpm at 4°C for 7 min, the supernatant was aspirated. For intracellular staining, the cell pellets were resuspended with 0.2% Tween-20 in 1xPBS containing an intracellular antibodies cocktail (anti-IFN γ PE, anti-IL-4 Vio515, anti-IL-17A APC, Miltenyi Biotec, Bergisch Gladbach, Germany). For detection of nuclear proteins FoxP3 and Ki67, the antibodies (anti-FoxP3 PE, anti-Ki67 APC, Miltenyi Biotec, Bergisch Gladbach, Germany) were diluted in FoxP3 Staining Kit buffers (Miltenyi Biotec, Bergisch

Gladbach, Germany). The samples were incubated at 4°C for 15 min shielded from light. The cells were washed twice with 1XPBS and resuspended in 1XPBS for analysis by flow cytometry using a BD LSRII flow cytometer (Becton Dickinson, Franklin Lakes, NJ, USA).

Antigen recall assay

Lymph node and spleen cells are plated at 1×10^6 cells/mL in 2% fetal bovine serum, 10,000 I.U./mL Penicillin, 10,000 µg/mL Streptomycin in RPMI 1640 containing 10 µg/mL myelin oligodendrocyte glycoprotein fragment 35-55 (MOG₃₅₋₅₅) (GL Biochem, Shanghai, China) or ovalbumin (Sigma Aldrich, St. Louis, MO, USA) antigen control and incubated in 5% CO₂ at 37°C. After 48 hours, the culture media was collected, and flash frozen in liquid nitrogen. Cytokine levels in the culture media were analyzed by sandwich enzyme-linked immunosorbent assay (ELISA) using Ready-Set-Go! kits for IFN γ , IL-5, and IL-17 (eBioscience, San Diego, CA, USA).

RNA Extraction

TRIzol (Invitrogen, Carlsbad, CA, USA) was added to dissociated lymph node or spleen cell pellets (see cell suspension preparation) at approximately a ratio of 1 mL TRIzol buffer per 50-100 mg of tissue. The samples were passed through a 21-gauge needle 10x, and the homogenate was incubated at RT for 5 min. 200 µL of RNase-free chloroform was added and the samples were vortexed vigorously for 15 secs. The samples were incubated at RT for 3 min, then centrifuged at 13,000 g for 10 min at 4°C. The aqueous phase was transferred to new 1.5 mL microcentrifuge tube. One volume of isopropanol was added to tube to precipitate the RNA. The tube was incubated at -20°C for 1 hour to facilitate precipitation. Then, the samples were centrifuged at 20,000 g for 15 min at 4°C to pellet the precipitated RNA. The resulting RNA pellet

was washed twice with 70% ethanol before air-drying the pellet at RT for about 20 mins. The RNA pellet was resuspended with nuclease-free water. All centrifugation steps were performed with an Eppendorf 5417R (Eppendorf, Hamburg, Germany) refrigerated centrifuge.

RNA concentration and purity (determined by A260/280nm and A260/230nm ratios) were measured using a Thermo Scientific NanoDrop One Microvolume UV-Vis Spectrophotometer. 250 ng of each sample of RNA was denatured with 2x RNA Loading Dye (Thermo Scientific, Canoga Park, CA, USA) for 70°C at 10 min using a MJ Mini Thermal Cycler (Bio-Rad, Hercules, CA, USA). Denatured RNA samples were run alongside 1 µg of RiboRuler Low Range RNA Ladder (Thermo Scientific, Canoga Park, CA, USA) in a 1.2% agarose gel in Tris-Buffered EDTA buffer pre-cast with 5% GelRed (Biotium, Fremont, CA, USA) at 90V for 20 mins to check for intact 28S and 18S RNA bands. Gels were imaged using a Universal Hood Gel Doc System (Bio-Rad, Hercules, CA, USA).

Real-time qRT-PCR

Complementary DNA (cDNA) was synthesized from 500 ng of purified RNA in a 20 µL reaction using SuperScript IV VILO Master Mix (Invitrogen, Carlsbad, CA, USA). Quantitative polymerase chain reaction (qPCR) was performed using PowerUp SYBR Green Master Mix (Applied Biosystems, Foster City, CA, USA). cDNA was diluted 10x and 7.5 ng of cDNA was used per 20 µL qPCR reaction. The target genes and the primers used are listed in **Table 2-1**. PCR primers were used at a final concentration of 500 nM. Amplifications were performed using the following cycling protocol: UDG activation at 50°C for 2 min, Dual-Lock™ DNA polymerase hot-start at 95°C for 2 min, then 40 cycles of denaturing at 95°C for 15 min and annealing/extending at 60°C for 1 min. Reactions were performed and read using an StepOnePlus

Real-Time PCR System (Applied Biosystems, Foster City, CA, USA). A melt curve was performed at the end of each assay to check for single product amplification. A standard curve made by sequential 10-fold dilution from the most concentrated standard (containing 5 μ L from all cDNA samples and diluted to a total volume of 200 μ L with nuclease-free water) was used to determine amplification efficiency. Glyceraldehyde-3-Phosphate Dehydrogenase (GAPDH) was used as the housekeeping gene for all qPCR assays.

Tissue collection and sectioning for immunofluorescence and RNA in situ hybridization assays

Mice were euthanized by isoflurane overdose. For immunofluorescence assays, superior cervical ganglia were collected and fixed overnight at 4°C. The next day the tissues were cryoprotected in 15% sucrose 0.05% sodium azide in 1xPBS. The following day, the tissues were incubated in 30% sucrose 0.05% sodium azide in 1xPBS until they no longer floated in the solution. Cryoprotected tissues were embedded in Tissue-Tek Optimum Cutting Temperature compound (Sakura Finetek, Torrance, CA, USA) and cryosectioned using a Leica CM1950 (Wetzlar, Germany) cryostat at 10 μ m onto Fisherbrand Super Frost Plus slides (Fisher Scientific, Hampton, NH, USA). Slides were stored at -80°C until use.

For RNA *in situ* hybridization, brain and superior cervical ganglion were harvested and fresh frozen on dry ice. The tissues were cryosectioned using a Leica CM1950 (Wetzlar, Germany) cryostat at 10 μ m onto Fisherbrand Super Frost Plus slides (Fisher Scientific, Hampton, NH, USA). Slides were stored at -80°C until use.

Immunofluorescence assays

For the immunofluorescence detection assay, slides were blocked and permeabilized with 10% normal goat serum 0.5% TritonX-100 1% BSA in 1xPBS for 1 hour at RT. Following a rinse slide with 1xPBS, slides were incubated with an appropriate dilution ((1:1000) Rabbit anti-tyrosine hydroxylase (Abcam, Cambridge, UK)) of primary antibody in 5% goat serum 1% BSA in 1xPBS overnight at 4°C. The next day, slides were washed 3x10min with 1xPBS then incubated in an appropriate dilution of fluorophore-conjugated antibody ((1:500) Goat anti-rabbit IgG (H+L) polyclonal cross-adsorbed secondary Alexa Fluor 488 (Invitrogen, Carlsbad, CA, USA)) in 5% goat serum 1% BSA 1xPBS for 1 hour at RT. The slides are then stained with Hoechst 33342 (20mM at 1:1000) (Pierce, WI, USA) in 1XPBS for 5 min at RT, then washed 3x10 min with 1xPBS. Finally, Prolong Gold Antifade mounting media (Invitrogen, Carlsbad, CA, USA) and glass coverslips were applied and sealed with nail polish.

RNA in situ hybridization

RNA *in situ* hybridization was performed following standard instructions accompanying the Advanced Cell Diagnostics RNAScope Fluorescent Multiplex kit (Biotechne, Minneapolis, MN, USA). Following, RNA *in situ* hybridization, an immunofluorescent assay was performed starting from the blocking step as described above, except the blocking buffer contained no TritonX-100.

Statistical Analysis

R (R Foundation for Statistical Computing, Vienna, Austria) and Microsoft Excel (Redmond, WA, USA) were used for statistical analysis and for generating graphs. Analysis of variance (ANOVA) and Student's t-test were used to determine statistical significance.

Microscopy

Fluorescent microscope images were captured using an Axio Imager 2 (Carl Zeiss, Oberkochen, Germany), and analyzed using ZEN lite (Carl Zeiss, Oberkochen, Germany).

RESULTS

Conditionally knockout of PAC1 receptors

To determine the efficiency of tamoxifen-induced recombination in catecholaminergic neurons, we crossed the PAC1^{flox/flox} DβH-CreER line to the Ai9 reporter line. These Ai9 mice were designed to express the red TdTomato fluorescent reporter in cells following Cre recombination. The DβH-CreER line has previously been shown to induce recombination with greater than 90% recombination efficiency in the locus coeruleus and adrenal medulla, and partial recombination in the SCG¹⁵⁹. Using the tdTomato reporter and a similar tamoxifen-treatment protocol, we detected about 50% recombination in tyrosine hydroxylase (TOH)-positive neurons SCG (**Figure 2-2a**). To determine if the PAC1 receptor gene underwent similar recombination, we combined RNA *in situ* hybridization for PAC1 receptor with immunofluorescence assay of TOH. Results demonstrated a partial loss of PAC1 gene transcripts in the SCG (**Figure 2-2b**) and a nearly complete loss in the locus coeruleus (**Figure 2-2c**)¹⁵⁹. The estimated percentage of TOH-expressing SCG neurons in which PAC1 receptor gene transcripts were eliminated was 30%,

which is comparable to that observed with a lacZ reporter ¹⁵⁹, but less than that observed when DβH-CreER mice were crossed with mice containing conditional alleles of choline acetyl transferase (ChAT) ¹⁶² and GATA3 ¹⁶³. In these cases, gene expression in SCG remained at about 20% of control levels after targeted deletion. Nonetheless, strong phenotypic alterations were reported in those mice, corroborating that incomplete elimination of a targeted gene can be sufficient to significantly impair gene function.

Conditional knockdown (cKD) of PAC1 led to early inhibition, then enhanced, severity of EAE clinical scores

As tamoxifen is known to affect the clinical severity of EAE, tamoxifen-treated PAC1^{flx/flx} mice were used as controls rather than vehicle-treated PAC1^{flx/flx} DβH-CreER mice. Tamoxifen was thus administered to PAC1 cKD and PAC1^{flx/flx} control mice at two months of age. After a four-week tamoxifen washout, acute EAE was induced with MOG₃₅₋₅₅ as described in our prior studies ⁹⁵. Conditional deficiency of PAC1 receptors resulted in a statistically significant inhibition of EAE during both the induction and peak periods of EAE (**Figure 2-3**). Thereafter, beginning on day 17, disease progression curves crossed, with clinical disease being more severe in PAC1 cKD mice compared to controls. PAC1 receptor signaling cells thus appears to facilitate disease in the early inductive phase of EAE and to promote recovery once disease is fully established.

Analysis of cytokine expression in lymph nodes and spleen

Because the SNS provides major innervation of lymphoid organs and regulates Th differentiation, we determined the effect of sympathetic PAC1 receptor diminution on helper T-

cells (Th) subtype abundance in the spleen and lymph nodes. Th cells are characterized based on the cytokines they produce. The most common phenotypes are Th1, Th2, and Th17. In autoimmune diseases, it is thought that Th1 and Th17 helper T-cells are generally pathogenic while Th2 cells are protective¹⁶⁴⁻¹⁶⁶. Previous research has shown that PACAP modulates Th phenotype in a way that protects against EAE. PACAP promotes the recruitment, expansion, and survival of antigen specific Th2 T-cells by modulating chemotactic molecules released by dendritic cells¹⁶⁷. Moreover, we previously showed that PACAP deficient mice exhibited a skewing of CD4⁺ Th phenotypes away from a Th2 phenotype towards the more pro-inflammatory Th1 and Th17 phenotypes^{92,153}.

To determine if PACAP regulated Th polarity through PAC1 receptors on postganglionic SNS neurons that target lymphoid tissues, we characterized by flow cytometry CD4⁺ Th phenotypes (Th1, Th2, and Th17) in spleen and lymph nodes of tamoxifen-treated mice 11-12 days after EAE induction, prior to peak EAE. In PACAP cKD mice, in contrast to that observed in global PACAP KO mice, we detected a significant reduction in the relative abundance of Th17 cells in the spleen and a significant increase in Th2 cells (**Figure 2-4a upper panels**). This indicates a shift to a less inflammatory state. No change was observed in the abundance of Th1 cells. Analyses of gene expression similarly showed a shift to less inflammatory state, in this case showing a reduction in T-bet and ROR γ t, transcription factors that are relatively specific for Th1 and Th17 cells, respectively (**Figure 2-4a upper panels**). No significant differences between genotypes were observed in splenic gene expression of IFN γ (a Th1 cytokine), IL-4 (a Th2 cytokine), GATA-3 (a Th2 transcription factor), or IL-17 (a Th17 cytokine). In the lymph nodes, no significant differences between genotypes were observed in the flow cytometric (**Figure 2-4b**) or by gene expression assays (data not shown).

To obtain antigen-specific information on Th differentiation, we performed *ex vivo* antigen recall assays on spleen and lymph node single cell suspensions cultured in the presence of purified MOG₃₅₋₅₅ or control stimulus ovalbumin. We observed robust MOG₃₅₋₅₅-induced inductions of IFN γ production in lymph node and spleen cultures of cKD and control mice (**Figure 2-5**). In cultures from cKD mice, mean IFN γ levels were decreased compared to controls, but only in the case of lymph nodes was the reduction significant. We also observed robust MOG-induced inductions of IL-17 production in spleen and lymph node cultures of cKD and control mice, but no differences were observed between genotypes (data not shown). IL-4 in spleen and lymph node cultures was undetectable by ELISA. Overall, the data obtained by FACS, qPCR, and antigen recall assay indicate that loss of sympathetic PAC1 receptor signaling results in a shift in the immune response to a less inflammatory state, with lower Th1 and Th17, and higher Th2 activities.

PAC1 loss in the catecholaminergic cells led to a defect in T_{reg} production during EAE

We previously found that PACAP deficient mice exhibited a deficit in thymic T_{reg} proliferation^{92,153}. We hypothesized that the effects of PACAP in Th proliferation observed in those studies were in part mediated by PACAP/PAC1 receptor modulation of the SNS. We thus analyzed T_{reg} abundance in the thymus, the site where T_{regs} are produced *de novo*. Thymi from PAC1^{flox/flox} DBH CreER mice induced with EAE and were indeed found to have a reduction in T_{regs} during EAE (**Figure 2-6**).

Other genes potentially affected in the inflammatory response

To address potential downstream targets of PACAP/PAC1 in the control of the inflammatory response, several candidate genes were analyzed. IL-6, IL-10, and IL-33. IL-6 plays

a key role in inhibiting production of T_{regs} during EAE ¹⁶⁸, IL-6 deficient mice are resistant to developing EAE ^{169,170}, and administering neutralizing antibodies to IL-6 reduces EAE disease severity ¹⁷¹. We thus hypothesized that an increase in IL-6 may explain the reduction in T_{regs}. However no significant difference was observed between genotypes (data not shown), T_{regs}. It was previously demonstrated that T_{regs} from IL-10 deficient mice are unable to effectively suppress EAE, indicating that IL-10 is important for T_{reg} function ¹⁷². We found a significant decrease in IL-10 gene expression in the lymph node—but not spleen—of cKD EAE mice as compared to control mice (data not shown)

We also examined expression of NAD-dependent deacetylase sirtuin-1 (SIRT1), a histone deacetylase, which in EAE, is known to protect against oxidative stress and reduce retinal ganglion cell loss ¹⁷³. Additionally, in EAE, SIRT1 overexpression leads to lower peak disease severity, and reduces immune cell infiltration, demyelination, and apoptosis in the spinal cord ¹⁷⁴. SIRT1 was also previously found to deacetylate ROR γ t, thus promoting differentiation of Th17 T-cells ¹⁷⁵, and to deacetylate and destabilize FoxP3, thus inhibiting T_{reg} expansion during EAE ^{176,177}. In our study, SIRT1 significantly decreased (p<0.01) with EAE but does not differ between control and cKO mice in the spleen (data not shown).

Others have shown that mice with T-cells that cannot respond to TGF- β do not develop EAE and thus TGF- β is essential in EAE disease initiation ¹⁷⁸. On the other hand, TGF- β is also known to suppress Th1 and promote Th17 immune response ^{179,180}. We found that levels of TGF- β decreased with EAE in the lymph nodes and spleen but was not significant different between control and cKO animals (data not shown).

DISCUSSION

We sought to determine if the well-known anti-inflammatory actions of PACAP are mediated in part by PAC1 receptor-expressing sympathetic neurons that innervate lymphoid tissue. To accomplish this objective, we used a gene targeting approach to interfere with this pathway by conditionally inducing PAC1 receptor gene deletion in postganglionic sympathetic neurons. This approach resulted in a partial deletion of PAC1 in postganglionic sympathetic neurons. The results reported here support a model in which PACAP/PAC1 receptor signaling in sympathetic neurons serves to promote the ability of the SNS to build an inflammatory response early in the phase of EAE, and then facilitate recovery by shifting the immune response to a less inflammatory, pro-repair state. The inflammatory response in the different time points of EAE do differ. For example, gene expression data suggests that a FoxP3/IL-17 imbalance occurs early in EAE, while an IFN- γ /IL-4 imbalance may contribute to the peak injury¹⁸¹. Clinically, PAC1 receptor cKD mice showed less disease severity in the early inductive phase of EAE. This was associated with decreased Th1 and Th17, and increased Th2 responses in cKD mice. Later, as disease progressed, clinical severity scores of cKD mice surpassed those of control mice. Our analyses suggest that this reversal was due to impaired T_{reg} production in PAC1 cKO mice. T_{regs} are known to increase in abundance during EAE and promote recovery¹⁸², but they do not prevent the onset of disease¹⁸³.

A time-dependent action of the SNS to promote the induction of inflammatory disease and then restrict inflammation has to our knowledge not yet been demonstrated in an acute monophasic EAE model such as employed here. However, this type of regulation is known to occur in other autoimmune disease models. For example, a time-dependent SNS enhancement, then inhibition of disease severity and Th polarization was observed in a murine collagen-induced arthritis model

¹⁸⁴. Moreover, in an acute MOG₃₅₋₅₅ C57BL/6 model such as ours, 6-OHDA-induced peripheral sympathetic innervation ablation prior to MOG₃₅₋₅₅ immunization resulted in significantly diminished and delayed disease ¹⁸⁵, suggesting that sympathetic signaling facilitates inflammatory responses in the course of disease induction. In agreement, diminished Th1-responses to pathogen challenge were observed in dopamine β -hydroxylase (D β H) deficient mice ¹²⁶.

We used a tamoxifen-inducible Cre-Lox system to restrict PAC1 receptor loss to catecholaminergic cells. Such cells are located in various areas of the brain, in sympathetic neurons, and in the adrenal medulla. Thus, sympathetic neurons are not the sole cell type in which PAC1 receptors were eliminated on PAC1 cKD mice. Because of this, we cannot rule out that the phenotype we observed is due to loss of PAC1 receptors in these other sites rather than sympathetic neurons. On the other hand, our analyses of Th cells and T_{regs} were performed on lymphoid tissues that are directly innervated by postganglionic sympathetic neurons. Of course, the possibility exists that the effects on immune cells were mediated indirectly by catecholaminergic cells in the brain or adrenal medulla.

The results obtained in the present study were quite different from that we reported in our previous studies in which EAE was examined in mice globally deficient in PACAP ^{92,153}. For example, the reduction of disease severity we observed at early time points in cKD mice was not observed in PACAP KO mice. Moreover, the Th balance was skewed toward greater inflammation in PACAP KO mice, whereas in PAC1 receptor cKD mice, the balance was tipped towards reduced inflammation. The differing results in PACAP KO vs. PAC1 receptor cKD mice can potentially be explained by the fact that PACAP acts in many different sites and on many cell types, including directly on inflammatory cells. PACAP is also known to regulate the hypothalamic-pituitary-adrenal axis via induction of corticotropin releasing factor gene expression in the hypothalamus.

In addition, PACAP also acts on two other known PACAP receptors, VPAC1 and VPAC2, which are also expressed on many cell types including most types of immune cells. Use of mice in which a specific PACAP receptor (PAC1) is eliminated in a specific cell type (catecholaminergic), represents a step towards dissecting the complex actions of PACAP in autoimmune and other diseases modified by sympathetic function. The delineation of the mechanisms by which PACAP regulates sympathetic function could have therapeutic implications in other diseases impacted by the SNS, including diabetes and other metabolic diseases, obesity, and cardiovascular disorders.

ACKNOWLEDGEMENTS

We would like to thank Dr. Joseph Pisegna (University of California, Los Angeles, Los Angeles, CA, USA) for helping to generate the PAC1 floxed mouse line, Dr. Hermann Rohrer (Max Planck Institute for Brain Research, Frankfurt, Germany) for the D β H-CreER mouse line, and Dr. Anton Maximov (Scripps Research Institute, La Jolla, CA, USA) for the Ai9 reporter mouse line.

This project received support from the National Multiple Sclerosis Society (RG 1501-02646), the Cousins Center for Psychoneuroimmunology, UCLA Semel Institute, and the NIH/NCATS UCLA CTSI Grant Number UL1TR000124). The latter award helped fund the generation of the PAC1^{flox/flox} D β H-CreER mice.

Microscopy and cryosectioning was performed using instruments made available through the UCLA Intellectual and Developmental Disabilities Research Center (IDDRC) Core. The IDDRC is supported by a grant from the Eunice Kennedy Shriver National Institute of Child Health (5U54HD087101-03) and is an Organized Research Unit supported by the Jane and Terry Semel Institute for Neuroscience and Human Behavior.

Flow cytometry was performed in the UCLA Jonsson Comprehensive Cancer Center (JCCC) and Center for AIDS Research Flow Cytometry Core Facility that is supported by National Institutes of Health awards P30 CA016042 and 5P30 AI028697, and by the JCCC, the UCLA AIDS Institute, the David Geffen School of Medicine at UCLA, the UCLA Chancellor's Office, and the UCLA Vice Chancellor's Office of Research.

TABLES

Gene	Forward primer	Reverse primer
FoxP3	CACACCTCTTCTTCCTTGAACC	GATCATGGCTGGGTTGTCCA
GAPDH	GGCCTTCCGTGTTCTAC	TGTCATCATACTTGGCAGGTT
GATA3	CAGATAGCATGAAGCTGGAG	CCTTCTGTGCTGGATCGTG
IFN γ	CAATGAACGCTACACACTGC	GCTTTCAATGACTGTGCCG
IL-4	GTCATCCTGCTCTTCTTTCTCG	CTTCTCCTGTGACCTCGTTC
IL-6	ACAACCACGGCCTTCCCTACTT	CACGATTTCCCAGAGAACATGTG
IL-7	CCTCCACTGATCCTTGTTCTGC	GCAGCTTCCTTTGTATCATCAC
IL-10	CAGCCGGGAAGACAATAAC	CATTTCCGATAAGGCTTGGC
IL-17	GTGTCTCTGATGCTGTTGCTG	CATTCTGGAGGAAGTCCTTGG
IL-33	CTACTGCATGAGACTCCGTTC	GTGTCAACAGACGCAGCAAATG
ROR γ t	CAGTGTAATGTGGCCTACTCC	CTTGACAGCATCTCGGGAC
SIRT1	CCTTGGAGACTGCGATGTTA	GTGTTGGTGGCAACTCTGAT
T-bet	GCAGTGTGGAAAGGCAGAAG	CTGGGTCACATTGTTGGAAGC

Table 2-1. List of primers used in qPCR assays.

FIGURES

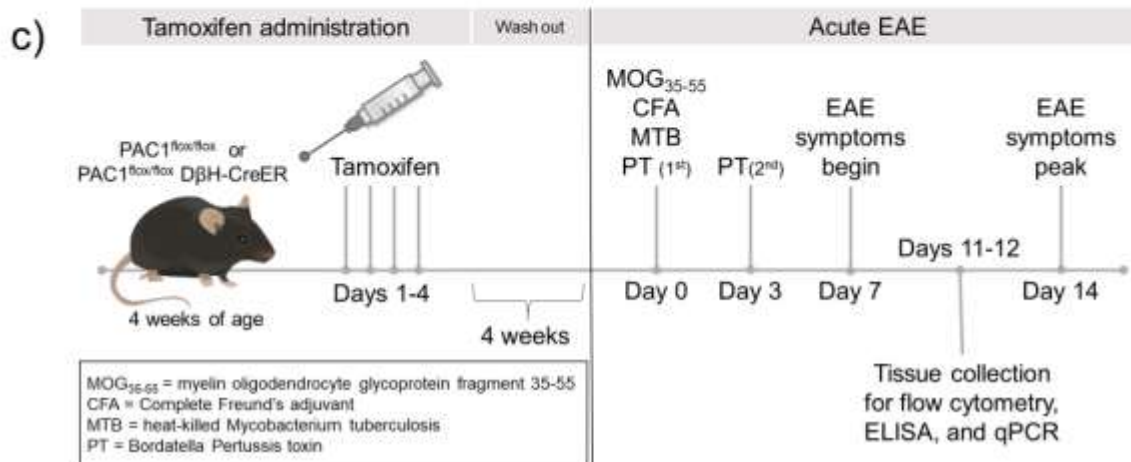
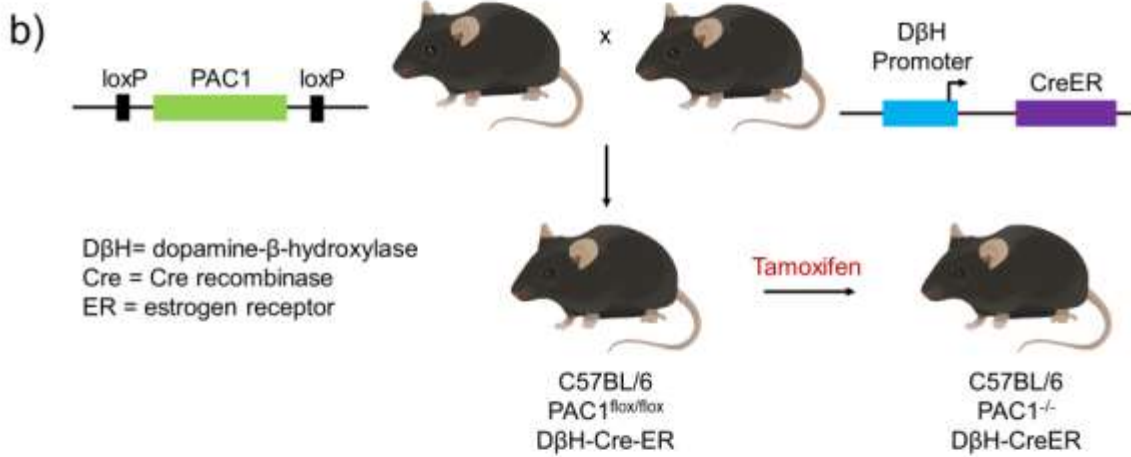
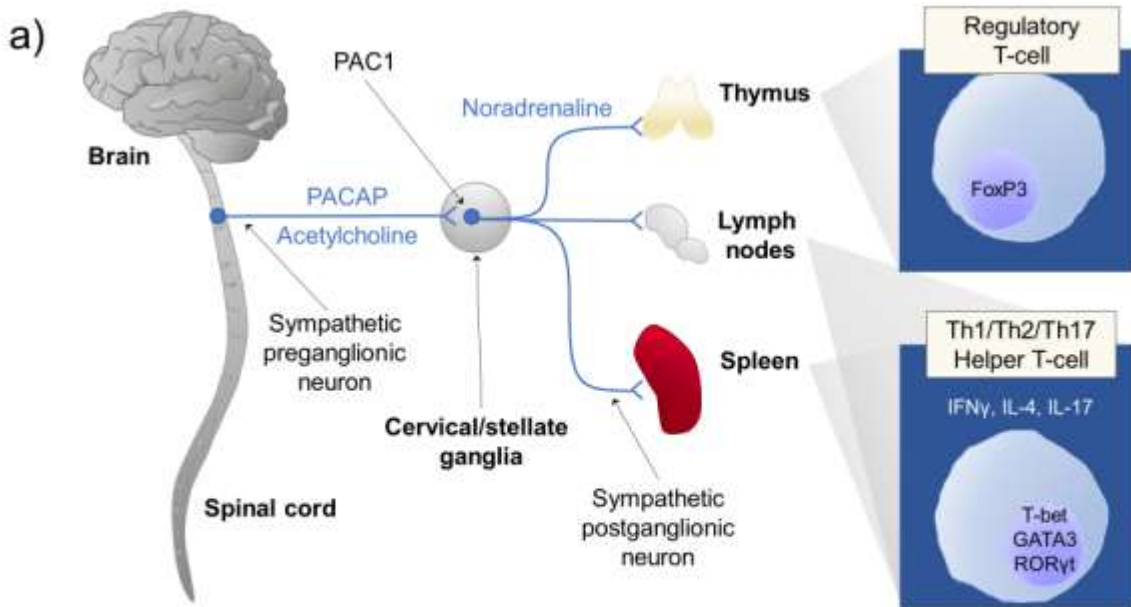


Figure 2-1. Experimental approach

(a) Potential neural circuitry by which PACAP modulates peripheral immune cell activity during inflammatory stress. During inflammatory stress, neurons in the brain stem and hypothalamus activate preganglionic sympathetic neurons in the spinal cord. PACAP is expressed along with acetylcholine in the preganglionic neurons in thoracic spinal cord. When released during stress or inflammation, PACAP acts via PAC1 receptors expressed on sympathetic neurons in cervical/stellate ganglia to alter the immune response in the thymus, lymph nodes, and spleen. **(b)** Approach to conditionally knockout PAC1 receptors in postganglionic neurons in the SNS. C57BL/6 mice were genetically engineered to introduce loxP sites that flank critical sequences in the PAC1 receptor gene. Such mice (PAC1^{lox/lox} mice) are bred to C57BL/6 mice which express Cre enzyme physically linked to the ligand-binding portion of the estrogen receptor driven by the dopamine β -hydroxylase (D β H) promoter (D β H-CreER). Administration of tamoxifen to PAC1^{lox/lox} D β H-CreER mice allows Cre recombinase to translocate into the nucleus specifically in D β H-expressing cells, and subsequently disrupt the endogenous PAC1 receptor gene. **(c)** Experimental timeline to conditionally knockout PAC1 and induce EAE. PAC1^{lox/lox} and PAC1^{lox/lox} D β H Cre-ER mice are administered tamoxifen (Sigma Aldrich, St. Louis, MO, USA) (100 μ L of 20 mg/mL dissolved in peanut oil) by daily oral gavage for four consecutive days at 4 weeks of age, the age at which the pups are weaned. Because tamoxifen is a known estrogen receptor agonist, we allow four weeks for tamoxifen washout to minimize any confounding effects of tamoxifen before proceeding with immunization to MOG₃₅₋₅₅.

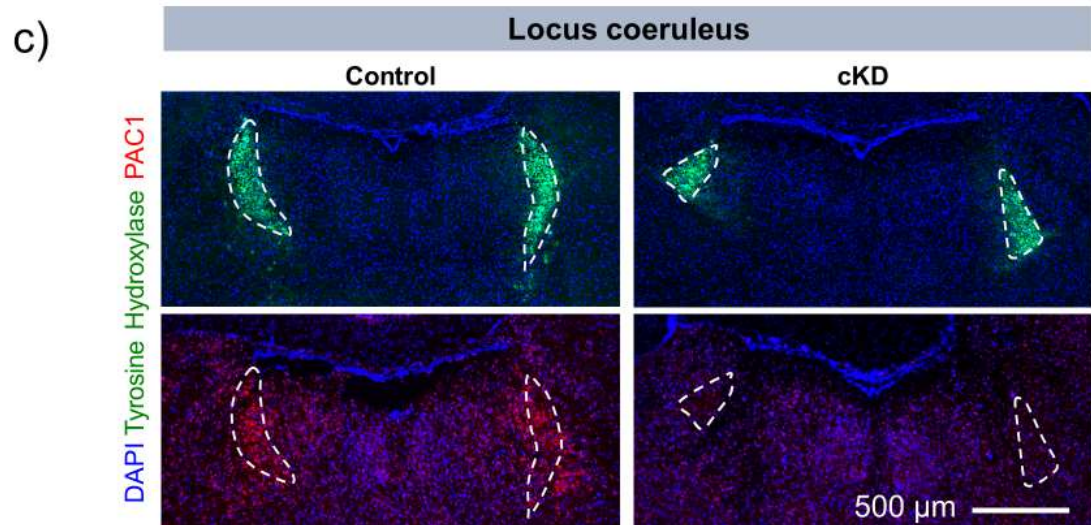
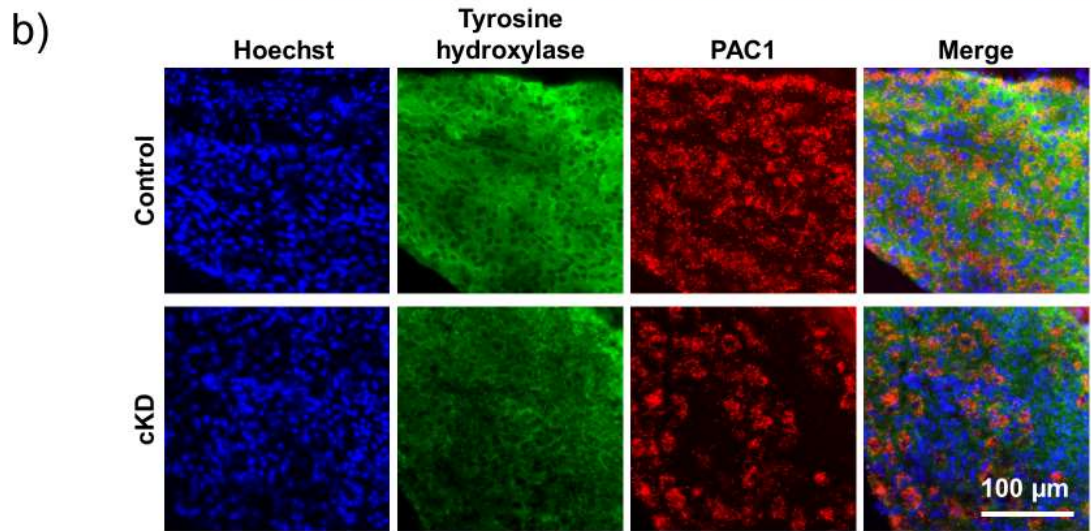
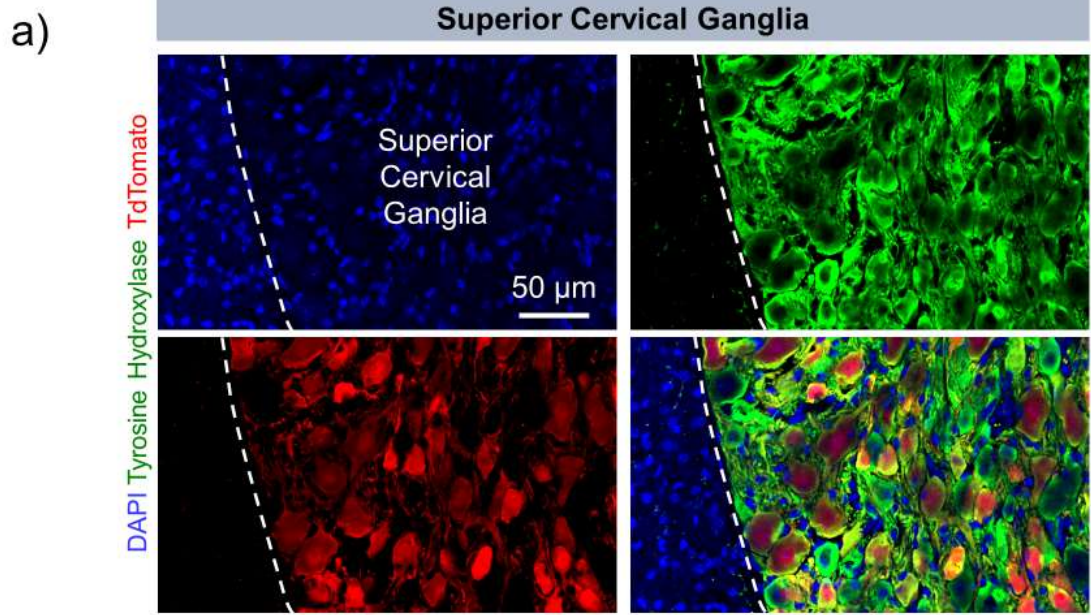


Figure 2-2 PAC1 receptor gene expression is specifically knocked down in catecholaminergic cells.

(a) Use of PAC1^{flox/flox} DβH-CreER Ai9 reporter triple transgenic mouse confirms cell-specific targeting of Cre in the superior cervical ganglion. We generated a triple transgenic mouse which only expresses the red reporter protein, TdTomato, when an upstream floxed stop sequence is excised by tamoxifen-induced Cre. Within the superior cervical ganglion, TdTomato is expressed only in cells which express tyrosine hydroxylase, an enzyme which is highly expressed in DβH⁺ cells. This demonstrates specific targeting of Cre activity. The mice were euthanized, and brains and superior cervical ganglia were collected 4 weeks after the last dose of tamoxifen. (b) Superior cervical ganglion sections and (c) coronal brain sections from control and cKD mice at the level of the locus coeruleus were labeled by RNA in situ hybridization using with a DNA probe against PAC1 mRNA and co-labeled by immunofluorescence assay using antibody against tyrosine hydroxylase to label catecholaminergic neurons

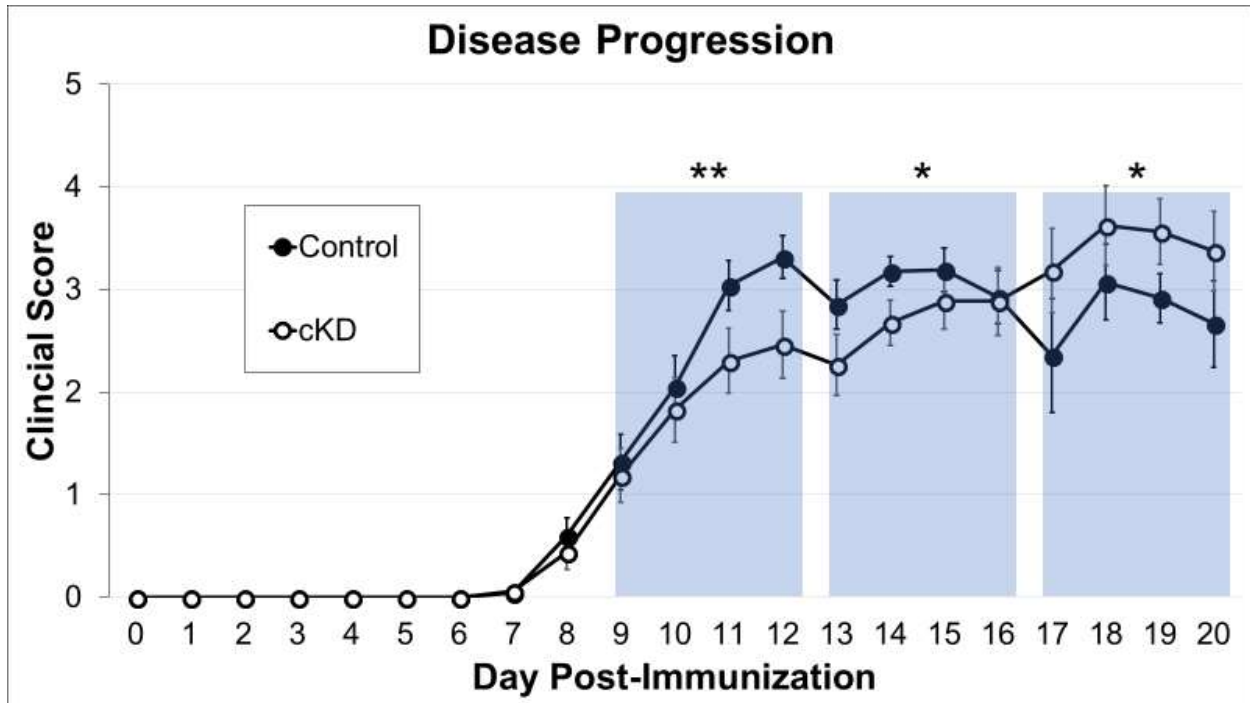
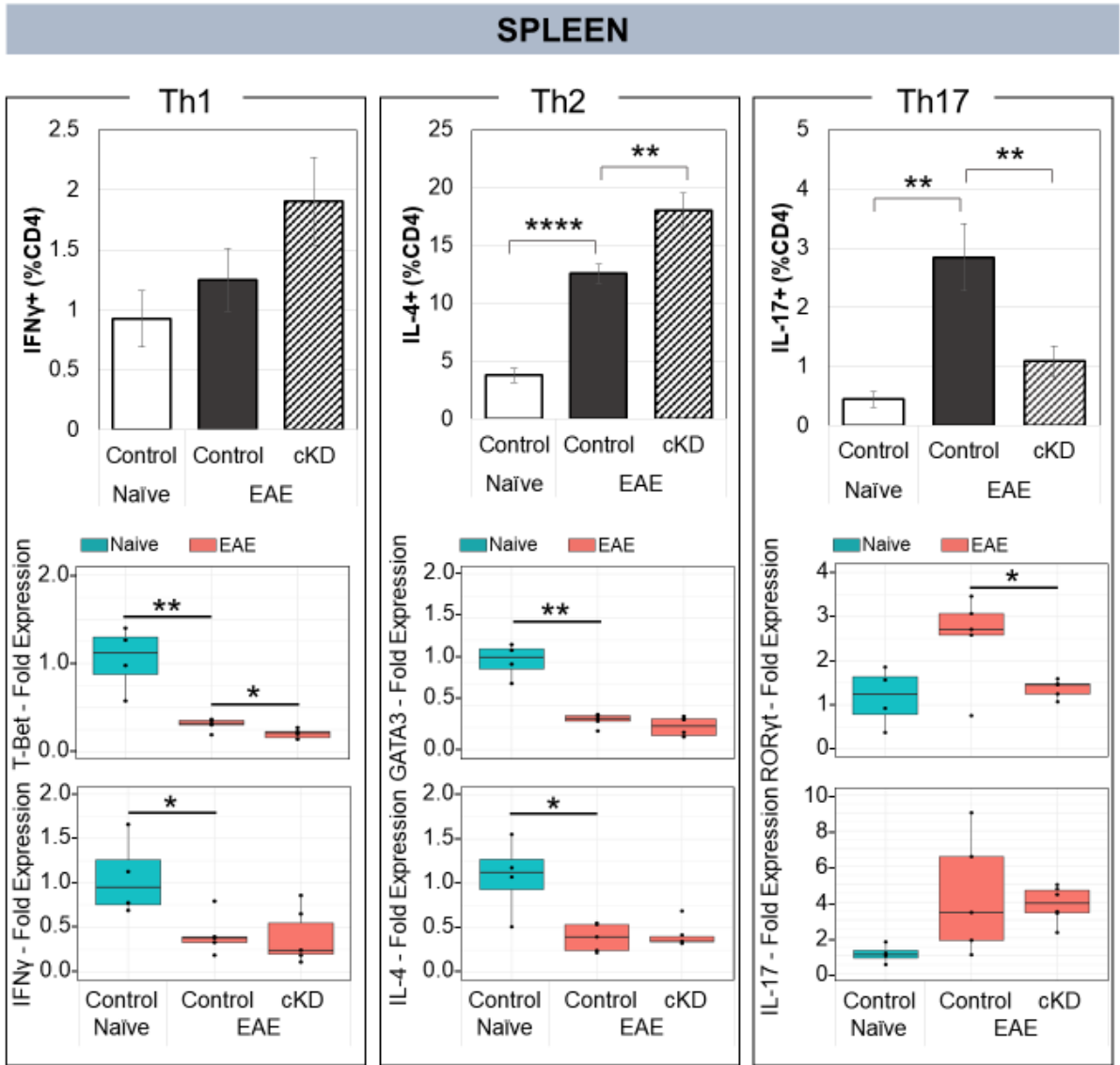


Figure 2-3 Conditional knockdown of PAC1 receptors in catecholaminergic cell led to early inhibition of, then enhanced, EAE severity.

PAC1^{flox/flox} D β H-CreER and PAC1^{flox/flox} control mice were treated with tamoxifen at 4 weeks of age to induce CreER-dependent excision of PAC1 gene. At 8 weeks of age, the mice were immunized against MOG₃₅₋₅₅ to induce acute EAE. Data shown combines data from 4 independent experiments, including a total of 36 WT and 32 cKD mice. EAE was established by day 9 post MOG₃₅₋₅₅-immunization and allowed to progress until day 20, a time point in which clear differences in Th1/Th2/Th17 CD4⁺ phenotype shifts were observed in PACAP deficient mice⁹². The twelve days of EAE disease were divided into three bins aggregating scores from four consecutive days. This binning strategy divides the twelve days of EAE evenly for analysis and avoids combing data from EAE scores before day 16 with scores after day 16, the time point at which the EAE clinical scores curves for the two groups cross. *p<0.05, **<0.01. Statistical significance was determined by 2-tailed t-tests. Standard error bars are shown

a)



b)

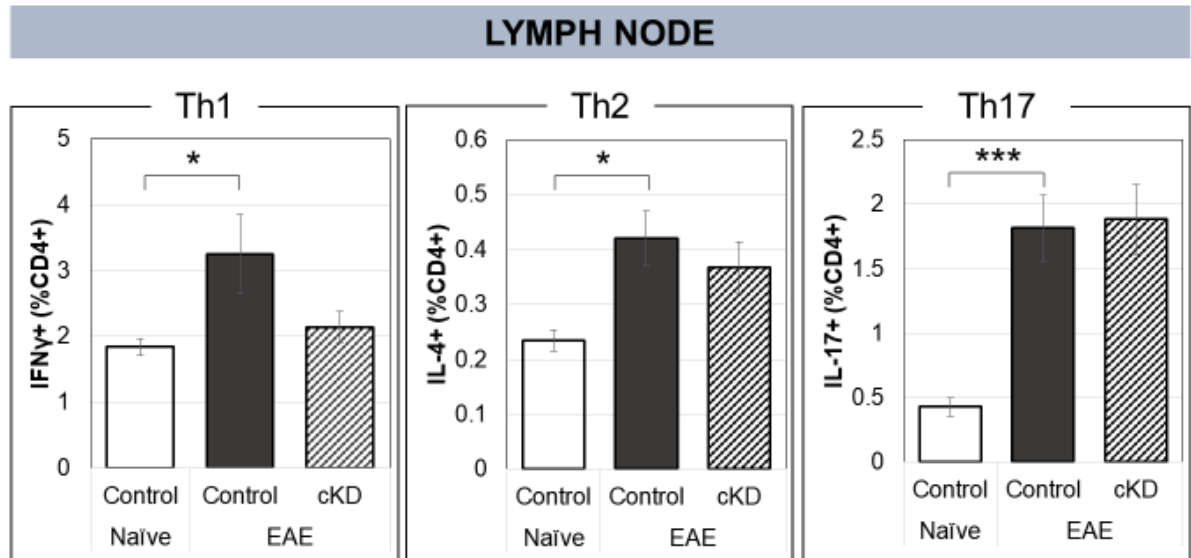


Figure 2-4 Conditional knockdown of PAC1 in sympathetic ganglia alters CD4⁺ helper T-cell polarization during EAE.

Cell suspensions from **(a, top portion)** spleen and **(b)** lymph nodes were stained with antibodies against CD4, IFN γ , IL-4, and IL-17 and analyzed by flow cytometry to characterize the populations of Th1, Th2, and Th17 CD4⁺ helper T-cells. Naïve floxed=5, EAE floxed=14, EAE cKD=9. RNA was extracted from whole lymph nodes (data not shown) and spleen **(a, bottom portion)**, and analyzed by qPCR for signature transcription factors and cytokines associated with Th1, Th2, and Th17 CD4⁺ T-cells. Naïve floxed=4, EAE floxed=5, EAE cKD=6. *p<0.05, **<0.01. Statistical significance was determined by 2-tailed t-tests. Standard error bars are shown

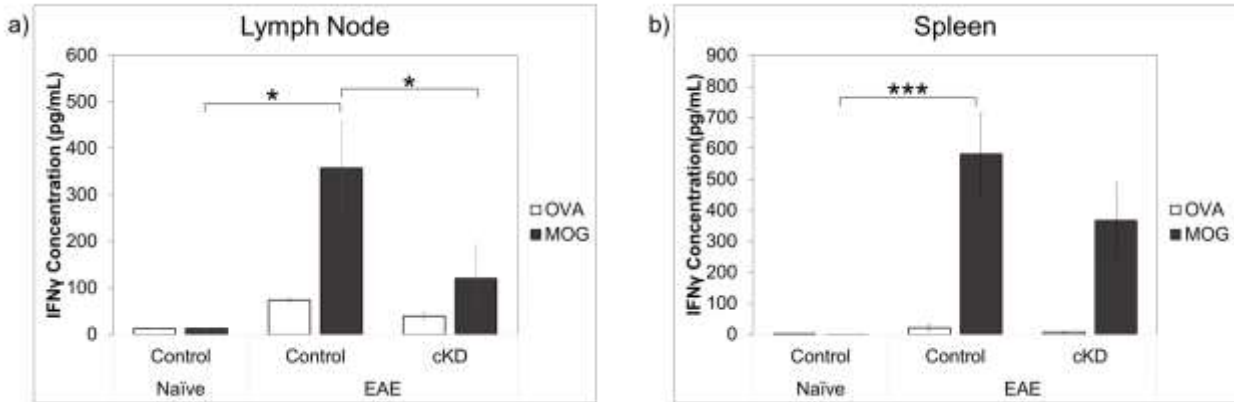


Figure 2-5 Conditional knockdown of PAC1 in catecholaminergic neurons led to decreased production of IFN γ from spleen and lymph node cells cultured with MOG₃₅₋₅₅.

Lymphocytes (**a**) and splenocytes (**b**) were harvested from naïve and EAE animals and cultured in media containing the control antigen ovalbumin control stimulus or specific antigen MOG₃₅₋₅₅ stimulus. Media was collected and analyzed for IFN γ secretion by ELISA. Standard error bars shown. * <0.05 . Statistical significance was determined by 1-tailed t-tests. Standard error bars are shown. Naïve floxed=4, EAE floxed=6, EAE cKD=5

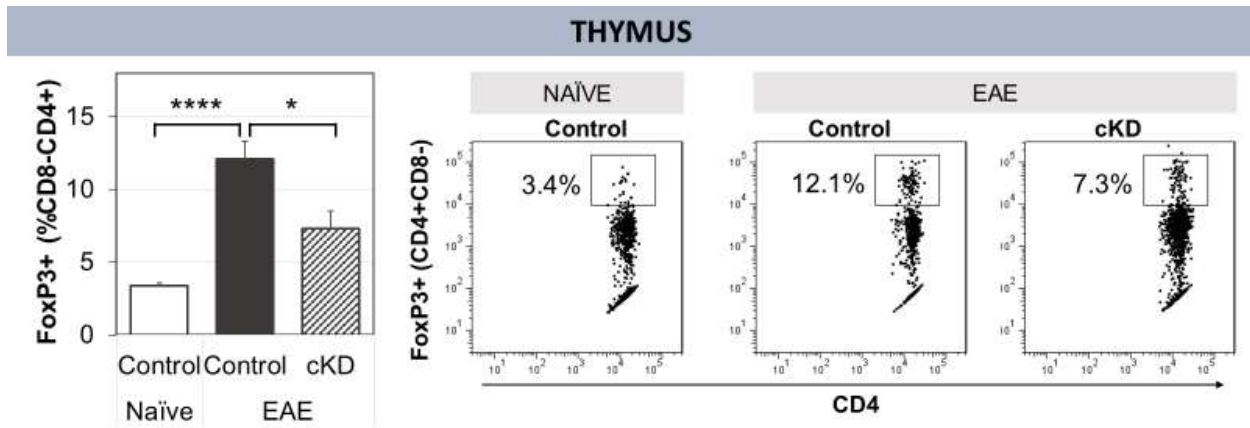


Figure 2-6 Flow cytometry analysis of T_{regs} in thymus.

On day 11 post-EAE induction, thymi were harvested for analysis by flow cytometry. There are fewer T_{regs} in the thymus of tamoxifen-treated PAC1 cKD mice during EAE as compared to floxed mice. Naïve floxed=5, EAE floxed=14, EAE cKD=9. Statistical significance determined by two-tailed T-test. *p<0.05 **p<0.01 ***p<0.001 ****p<0.00001. Standard error bars shown

Chapter 3 – Roles of PACAP/PAC1 signaling on neuroprotection and modulating optic neuritis in a model of multiple sclerosis

ABSTRACT

Diseases involving chronic inflammation in the central nervous system lead to neurodegeneration and neuron loss. Many currently available treatments focus on reducing inflammation but continual low -level inflammation leads to accumulated neuronal damage and worsening disease with time. Many studies in model of inflammatory, neurodegenerative diseases have demonstrated the anti-inflammatory and neuroprotective properties of a protein called pituitary adenylate cyclase-activating polypeptide (PACAP). However, the mechanisms for these properties are not yet clear. In these studies, we use an inducible Cre-Lox approach to conditionally delete PAC1 receptors from cells in the retina in a model of multiple sclerosis and optic neuritis. These studies indicate that loss of PAC1 in the retina leads to the loss of a subset of retinal ganglion neurons in the retina and pathology in the axons in optic nerves from both healthy and diseased mice. Furthermore, PAC1 deletion in the retina also leads to increased immune cell presence, including microglia/macrophages, in the optic nerves of diseased mice. The findings of these studies demonstrate the *in vivo* ability of PACAP action on PAC1 in the CNS to protect neurons and reduce inflammation in an inflammatory, neurodegenerative disease.

INTRODUCTION.

Multiple sclerosis (MS) is an autoimmune, neurodegenerative disease characterized by autoreactive immune cell destruction of myelin, resulting in loss of neurons and their axons in the central nervous system (CNS), which includes the brain, spinal cord, eye, and optic nerve. Most descriptions

of MS focus on the symptoms such as pain and paralysis that occurs in the limbs of these patients. However, the specific pathological state in the optic nerve, optic neuritis (ON), is the presenting clinical symptom in about 20%, and eventually occurs in about 50% of those diagnosed with MS ^{186,187}. Moreover, approximately 30-70% of those of experience optic neuritis will develop MS within 15 years ^{188,189}. ON is characterized by inflammation and demyelination of the optic nerve and often experienced as monocular vision loss, pain, and decreased color detection. In MS patients who experienced optic neuritis, thinning of the retinal fiber layer, which contains glia and as well as axons of retinal ganglion neurons, is correlated with decreased visual acuity, and reduced macular volume predicted worse color vision ^{190,191}. However, most patients recover visual function within approximately a ten year period ¹⁹². In addition to optic nerve damage, retinal ganglion neuron (RGN) loss occurs in some MS patients, and is associated with visual impairment ¹⁹³. Even in absence of clinical optic neuritis, progressive loss of RGNs—the principle neurons that transmit visual signals to the brain—and their axons has been documented in MS patients ^{187,193}.

Patients are typically initially diagnosed with the relapsing-remitting form of MS in which they experience MS attacks punctuated by asymptomatic periods. The most commonly prescribed drugs for MS act primarily to reduce inflammation. Although these drugs are somewhat effective in modifying relapsing-remitting MS, a chronic low level of inflammation persists, and eventually induces neurodegeneration. Chronic inflammation and additive neuron damage over time can lead to the secondary progressive form of the disease in which patients experience more and more severe symptoms without relief. How does the central nervous system protect itself from harmful inflammation, and how can such mechanisms be exploited to halt neurological decline in MS? We focus this study on the roles of pituitary adenylate cyclase-activating polypeptide (PACAP), an endogenous, evolutionarily highly conserved protein which is upregulated in response to injury,

ischemia, and inflammation and has been shown to protect neurons and reduce inflammation in animal models of neurodegenerative diseases such as Alzheimer's, Parkinson's Disease, stroke, and MS^{72-76,78,79,91,92}. These dual properties of neuroprotection and modulation of inflammation make PACAP a strong candidate for treatment of MS and other neurodegenerative diseases. In these studies, we investigate how PACAP/PAC1 interaction in a model of MS and ON, called experimental autoimmune encephalomyelitis (EAE), provides protection to neurons and their axons and modulates inflammation in the retina and optic nerve.

Current treatments of optic neuritis

For the acute treatment of ON, high dose intravenous administration of corticosteroids such as prednisone or methylprednisone are used (reviewed in^{194,195}). Less common treatments for patients with severe, acute ON that is resistant to standard cortical steroid treatments are plasma exchange and intravenous immunoglobulin¹⁹⁶. A large, multi-center study found that treatment with intravenous methylprednisone treatment sped up the visual function recovery time, reduced the risks of additional attacks of optic neuritis and of developing multiple sclerosis, but does not improve long term visual function¹⁹⁷. Long term management of ON for patients with high MS conversion risk, as defined as the presence of lesions, white matter abnormalities (indicating demyelination), shown by magnetic resonance imaging (MRI), may be treated with disease-modifying therapies such as interferon beta. A small observational study found that the 10-year likelihood of a patient presenting with acute ON to develop MS is approximately 22% if they had a normal baseline MRI versus 56% if they had at least one lesion¹⁹⁵. Within 12 months after the incident of ON, about 95% of the patients had shown some recovery of their vision¹⁹⁵.

PACAP and its receptors

PACAP was originally discovered in 1989 as a 38-amino acid hypothalamic peptide that potently induced cyclic adenosine monophosphate levels in pituitary cells⁷⁰. PACAP binds receptors PAC1, VPAC1, and VPAC2. While the latter two also bind a homologous ligand called vasoactive intestinal peptide, PAC1 is highly selective for PACAP. VPAC1 and VPAC2 mediate some of the immunomodulatory actions of PACAP⁸³, whereas PAC1 mediates its growth factor/neuroprotective actions^{76,78,79}. In prior work, we investigated the actions of PACAP and its receptors in EAE using mice deficient in PACAP, PAC1, VPAC1, or VPAC2^{91,92,96,198}. PACAP KO mice exhibited enhanced and more prolonged EAE compared to wild type (WT) mice^{91,92}. Mice deficient in VPAC2 or PAC1 mimicked the more severe EAE observed in PACAP-deficient mice. Intriguingly, whereas the enhanced EAE phenotype of VPAC2 KO mice can be explained by loss of anti-inflammatory VPAC2 on immune cells, PAC1 is expressed in neurons. Thus, we hypothesize that the PACAP acts directly on neurons to protect them and to also modulate inflammation during EAE.

PACAP and receptor expression in the eye

PACAP is expressed in RGNs, amacrine and horizontal cells^{199,200} while the PAC1 receptor is expressed in RGNs and amacrine cells^{201–203}. Both PACAP and PAC1 protein are upregulated following injury in an optic crush model²⁰⁴. Furthermore, protective effects of intravitreal PACAP treatment have been demonstrated in multiple *in vivo* models of retinal degeneration in rats^{200,205}. Studies in PACAP-deficient mice indicate that the absence of one PACAP allele resulted in greater apoptosis and neuron loss after interocular injection of excitotoxin N-methyl-D-aspartate (NMDA)²⁰⁶. PACAP administration reduces neuron apoptosis

in a model of diabetic retinopathy²⁰⁷. We hypothesized that PACAP/PAC1 signaling in the retina provides protection to neurons and their axons during EAE and reduces inflammation in the optic nerve.

Model of optic neuritis

The EAE model of MS also serves as a model for optic neuritis and it recapitulates many aspects of pathology observed in human patients. In EAE, retinal ganglion cell loss occurs with EAE²⁰⁸. Astrocytes, as labeled by glial fibrillary acidic protein (GFAP), are seen to move into the inter-plexiform layer from the retina²⁰⁸. There is also increased GFAP expression in the optic nerve indicating astrogliosis during EAE²⁰⁹. In the EAE model, retinal ganglion neuron loss, demyelination, and increased inflammatory infiltrates have also been observed^{210,211}. Increased expression of Iba1 in the retina and optic nerve during EAE indicates microglia/macrophage presence and activation²⁰⁹.

Approach

To study long term pathology, we use the chronic model of EAE and optic neuritis. To induce EAE, mice were subjected to a well-characterized protocol in which a fragment of myelin oligodendrocyte glycoprotein, MOG₃₅₋₅₅, is administered peripherally in adjuvant. This results in the production of T-cells autoreactive to myelin⁶². We used Cre-Lox recombination in a transgenic mouse line which possesses floxed endogenous PAC1 alleles with viral delivery of Cre as a critical tool to allow us to determine if endogenous PACAP/PAC1 signaling in neurons provides direct neuroprotection as well as indirect neuroprotection by inhibiting inflammation during EAE. We

focused specifically on retinal ganglion neurons because of their high vulnerability in MS and ON, and the well-established methodologies to track their survival and axon integrity.

MATERIALS AND METHODS

Animals

Mice were housed under environmentally controlled conditions in a 12-hour light/dark cycle with access to food and water *ad libitum*. All animal studies were approved by the UCLA institutional animal care and use committee (IACUC) and Animal Research Committee (ARC).

Transgenic mice

We generated C57BL/6 PAC1 floxed ($PAC1^{loxP/loxP}$) mice through the NIH-funded Knockout Mouse Project. These animals have loxP sites flanking either side of both alleles of their endogenous PAC1 gene. Approximately equal numbers of males and females were used for the following experiments.

Conditional knockout of PAC1 in the retina

To conditionally induce PAC1 deletion in the eye, the mice were intraocularly injected at postnatal day 13, the day when the pups first open their eyes. We intravitreally injected $PAC1^{loxP/loxP}$ mice with the experimental virus (AAV2 Cre-GFP) in one eye and the reporter-only virus (AAV2 GFP) to the other eye. As both virus-injected eyes are from the same animal, differences from inter-animal systemic disease severity are mitigated. The mice were subcutaneously injected with carprofen, a nonsteroidal anti-inflammatory drug and analgesic, diluted in pharmaceutical grade saline at 5 mg/kg to manage post-operative pain. Isoflurane was

used as a general anesthetic. To propose the eye for injection, gentle pressure was applied to either side of the eye using the index and middle finger. With assistance of a stereo microscope, a small hole is made in the sclera posterior to the iris using a 30-gauge beveled needle. The adeno-associated viruses (AAVs) (AAV2 CMV-Cre-GFP (5×10^{12} gc/mL) and AAV2 CMV-GFP (5×10^{12} gc/mL) were purchased from the University of Carolina Vector Core (Chapel Hill, NC, USA). 0.1 μ L of 20 mg/mL Fluorescein-5-Isothiocyanate (FITC 'Isomer I') (Invitrogen, Carlsbad, CA, USA) dissolved in DMSO per 20 μ L of virus for visual confirmation of successful virus injection into the eye. A volume of 1.5 μ L of virus was injected into each eye until leakage occurred. The injections were made using a 10 μ L Hamilton 1700 Series Gastight syringe with RN (Removable Needle) termination (Reno, NV, USA) fitted with a blunt 33-gauge needle. An ophthalmic ointment, Vetropolycin, containing Neomycin-Polymyxin B, Bacitracin, and Hydrocortisone (Dechra Pharmaceuticals, Norwich, UK) was applied to the eye to protect the eye and prevent infection.

Experimental autoimmune encephalomyelitis. Experimental autoimmune encephalomyelitis (EAE)

To induce the chronic form of EAE, mice are subjected to a well-characterized protocol in which MOG₃₅₋₅₅, a fragment of myelin oligodendrocyte glycoprotein, is administered peripherally in adjuvant⁶⁶. 200 μ g of MOG₃₅₋₅₅ in a 1:1 emulsion of phosphate-buffered saline (PBS) and Difco Complete Freund's Adjuvant (BD, Franklin Lakes, NJ, USA) supplemented with an additional 100 mg of Difco Mycobacterium tuberculosis H37RA (BD, Franklin Lakes, NJ, USA) is split and subcutaneously injected in the left and right flanks posterior to the forelimbs. This was specified as day 0 of EAE (**Figure 3-1**). This results in the expansion of T-cells autoreactive to myelin⁶². Additionally, the mice receive a peritoneal injection of 300 ng of pertussis toxin (List

Biological Laboratories, Campbell, CA, USA) dissolved in PBS. Pertussis toxin causes permeabilization of the blood brain barrier, thus allowing the T cells targeting MOG to enter the CNS. After two days, the mice are given an additional 300 ng booster injection of pertussis toxin to maintain permeabilization of the blood brain barrier. On the seventh day of EAE, the mice receive a second injection of the emulsion of MOG₃₅₋₅₅, Complete Freund's Adjuvant, and Mycobacterium tuberculosis. This second immunization is crucial for inducing the chronic form of EAE in which the mice maintain EAE symptoms for the full extent of these studies. Mice reproducibly begin to develop demyelination and paralysis within 13-16 days post initial EAE induction. Clinical scores of EAE severity were given based on a 5 point-scale in which 0=asymptomatic, 1=loss of tail tonicity, 2=partial paralysis or failure to resist inversion, 3=complete paralysis of one hind limb, 4=complete paralysis of both hind limbs, and 5=moribund or death. In cases where mice reached the moribund state, they were euthanized as dictated by federal and university policy. For these studies, tissues were collected 60 days post-EAE induction, a time when significant neurodegeneration and retinopathy has been observed ²¹¹. For these studies, approximately half of the littermates were kept naïve and half were induced with EAE. The mice chosen for EAE was based on their identification number where every other number was chosen to be EAE.

Immunofluorescence assays

Flat mount samples: Eyes were enucleated, and retinas and optic nerves were collected using a method previously described ²¹². To harvest the retina from the whole eye, the anterior chamber including the lens was removed, the retinal pigmental layer was peeled away, and four equidistant cuts radiating away from the optic nerve head were made to allow the retinal cup to be

flattened. Whole retinas were flat mounted on nylon membranes (**Figure 3-1**). Optic nerve samples analyzed include the entire length of the optic nerve immediately posterior to the optic nerve head to the optic chiasm. The retinas and optic nerves were fixed in 4% paraformaldehyde in phosphate-buffered saline (PBS) overnight at 4°C. The following day, the retinas and optic nerves were rinsed twice with 1x PBS and stored in 1x PBS until the assay. For the assay, samples were blocked in 10% normal donkey serum 1% bovine serum albumin (BSA) 0.5% TritonX-100 in 1x PBS overnight at 4°C protected from light. The following day, the samples were incubated with primary antibodies in 10% normal donkey serum 1% BSA 0.5% TritonX-100 in 1x PBS overnight at 4°C protected from light. Samples were then washed with 5 x10 min 1x PBS. Then, the samples were incubated with secondary antibodies in 10% normal donkey serum 1% BSA 0.5% TritonX-100 in 1x PBS overnight at 4°C protected from light. To label nuclei, the samples were incubated with 20 mM Hoechst 3341 (Thermo Fisher Scientific, Canoga Park, CA, USA) in 1x PBS at 1:1000 for 5 minutes at room temperature (RT) in the dark. Samples were then washed 5 x 10 min with 1x PBS and mounted on microscope slides with Prolong Gold Mounting Media (Life Technologies, Carlsbad, CA, USA). Images were taken with a Zeiss LSM 800 confocal microscope (Zeiss, Oberkochen, Germany).

Sectioned samples: For cryosectioned retinas and optic nerves, retinas and optic nerves were fixed overnight at in 4% paraformaldehyde in 1x PBS. The next day, retinas and optic nerves were incubated in 15% sucrose in 1x PBS 0.05% sodium azide overnight at 4°C, and the following day in 30% sucrose in 1x PBS 0.05% sodium azide at 4°C until the tissue sank. Samples were then embedded in Optimal Cutting Temperature media (Sakura Finetek, Torrance, CA, USA), cryosectioned with a Leica CM1950 (Wetzlar, Germany) at 10 µm and mounted onto Fisher Finest Superfrost microscope slides (Fisher Scientific, Hampton, NH, USA). Slides were stored at -80°C

until use. For the immunofluorescence assay, tissue sections were rehydrated with 1x PBS at RT for 5 min and rinsed twice with PBS. Sections were then blocked with 10% normal goat serum (or donkey serum, depending on the assay) 1% BSA 0.05% TritonX-100 in 1x PBS for 1 hour at RT. After a rinse with 1x PBS, sections were incubated with primary antibody diluted in 5% serum (donkey or goat (Equitech Bio, Kerville, TX, USA), depending on the assay) 1% BSA in 1x PBS overnight at 4°C. The next day, sections were washed with 3 x 10 min 1x PBS. Then, sections were incubated in secondary antibody solution diluted in 5% goat (or donkey serum, depending on the assay) 1% BSA in 1x PBS at RT for 1 hour in the dark. Hoechst 33342 (20mM at 1:1000) (Pierce, WI, USA) was applied at 1:1000 at RT for 5 min. Following 3 x 10 min washes with 1x PBS, Prolong Gold Mounting media (Invitrogen, Carlsbad, CA, USA) was applied, and a glass coverslip was sealed with nail polish. Images were taken with a Zeiss Imager.M2 Microscope (Zeiss, Oberkochen, Germany).

The following is the list of antibodies used in this study along with the specific dilution used:

Primary Antibodies

- (1:1000) Rabbit anti-Iba1 (Wako Pure Chemical Industries, Osaka, Japan)
- (1:500) Rabbit anti-GFP (Life Technologies, Carlsbad, CA, USA)
- (1:500) Goat anti-GFP (Abcam, Cambridge, UK)
- (1:500) Mouse anti-GFAP (Millipore, Clone GA-5, Burlington, MA, USA)
- (1:500) Rat anti-CD4 Clone RM4-5 (eBioscience, San Diego, CA, USA)
- (1:500) Goat anti-GFP (Abcam, Cambridge, UK)
- (1:1000) Mouse anti-SMI-32 (Covance/BioLegend, San Diego, CA, USA)
- (1:1000) Rabbit anti-NF200 (Abcam, Cambridge, UK)
- (1:500) Rat anti-CD45 PE (eBioscience, San Diego, CA, USA)
- (1:500) Rat anti-CD45 FITC (eBioscience, San Diego, CA, USA)

Secondary Antibodies

- (1:500) Donkey anti-Rabbit Cy3 (Jackson Immunoresearch, West Grove, PA, USA)
- (1:500) Donkey anti-Goat Alexa Fluor 488 (Life Technologies, Carlsbad, CA, USA)
- (1:500) Goat anti-Rabbit Alexa Fluor 488 (Life Technologies, Carlsbad, CA, USA)
- (1:500) Donkey anti-Rat Cy3 (Jackson Immunoresearch, West Grove, PA, USA)
- (1:500) Donkey anti-Mouse Alexa Fluor 647 (Life Technologies, Carlsbad, CA, USA)

(1:500) Donkey anti-Rabbit Alexa Fluor 647 (Life Technologies, Carlsbad, CA, USA)
(1:500) Goat anti-Rat Alexa Fluor 488 (Life Technologies, Carlsbad, CA, USA)

RNA in situ hybridization

RNA *in situ* hybridization was performed following standard instructions accompanying the Advanced Cell Diagnostics RNAScope Fluorescent Multiplex kit (Biotechne, Minneapolis, MN, USA). Following, the hybridization step, an immunofluorescent assay was performed starting from the blocking step as described above for cross sectioned samples, except the blocking buffer contained no TritonX-100.

Microscopy and image processing

Images of fluorescent cross section samples were captured using an Axio Imager 2 (Carl Zeiss, Oberkochen, Germany) while images of fluorescent whole mount samples were captured using a Zeiss LSM 800 confocal microscope (Carl Zeiss, Oberkochen, Germany) with ZEN Blue software (Carl Zeiss, Oberkochen, Germany). A 5x objective was used to capture whole retina images for axonal quantitation. A 10x objective was used to capture whole optic nerve, retina images for neuronal quantitation, and whole brain images. Z-stack, stitched images were imported into ImageJ (National Institutes of Health, Bethesda, MD, USA) using BioFormat Importer (Open Microscopy Environment) and processed into maximum intensity projection images.

Quantification of neuron loss

To quantitate total loss of SMI-32⁺ neuronal axons, flat mount retinas were labeled for RNA-binding protein with multiple splicing (RBPMS) which labels retinal ganglion neurons (RGNs) ²¹³. Four non-overlapping images from each retina were used to calculate measurements for each retina. Each image was captured approximately two-thirds the distance from the optic

nerve head to the edge of the retina. To quantitate subpopulation of neurons which have been shown to be vulnerable in the glaucoma model of disease ²¹⁴, antibodies to SMI-32 were used. Measurements were made in a blinded manner.

Quantification of axonopathy

Retina: To quantitate axon loss, flat mount retinas were labeled for SMI-32 as described above. SMI-32 immunopositive axons were counted using the ImageJ (National Institute of Health, Bethesda, MD, USA) Point Tool 500 μ m from the optic nerve head.

Optic nerve: To visualize the morphology of axons associated with RGNs in which virus-mediated PAC1 deletion occurred, the viral reporter (GFP or mCherry) were used. To visualize the morphology of all axons, the marker for heavy neurofilament, NF200, was used.

For both quantifications, measurements were made in a blinded manner.

Quantitation of inflammation

Antibodies against Glial fibrillary acidic protein (GFAP) were used to label astrocytes, Ionized calcium binding adaptor molecule 1 (Iba1) to label microglia and macrophages, and cluster of differentiation 45 (CD45) to label leukocytes. Cell counting was performed with the ImageJ (NIH, Bethesda, MD, USA) Cell Counter tool. Immunopositive fluorescence intensity was measured using the Histogram tool by an investigator blinded to the sample groups.

Statistical analysis

Microsoft Excel (Redmond, WA, USA) were used for statistical analysis and for generating graphs. Analysis of variance (ANOVA) and Student's t-test were used to determine statistical

significance. Any statistical data point 1.5 times greater than or less than the interquartile range of the data set were considered outliers and excluded from analysis.

RESULTS

Infection of retina with AAV2 GFP

We have shown that intraocular AAV2 GFP administration results in expression of the GFP reporter in several cell layers of the retina, including retinal ganglion neurons as well as their axons in the optic nerve (**Figure 3-2**). The virus does not infect cells in the brain as expression of the viral reporter in the brain is limited to regions directly innervated by neurons in the retina (**Figure 3-3**). Thus, these axons are mostly likely associated with neurons infected in the retina. Approximately 70% of the retinal ganglion neurons (RGNs) are infected by the virus.

PAC1 deletion leads to the loss of a sub-population of retinal ganglion neurons and their axons

We observed statistically significant RGN loss due to EAE but did not detect further RGN loss due to PAC1 deletion (**Figure 3-4**). In neurodegenerative diseases, different cell types have varying degrees of vulnerability and resistance to degeneration and cell death. In a model of glaucoma, alpha neurons are resistant to cell death²¹⁴. These neurons were first described in cat retinas and later in many other mammalian retinas as well^{215,216}. Perhaps the resistance of alpha neurons against insult could be in part to protection due to the presence of PAC1 receptors on these neurons.

To detect these cells, we used the marker SMI-32, which labels unphosphorylated neurofilament H. SMI-32 is highly expressed in alpha retinal ganglion cells, as well as in axons²¹⁷. Indeed, we found that retinas with PAC1 deletion from EAE animals had greater reduction of SMI-32 immunopositive neurons than control retinas from the same animal. This finding suggests

that PAC1 signaling protects against axonopathy in both the eyes of naïve and EAE animals. In addition, in naïve animals, SMI-32⁺ neurons had fewer neurites (**Figure 3-5**) than eyes infected with the control virus, suggesting these neurons are not as healthy. That this observation was statistically significant in the naïve retinas and not in the EAE retinas points to PAC1's role in maintaining neuronal integrity even in the absence of disease. The reduction of neurite number in axons even in naïve eyes is not surprising, as it is known that PACAP promotes neuritogenesis *in vitro*²¹⁸. Moreover, there were fewer SMI-32 immunopositive axons in retinas with PAC1 deletion as compared to control eyes in EAE mice (**Figure 3-6**). It is known that PACAP loss delays axon regeneration in a facial nerve crush model²¹⁹. This protection may be due to direct action on neurons as it is known that PACAP stimulates neurite growth *in vitro* in both cell lines and primary cells^{220–224} in part by regulating mitochondrial activity²²⁵. Those *in vitro* effects were likely through the PAC1 receptor because related protein vasoactive intestinal peptide, which acts only on VPAC1 and VPAC2 receptors, failed to stimulate neurite growth²²¹.

No change in astrocyte or microglia activation in the retina due to targeted PAC1 deletion

There were no changes in GFAP expression with EAE or PAC1 loss (**Figure 3-7**). Total microglia numbers in the retina did not change but there were increased numbers of activated microglia with EAE. However, there were no statistically significant difference in number of total microglia or percentage of activated microglia with PAC1 deletion (**Figure 3-8**).

PAC1 deletion leads to axon pathology in the optic nerve.

In the conditional PAC1 knockout eyes of EAE mice, there is a significant increase in the number of morphological ovoids (**Figure 3-9**), which are indicative of pathological accumulation

of axonal proteins. In naïve mice, there was a trend for an increase in the number of these ovoids. These findings suggest that PACAP/PAC1 signaling is important for maintaining axon integrity even in the absence of disease and is also protective in disease.

PAC1 deletion leads to increased inflammation in the optic nerve

Furthermore, it is known that during EAE, there is increased activation of astrocytes and microglia and infiltration of T-cells and macrophages into the optic nerve and retina ^{208,226,227}. PAC1 deletion lead to a statistically significant increase in immunopositivity for CD45 (pan-immune cell marker) during EAE (**Figure 3-10**). This indicates that PACAP/PAC1 plays a role in regulating immune cell numbers in the optic nerve during EAE. Labeling with antibodies against Iba1, which labels microglia and macrophages, indicated that the majority of these CD45+ cells are microglia or macrophages. Increase in Iba1 immunopositivity increases with EAE but is significantly greater in eyes with PAC1 deletion (**Figure 3-11**).

DISCUSSION

It is well established that PACAP protects neurons against various insults, including in the context of models of neurodegenerative diseases. It was previously not known if this protection is conferred through the PAC1 receptor. In these studies, we use a model of EAE and optic neuritis to investigate the role of PACAP and PAC1 signaling on neuroprotection and its potential indirect effects on inflammation.

The loss of SMI-32 immunopositive neurons and the loss of neurites on remaining neurons, as well as the pathological ovoids which appear in the optic nerves of eyes with PAC1 deletion, in both naïve and EAE mice indicate that PACAP and PAC1 maintain the health of neurons in the

retina in both the context of health and disease. In this model of optic neuritis, inflammation, such as activation of microglia and an influx of inflammatory infiltrates into the optic nerve, are expected, however the loss of PAC1 lead to even increased numbers of immune cell numbers in the optic nerve as well as increased microglia/macrophage activation. The specific mechanisms by which PACAP action on PAC1 receptors on neurons regulates inflammation is not yet known. It is possible that PACAP can act directly on immune cells to regulate the inflammatory response by binding to PAC1 receptors on astrocytes or macrophages ^{228,229}, although these cells were not targeted in this study. Indirect regulation can occur when PACAP binds to PAC1 receptors on neurons which can release factors to communicate with immune cells ²³⁰⁻²³⁵. In addition, PACAP/PAC1 signalling can also indirectly affect inflammation by promoting the survival of neurons ^{78,236-238}, thereby preventing neuron death and reducing the amount of cellular debris that would attract and activate of immune cells in the vicinity. Additional studies are needed to dissect through which mechanisms by which PACAP regulates inflammation in a model of optic neuritis. In these studies, the role of PACAP and PAC1 is specifically investigated in the eye but these findings can provide insight to other regions of the CNS. Studying pathology in the retina and optic nerve is relevant to MS and it also provides a more simplistic organ to study. The neurons of interest are conveniently located in a single layer in the retina and the corresponding axons are neatly bundled in the optic nerve. Although these findings are derived from studies in the eye, the findings are applicable to other regions of the CNS. The results from these studies can inform development of treatments for other inflammatory, neurodegenerative diseases such as Alzheimer's Disease, Parkinson's Disease, and traumatic brain injury.

ACKNOWLEDGMENTS

We thank the National Multiple Sclerosis Society for funding this study (RG3928A2, RG-1501-02646).

Microscopy and cryosectioning was performed using instruments made available through the UCLA Intellectual and Developmental Disabilities Research Center (IDDRC) Core. The IDDRC is supported by a grant from the Eunice Kennedy Shriver National Institute of Child Health (5U54HD087101-03) and is an Organized Research Unit supported by the Jane and Terry Semel Institute for Neuroscience and Human Behavior.

FIGURES

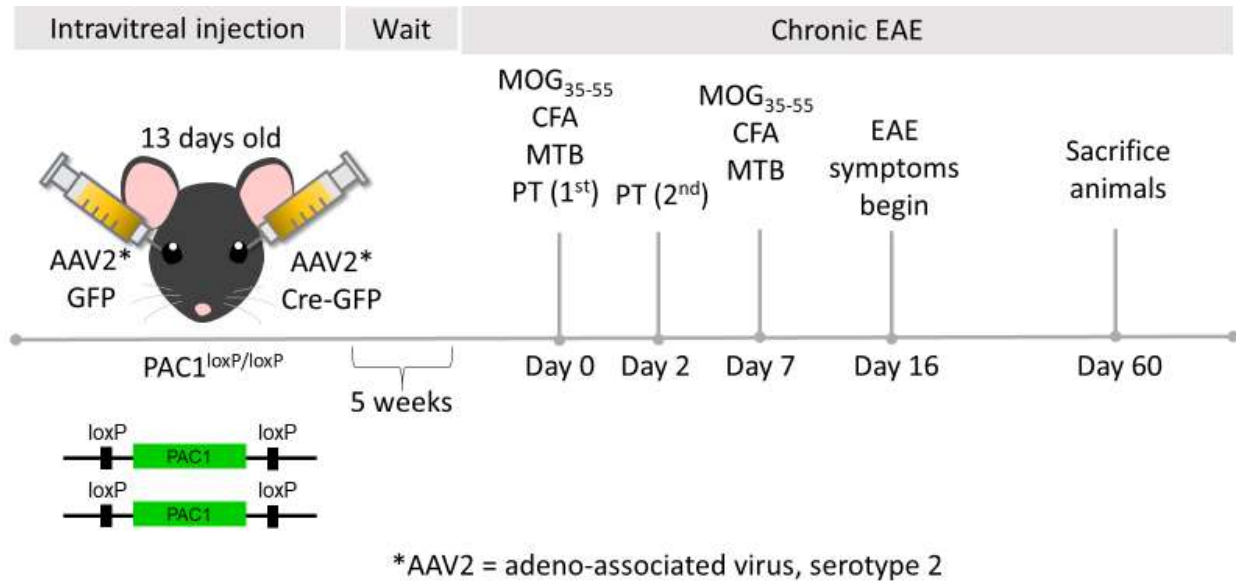


Figure 3-1. Approach for conditional knockout of PAC1 and induction of experimental autoimmune encephalomyelitis. At 13 days old when the animals first open their eyes, PAC1 floxed mice are intraocularly injected in one eye with the AAV2 GFP control virus and in the contralateral eye with the AAV2 Cre GFP virus. This approach allows for comparison of pairs of eyes from the same animal. This is important because from animal to animal, the EAE severity can vary greatly, but comparing eyes from the same mouse should mitigate inter-animal disease severity. After 5 weeks to allow for virus-delivered gene expression and for the animals to reach maturity, chronic EAE is induced. Symptoms begin around day 16 and the animals are sacrificed on day 60 when others have shown that long term neuronal damage has occurred with EAE.

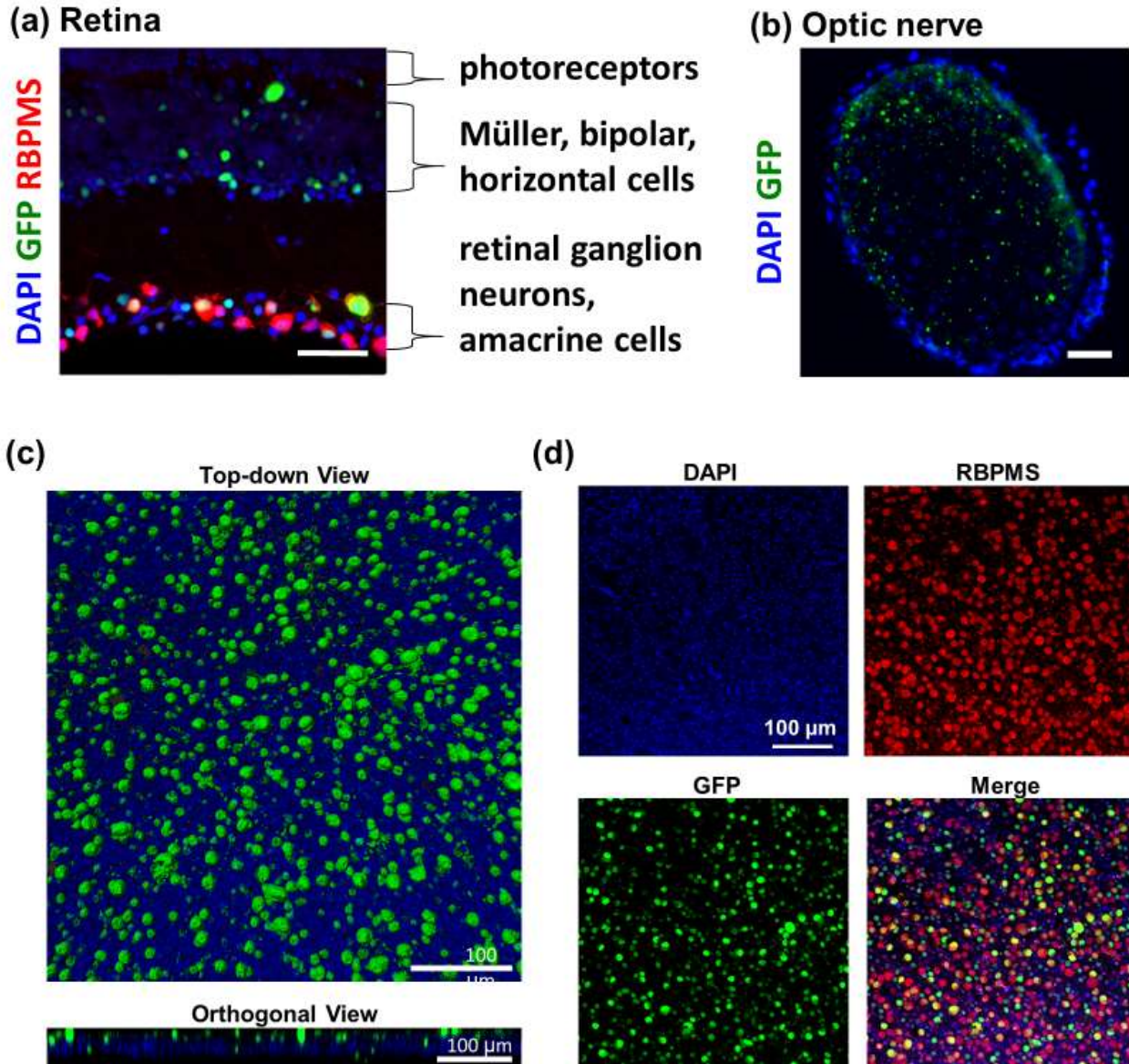


Figure 3-2. AAV2 infects retinal ganglion neurons.

(a) Viral reporter GFP expression can be seen throughout a cross section of a retina, including retinal ganglion neurons labeled with probed RNA-binding protein with multiple splicing (RBPMS). (b) GFP viral reporter expression can also be seen throughout an optic nerve cross section. (c) Viral reporter of AAV2 GFP in retina. The retina was harvested and flat mounted on a nylon membrane. Z-stack images were captured using a 10x objective. 3D blend mode in Imaris was used to visualize the image stack. Orthogonal view was used to visualize a YZ slice through the image stack. Blue = Hoescht, Red = native tDimer fluorescence. (d) Z-stack images of a whole mount retina were captured, and maximum intensity projections were created for each channel. A top-down view shows that the virus infects the RBPMS+ neurons of interest.

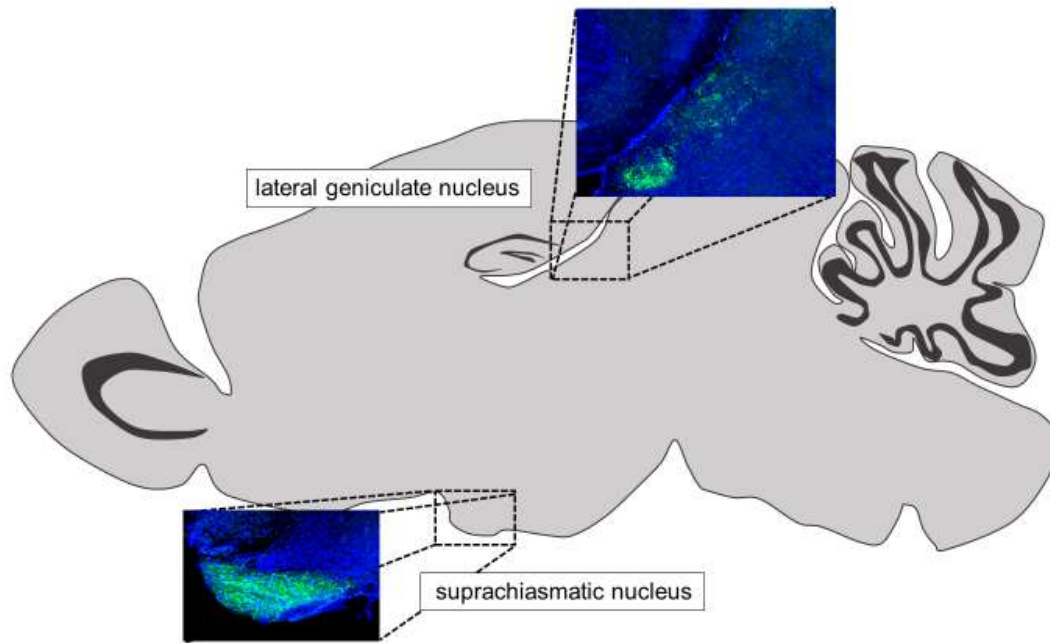


Figure 3-3. Viral reporter in brain.

At postnatal day 13, mice were intraocularly injected with AAV2 GFP. After 4 weeks, the animals were sacrificed, and brains collected to identify regions of native virus reporter expression. tDimer expression was detected in the fiber tracts of the lateral geniculate nucleus and the suprachiasmatic nucleus.

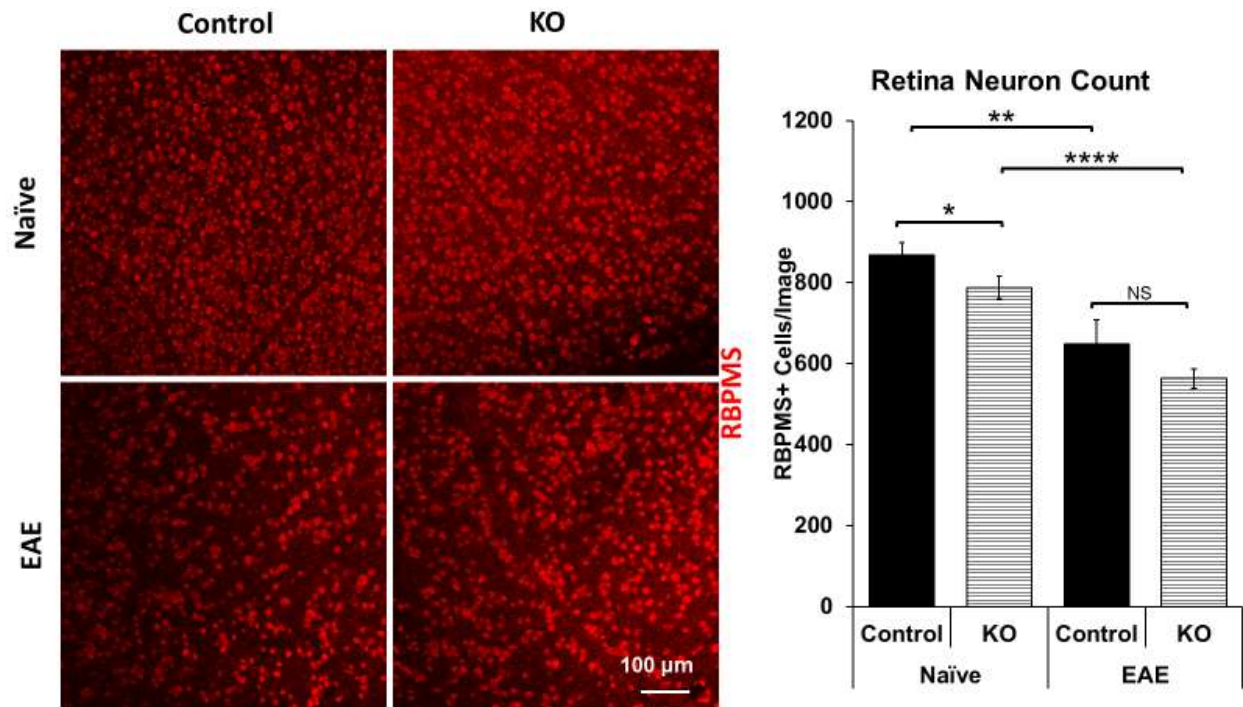


Figure 3-4. Retinal ganglion cell quantification.

Whole mount retinas were labeled with antibodies against the viral reporter, GFP, and against RNA-binding protein with multiple splicing (RBPMS), a marker for retinal ganglion neurons (RGNs). Four non-overlapping images from each retina was used to quantify retinal ganglion neuron loss. Number of animals: naïve control=16, Naïve KO=16, EAE control=17, EAE KO=14. 3 independent experiments. Student's t-test. NS=not statistically significant. * p<0.05 ** p<0.01 ***p<0.001 ****p<0.0001. Error bars show SEM.

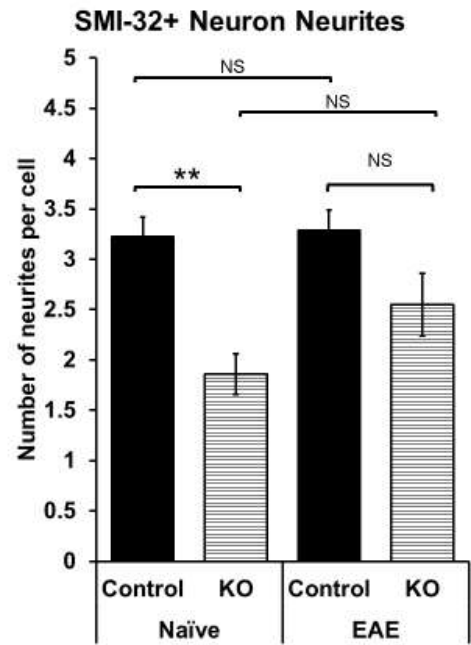
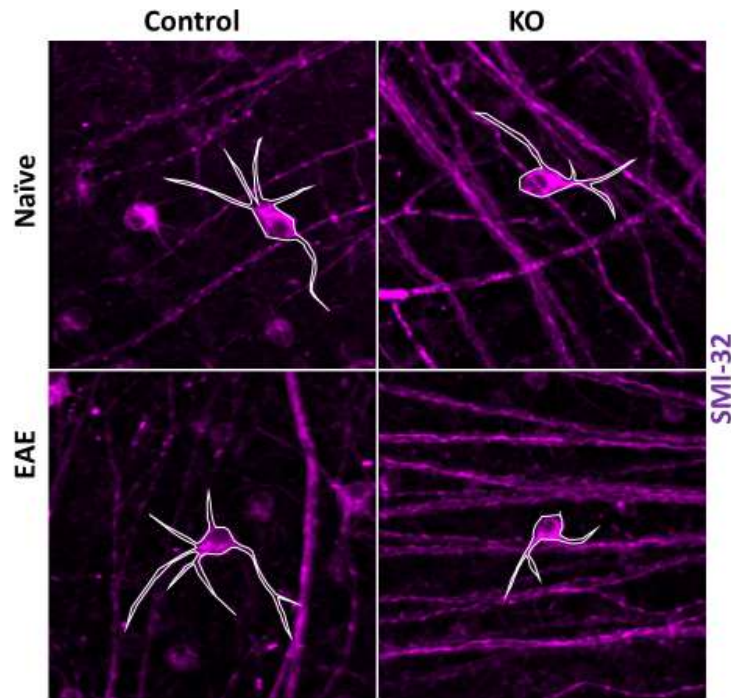
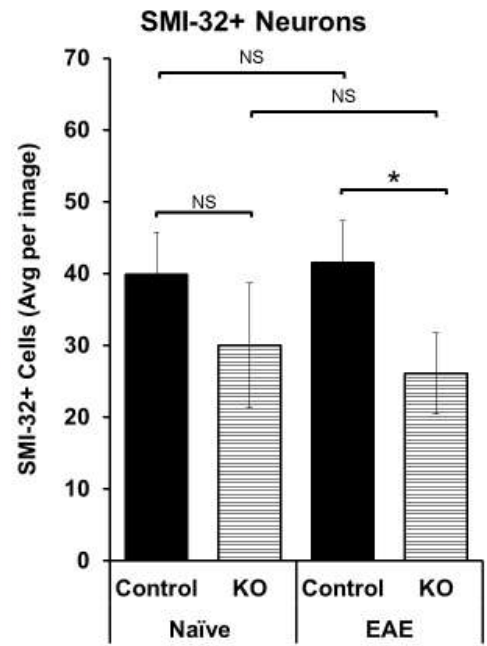
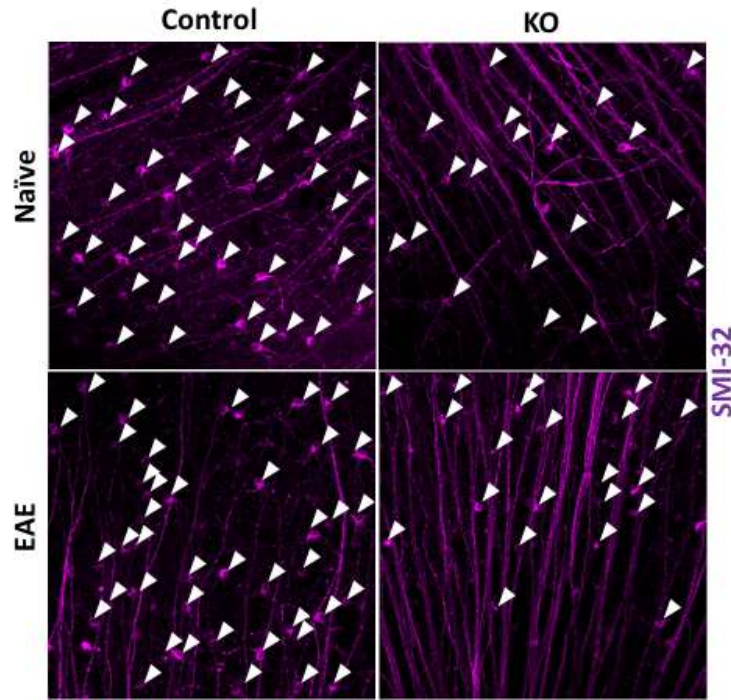


Figure 3-5. In naïve animals, AAV2 Cre GFP administration into the eye leads to loss of SMI-32 neurons and decreased number of dendrites per cell.

Whole mount retinas from PAC1 floxed mice had intravitreal administration of AAV2 GFP or AAV2 Cre GFP and were induced with chronic EAE. **(Top)** The number of SMI-32 immunoreactive neurons (indicated with white arrowheads) were quantified from four non-overlapping images of the retina. Number of animals (neuron quantification): naïve control=6, Naïve KO=5, EAE control=11, EAE KO=10. 2 independent experiments. **(Bottom)** The number of neurites per cell were counted averaged. Number of animals (neurite quantification): naïve control=3, naïve KO=3, EAE control=8, EAE KO=8. 1 independent experiment. Both quantification of neuron and neurite numbers were performed blinded. Student's t-test. NS=not statistically significant. * $p < 0.05$ ** $p < 0.01$. Error bars show SEM.

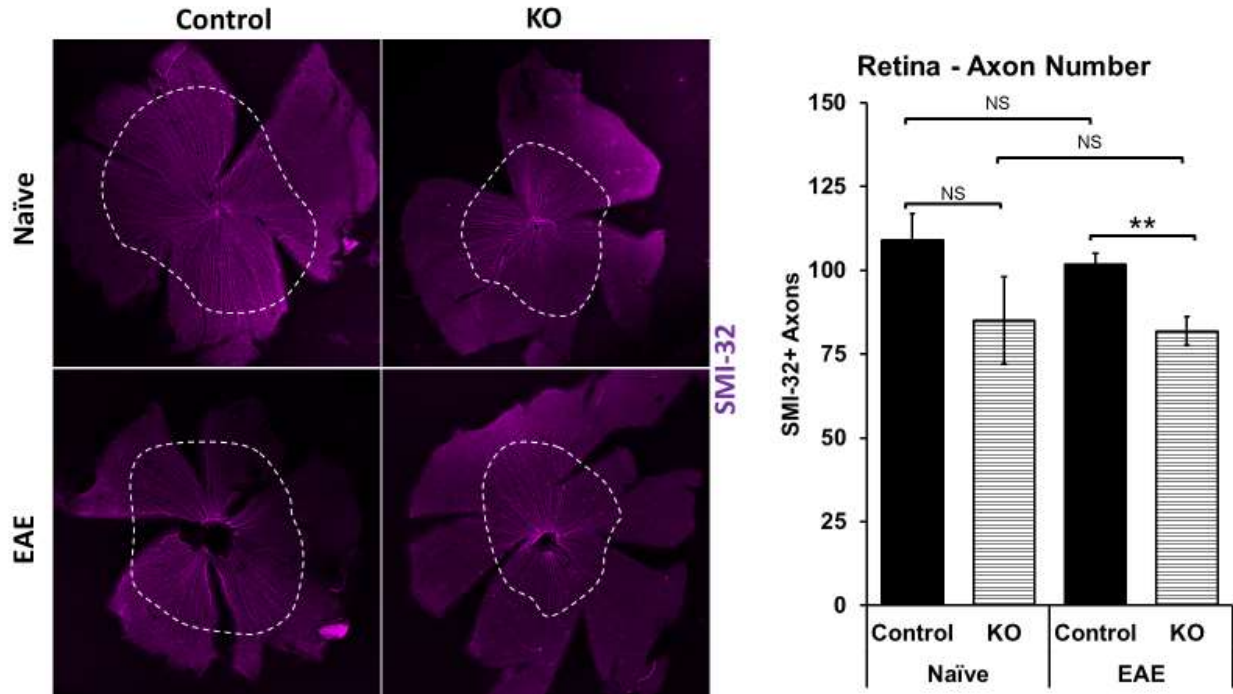


Figure 3-6. Eyes injected with AAV2 Cre GFP have fewer SMI-32 immunoreactive axons radiating from the optic nerve than eyes injected with AAV2 GFP.

Whole mount retinas from PAC1 floxed mice had intravitreal administration of AAV2 GFP or AAV2 Cre GFP and were induced with chronic EAE. Number of SMI-32+ immunoreactive axons were quantified by counting the number of immunopositive axons approximately 500 μm from the optic nerve head. Number of animals: naïve control=2, naïve KO=2, EAE control=8, EAE KO=6. 1 independent experiment. Student's t-test. For all graphs, NS=not statistically significant. * $p < 0.05$ ** $p < 0.01$. Error bars show SEM.

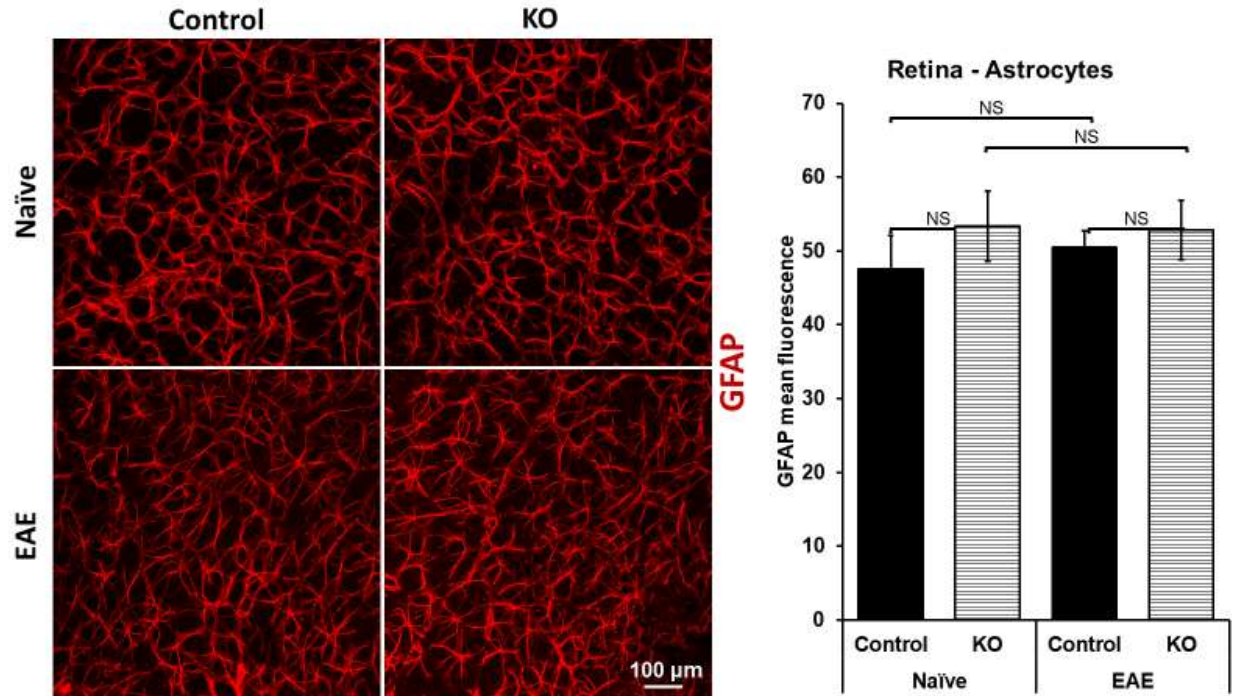


Figure 3-7 Astrocytes in the retina.

An antibody against GFAP was used to detect astrocyte activation. Number of animals: naïve control=6, naïve KO=6, EAE control=9, EAE KO=9. 1 independent experiment. Quantifications were performed blinded. Student's t-test. NS=not statistically significant. Error bars show SEM.

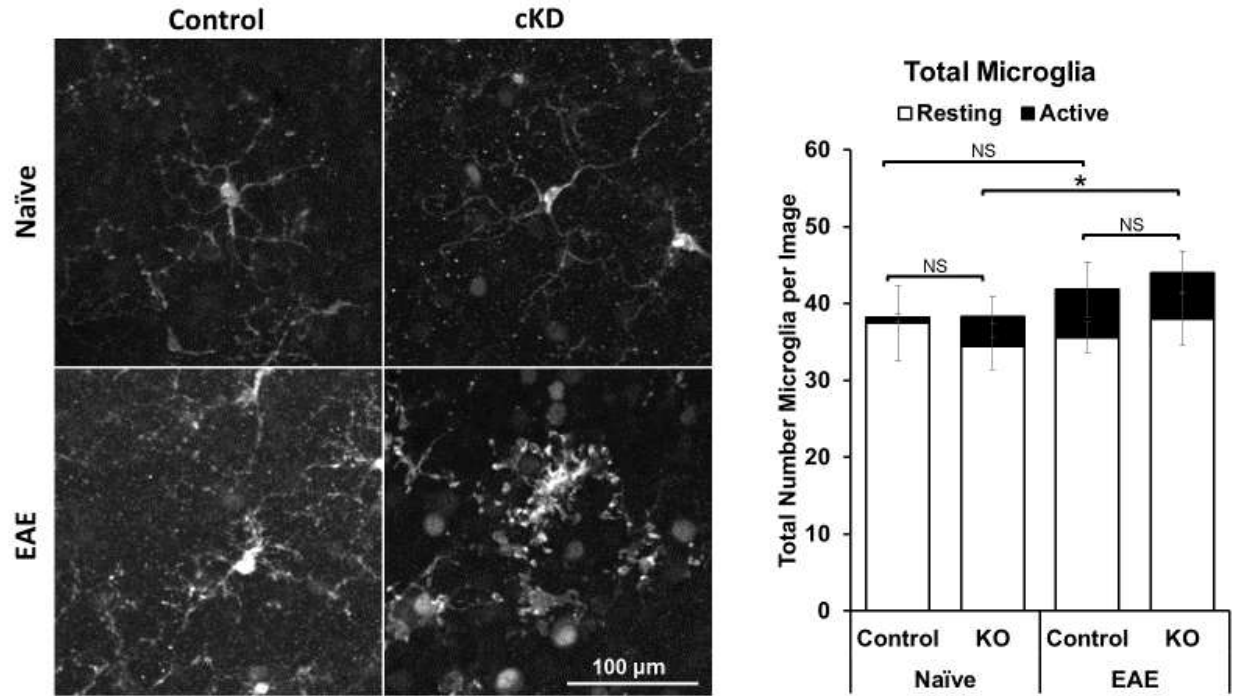


Figure 3-8. Microglia/macrophage characterization.

Microglia and macrophages were labeled with Iba1. The total number of microglia/macrophages did not change with EAE or PAC1 deletion. They were also characterized as “resting” or “active” based on their morphology. There was also no statistical difference in activation states except between naïve KO and EAE KO samples. Number of animals: naïve control=6, naïve KO=6, EAE control=9, EAE KO=9. Quantification was blinded. Student’s t-test. NS=not statistically significant. * p<0.05. Error bars show SEM.

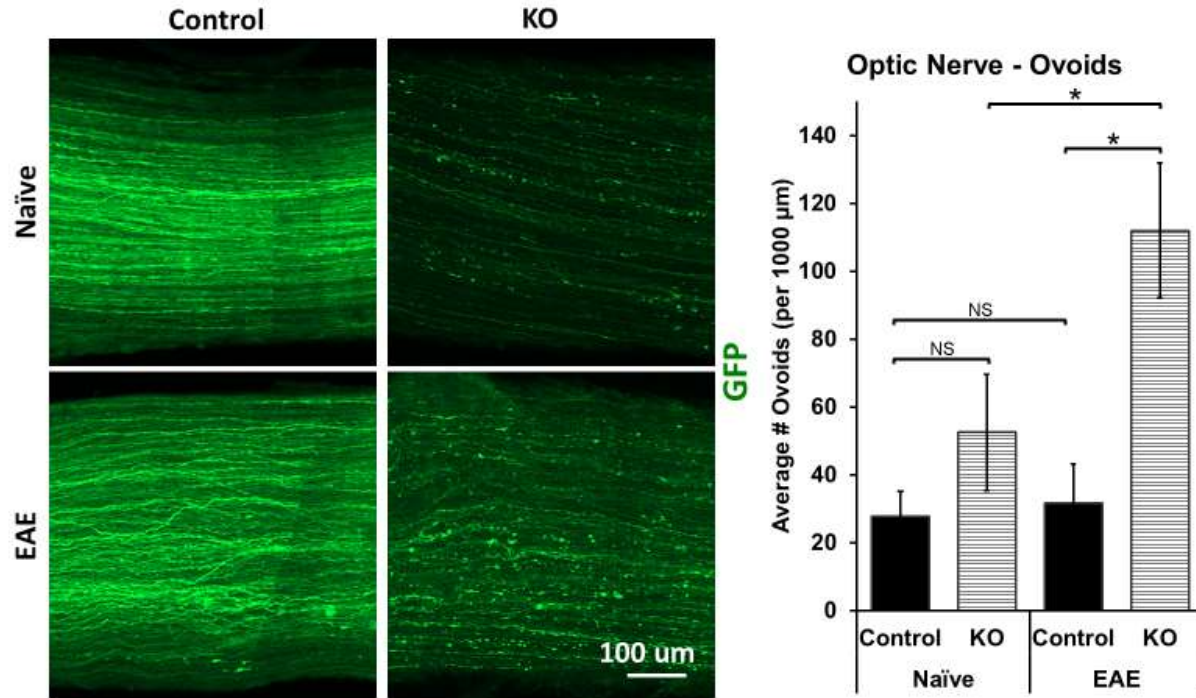


Figure 3-9. Loss of PAC1 in the eye leads to axonopathy in both naïve and EAE optic nerves.

Pairs of optic nerves from naïve and EAE animals are analyzed for abnormal ovoids in axons labeled by viral reporter GFP. Number of animals: naïve control=6, naïve KO=7, EAE control=8, EAE KO=8. Quantification performed blinded. Student's t-test. NS=not statistically significant. * $p < 0.05$. Error bars show SEM.

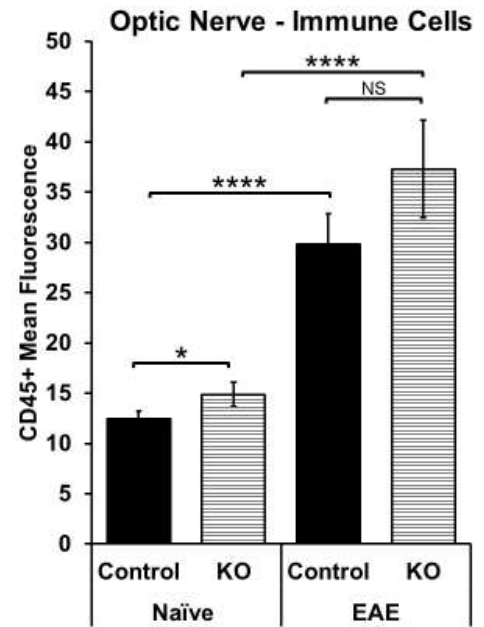
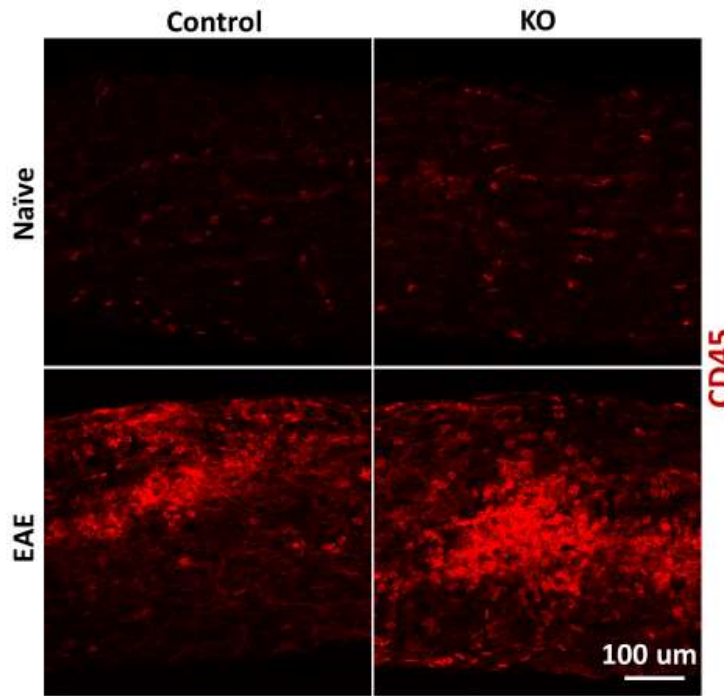
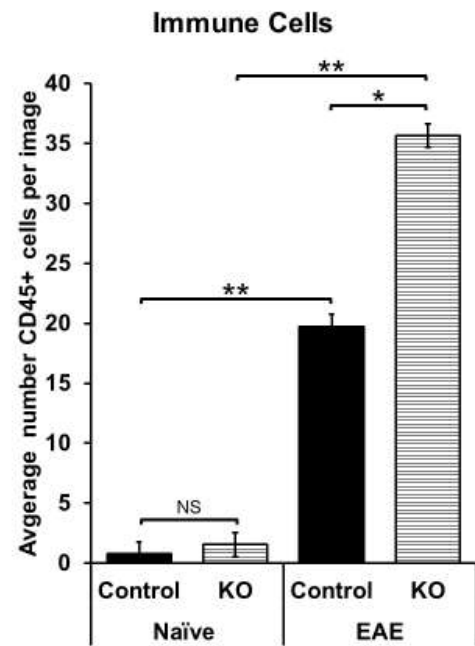
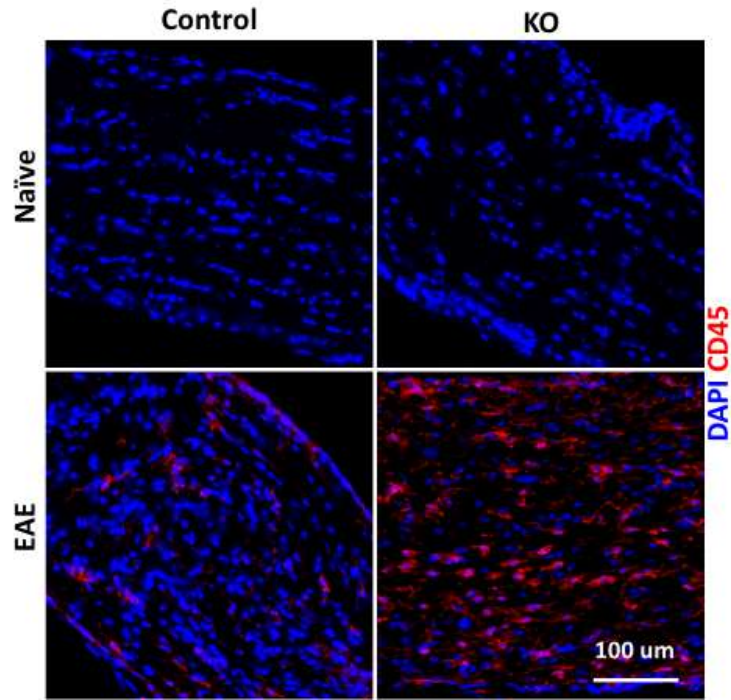


Figure 3-10. PAC1 deletion leads to increased CD45+ immunopositivity in the optic nerve during EAE.

Longitudinal optic nerve sections (**top**) (Number of animals: naïve control=3, naïve KO=3, EAE control=4, EAE KO=4) and whole mount optic nerve (**bottom**) (Number of animals: naïve control=14, naïve KO=14, EAE control=12, EAE cKD=12) were labeled with an antibody to the pan-immune marker CD45. CD45 was quantified by counting CD45 immunopositive cells or quantifying mean fluorescence. Quantification performed blinded. Student's t-test. NS=not statistically significant. * $p < 0.05$, ** $p < 0.01$. Error bars show SEM.

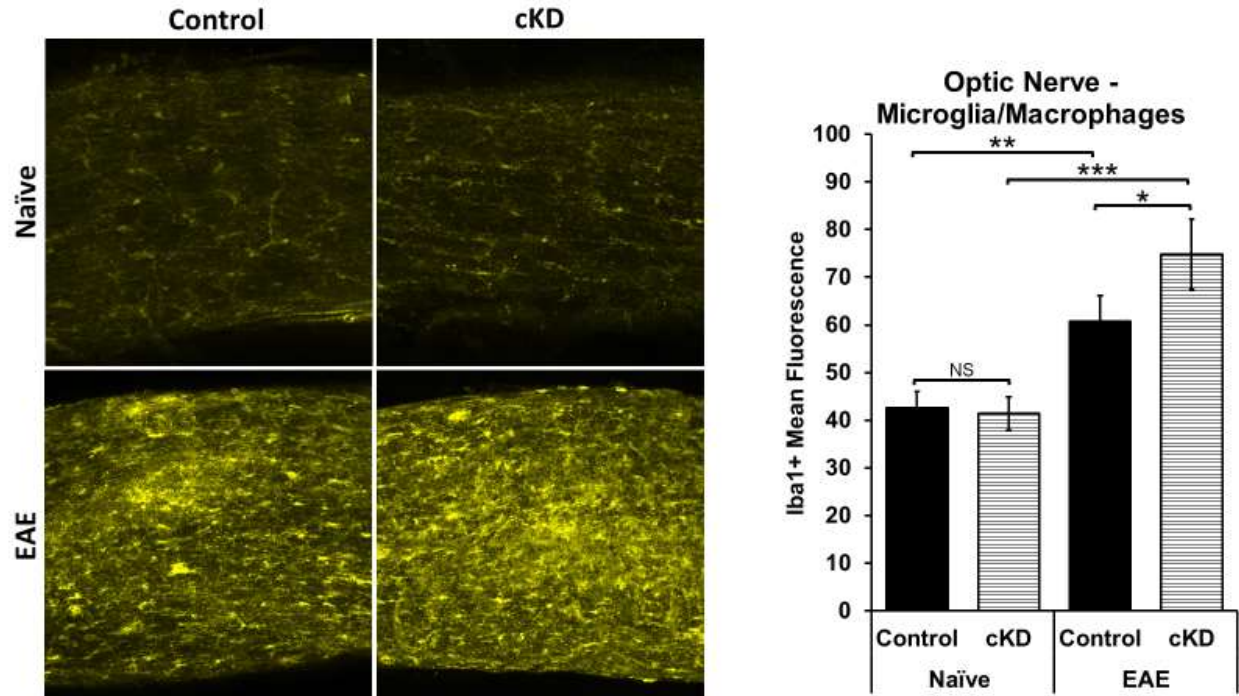


Figure 3-11. Microglia/macrophage presence.

The image above shows pairs of whole mount optic nerves from naïve and EAE animals labeled with an antibody to Iba1, which labels both resident microglia and infiltrating macrophages.

Number of animals: naïve control=14, naïve KO=14, EAE control=12, EAE KO=12.

Quantitation performed blinded. Student's t-test. NS=not statistically significant. * p<0.05 ** p<0.01 ***p<0.001. Error bars show SEM.

Chapter 4 – Test ability of AAV-mediated PACAP overexpression to ameliorate EAE

ABSTRACT

One of the challenges that continues to hamper efforts to develop treatments for neurodegenerative disease is targeting therapeutics to the central nervous system (CNS). In these studies, we use a CNS-homing recombinant adeno-associated virus (AAV) to target a gene of interest to the CNS to test its ability to protect against pathology and optic neuritis in a mouse model of multiple sclerosis called experimental autoimmune encephalomyelitis (EAE). This gene encodes pituitary adenylate cyclase-activating polypeptide (PACAP), a protein known for its anti-inflammatory and neuroprotective properties. We demonstrate successful overexpression of PACAP in the brain and showed that overexpression of PACAP in the brain leads to delayed development of EAE symptoms. Furthermore, overexpression of PACAP in the retina protects against neuron loss in the retina and against axonopathy and inflammation in the optic nerve. These results serve as a proof of principle that overexpressing an anti-inflammatory, neuroprotective protein in the CNS can protect against neuron loss and inflammation *in vivo*.

INTRODUCTION

Neurodegenerative diseases are typically chronic and can severely hamper daily life activities and comfort. A neuropeptide, PACAP has been shown to have neuroprotective effects in various neurodegenerative diseases such as multiple sclerosis, Alzheimer's Disease, Parkinson's Disease, and stroke^{72,73,75,78,79,155}. Given that PACAP functions uniquely as both a neuroprotective and an anti-inflammatory agent, it is a promising candidate for therapeutic development. These

studies assess the ability of AAV-delivered PACAP to rescue neuronal death and axonopathy in a model of multiple sclerosis and optic neuritis.

Current efforts to develop PACAP as a therapeutic

PACAP has not yet been used in clinical trials for any type of disease. There is presently interest in developing drugs that target PACAP and/or its receptors to treat neurodegenerative diseases²³⁹ such as stroke^{74,240}, Alzheimer's Disease^{241–244}, Parkinson's Disease²⁴⁵, and traumatic nerve injury^{246,247}, as well as other diseases such as diabetes^{248,249}, diabetic retinopathy²⁵⁰, dry eye²⁵¹. There have been efforts to stabilize PACAP to use as a therapeutic drug. Some have generated a more stable recombinant protein²⁵² while others have engineered stable analogs²⁵³. However, another strategy of interest is virus-mediated gene therapy.

Use of adeno-associated virus as a vector for gene therapy

One way to deliver therapeutic PACAP is by overexpressing the gene using a viral vector. Potential viral vectors include adeno-associated viruses (AAVs). AAVs are viruses of the Parvovirus family. They are approximately 20-30 nm in diameter and possess an unenveloped protein capsid containing a single-strand of genomic DNA of approximately 4.7 kb in length. The major concerns regarding using AAV for gene therapy include: immunogenicity, efficacy, genotoxicity, and persistence²⁵⁴. Nonetheless, AAVs are of interest to use as vectors for gene therapy because AAVs: 1) are considered non-pathogenic in humans, 2) have low immunogenicity²⁵⁵, 3) can infect not only dividing but also quiescent cells, 4) persist for long periods of time²⁵⁶, and 5) can integrate with the genome in more predictable sites than lentivirus, the other virus often chosen for developing virus-mediated gene therapy²⁵⁷. The transferred DNA can also exist as

extrachromosomal DNA in the infected cell. Due to an engineered replication defect and the lack of ability to produce its own capsid proteins, currently used AAVs cannot replicate and spread into other cells. There are at least 9 different serotypes of AAVs that infect human cells. The serotype refers to the composition of the capsid proteins and genome. The different AAV serotypes have varied tropism for different organs. The tropism is likely due to the different methods of host cell entry used by the AAVs ²⁵⁸. According to an *in vivo* murine study in postnatal day 2 mice injected via the superficial temporal vein comparing the different AAV serotypes on long-term spatial expression of a luciferase reporter gene, AAV8 and AAV9 demonstrate the highest reporter expression in the brain at 100 days post viral administration ²⁵⁶. A study in humans found that although most subjects have evidence of previous AAV and adenovirus infection as evidenced by the presence of antibodies against both viral type, the lymphoproliferative responses against adenovirus were approximately 10-fold greater against adenovirus than AAV ²⁵⁹, and the induction of host-neutralizing antibody production is much less than adenovirus ²⁶⁰. Nonetheless, there are several limitations to using AAVs for gene therapy.

Despite the above, the host immune response to AAV, including the production of neutralizing antibodies, can significantly impact the successful infection of target cells by AAV. Another concern is the possible need for repeated administration of AAV such as in the cases of reduced transgene expression over time or failure of the first administration to reach target organs. A study in rats demonstrated that second administration of AAV into the CNS is effective as long as at least 4 weeks have passed since the first AAV administration ²⁶¹. Another group showed that a single intramuscular administration of AAV in humanized mice generates neutralizing antibodies, however treatment of the animals with a monoclonal antibody against CD4 at the time of viral administration reduced the concentration of neutralizing made against AAV ²⁶². Therefore,

a treatment to reduce the immune response at the time of virus injection may improve outcomes if a second AAV injection is needed. It must also be noted that the route of administration (intraperitoneally, intravenously, or subcutaneously) also affects the immune response against AAV ²⁶³. Cell-mediated immune response appear to be serotype specific ²⁶⁴. Capsid library screening and serotype engineering can perhaps be performed to generate a synthetic AAV which can both efficiently target the desired organs and have lower immunogenicity.

Additionally, another concern is regarding the site of integration of the transgene into the genome. Native AAV is the only mammalian DNA virus thought to integrate into host genome in a site-specific manner into chromosome 19q13.4 ^{265,266}. However, more recent evidence shows that the integration sites varies amongst the different AAV serotypes and recombinants ²⁶⁷. The small size of the genomic DNA greatly limits possible genomic insert size. The maximum size of material that can be inserted into the vector is approximately 5 kb ^{268,269}. This size limitation is not a problem when wanting to overexpress PACAP as the complete coding sequence for the PACAP mRNA is only 528 base pairs in length.

Lentiviruses are the other predominate viral vector being developed for gene therapy. However, lentivirus genomes can integrate unpredictably into the human genome and there is a concern of these viruses reverting into replication competent retroviruses ²⁷⁰. In a clinical trial in 20 patients using a retrovirus to treat SCID-X1, vector insertional mutagenesis purportedly led to leukemia in 4 patients ^{271,271,272}. Thus, the unpredictable integration of retroviruses presents a serious safety concern in using lentiviruses as a vector for gene therapy *in vivo*.

On the other hand, AAV is already being used in clinical trials for many retinal diseases, including dry age-related macular degeneration, wet age-related macular degeneration, Leber Congenital Amaurosis, MERTK-associated retinitis pigmentosa, Usher syndrome, Stargardt disease,

choroideremia, achromatopsia, and X-linked retinoschisis^{273,274} and has been demonstrated to be safe. In these studies, we use AAV vectors to test a proof-of-principle that targeted over-expression of PACAP to the retina can diminish the pathology of optic neuritis in a model of MS.

MATERIALS AND METHODS

Animals

Mice were housed under environmentally controlled conditions in a 12-hour light/dark cycle with access to food and water *ad libitum*. All animal studies were approved by the UCLA institutional animal care and use committee (IACUC) and Animal Research Committee (ARC).

Mice strains

The animals used in the following studies are C57BL/6 mice. Approximately equal numbers of males and females were used for the following experiments.

Recombinant AAV and expression cassette

To investigate whether virus-mediated over expression of PACAP in the retina can protect against neuron loss and inflammation in the retina and optic nerve, we first engineered a construct to express PACAP and a tandem red fluorescent protein reporter, tDimer, separated by a P2A sequence²⁷⁵ under the human synapsin promoter (**Figure 4-1**). This construct is designed to express PACAP in specifically neurons. The control construct expresses only tDimer under the human synapsin promoter. In collaboration with Dr. Benjamin Deverman (California Institute of Technology, CA, USA), we used a newly-established AAV vector system derived from the screen of a capsid library to detect capsids that permit passage of AAV into the CNS²⁷⁶. One variant,

AAV-PHP.B, was found to transfer genes to the majority of neurons and astrocytes across multiple CNS regions with 40-fold greater efficacy than that of the current standard, AAV9.

Systemic delivery of AAV

Pups were systemically administered PHP.B AAV PACAP P2A tDimer or PHP.B AAV tDimer via the facial temporal vein at postnatal day 2 (**Figure 4-2**). Animals were injected at a dose of 1×10^{10} gc/gram. Virus was diluted using pharmaceutical grade saline to a total volume of 50 μ L. Fluorescein isothiocyanate was added to the solution to allow for visual confirmation of successful injection. The injections were performed using a 30-gauge needle syringe. Upon withdrawal of the needle, a cotton swab was immediately placed over the injection site with gentle pressure to until bleeding stopped. Animals were sacrificed at four weeks of age.

PACAP overexpression in the retina.

To overexpress PACAP in the retina, the mice were intraocularly injected at postnatal day 13, the day when the pups first open their eyes. We intravitreally inject the PACAP overexpression virus (PHP.B AAV PACAP P2A tDimer) in one eye and the reporter-only virus (PHP.B AAV tDimer) to the other eye. As both virus-injected eyes are from the same animal, differences from inter-animal systemic disease severity are mitigated. The mice were subcutaneously injected with carprofen, an analgesic, diluted in phosphate-buffered saline at 5mg/kg to manage pain. Isoflurane was used as a general anesthetic. To propose the eye for injection, gentle pressure was applied to either side of the eye using the index and middle finger. With assistance of a stereo microscope, a small hole is made in the sclera posterior to the iris using a 30-gauge beveled needle. 0.1 μ L of 20 mg/mL Fluorescein-5-Isothiocyanate (FITC 'Isomer I') (Invitrogen, Carlsbad, CA, USA) dissolved

in DMSO per 20 μL of virus for visual confirmation of successful virus injection into the eye. A volume of 1.5 μL of virus mixture was injected into each eye until leakage occurred. This results in a dosage of approximately 5×10^9 viral particles per mouse. The injections were made using a 10 μL Hamilton 1700 Series Gastight syringe with RN (Removable Needle) termination (Reno, NV, USA) fitted with a blunt 33-gauge needle. An ophthalmic ointment, Vetropolycin, containing Neomycin-Polymyxin B, Bacitracin, and Hydrocortisone (Dechra Pharmaceuticals, Norwich, UK) was applied to the eye to protect the eye and prevent infection. Four weeks are allowed for transgene expression and recovery from injection before EAE induction.

Experimental autoimmune encephalomyelitis. Experimental autoimmune encephalomyelitis (EAE)

To induce the chronic form of EAE, mice are subjected to a well-characterized protocol in which MOG₃₅₋₅₅, a fragment of myelin oligodendrocyte glycoprotein, is administered peripherally in adjuvant⁶⁶. 200 μg of MOG₃₅₋₅₅ in a 1:1 emulsion of phosphate-buffered saline (PBS) and Difco Complete Freund's Adjuvant (BD, Franklin Lakes, NJ, USA) supplemented with an additional 100 mg of Difco Mycobacterium tuberculosis H37RA (BD, Franklin Lakes, NJ, USA) is split and subcutaneously injected in the left and right flanks posterior to the forelimbs. This was specified as day 0 of EAE (**Figure 4-2**). This results in the expansion of T-cells autoreactive to myelin⁶². Additionally, the mice receive a peritoneal injection of 300 ng of pertussis toxin (List Biological Laboratories, Campbell, CA, USA) dissolved in PBS. Pertussis toxin causes permeabilization of the blood brain barrier, thus allowing the T cells targeting MOG to enter the CNS. After two days, the mice are given an additional 300 ng booster injection of pertussis toxin to maintain permeabilization of the blood brain barrier. On the seventh day of EAE, the mice receive a second injection of the emulsion of MOG₃₅₋₅₅, Complete Freund's Adjuvant, and

Mycobacterium tuberculosis. This second immunization is crucial for inducing the chronic form of EAE in which the mice maintain EAE symptoms for the full extent of these studies. Mice reproducibly begin to develop demyelination and paralysis within 13-16 days post initial EAE induction. Clinical scores of EAE severity were given based on a 5 point-scale in which 0=asymptomatic, 1=loss of tail tonicity, 2=partial paralysis or failure to resist inversion, 3=complete paralysis of one hind limb, 4=complete paralysis of both hind limbs, and 5=moribund or death. In cases where mice reached the moribund state, they were euthanized as dictated by federal and university policy. For these studies, tissues were collected 60 days post-EAE induction, a time when significant neurodegeneration and retinopathy has been observed ²¹¹. For these studies, approximately half of the littermates were kept naïve and half were induced with EAE. The mice chosen for EAE was based on their identification number where every other number was chosen to be EAE.

RNA Extraction

The anterior, right quarter of the brain was collected for gene expression analysis. The samples were placed in microfuge tubes, frozen on dry ice, and stored at -80°C until use. For RNA extraction, tubes were kept on wet ice for the duration of the procedure. A tungsten carbide metal bead was added, along with TRIzol Reagent (Invitrogen, Carlsbad, CA, USA). To homogenize the tissue, a TissueLyser (QIAGEN, Venlo, Netherlands) was used. The homogenizer frequency was set to 25 1/2, for 40 seconds. After the initial lyse step, the tubes were placed back on ice for 5 minutes to cool again. The tissue samples were homogenized again at a frequency of 25 ½ for 30 seconds. The tubes were chilled for another 5 minutes before proceeding. The tubes were centrifuged at 13,000 rpm for 2 min at 4°C, and floating debris was aspirated from the surface of

the supernatant. Then, 200 μ L of chloroform was added and tubes were manually inverted for 15 seconds. After incubating the tubes at room temperature (RT) for 2 minutes, the samples were centrifuged at 13,000 rpm 4°C for 5 minutes. The aqueous phase was transferred to clean 1.5 mL tubes and centrifuged at 13,000 rpm 4°C for 10 minutes to remove additional debris. The aqueous solution was again transferred to new tube. Then, 0.5 mL of 100% isopropanol was added to precipitate RNA. After inverting the tubes several times to mix the contents, the tubes were incubated at RT for 10 minutes. After centrifuging the samples at 13,000 rpm at 4°C for 10 min, the supernatant was aspirated. The RNA pellets were washed with 75% ethanol in diethyl pyrocarbonate (DEPC)-treated water. Tubes were centrifuged at 10,000 rpm at 4°C for 5 min and the wash step was repeated one more time. After an additional centrifuge step, the supernatant was aspirated, and the RNA pellet was allowed to dry at RT for 20 minutes. Pellets were resuspended in 100 μ L DEPC-H₂O and stored at -20°C until use. All centrifugation steps were performed with an Eppendorf 5417R (Eppendorf, Hamburg, Germany) refrigerated centrifuge.

RNA concentration and purity (determined by A₂₆₀/A₂₈₀nm and A₂₆₀/A₂₃₀nm ratios) were measured using a NanoDrop One Microvolume UV-Vis Spectrophotometer (Thermo Fisher Scientific, Waltham, MA, USA). 250 ng of each sample of RNA was denatured with 2x RNA Loading Dye (Thermo Scientific, Canoga Park, CA, USA) for 70°C at 10 min using a MJ Mini Thermal Cycler (Bio-Rad, Hercules, CA, USA). Denatured RNA samples were run alongside 1 μ g of RiboRuler Low Range RNA Ladder (Thermo Scientific, Canoga Park, CA, USA) in a 1.2% agarose gel in Tris-Buffered EDTA buffer pre-cast with 5% GelRed (Biotium, Fremont, CA, USA) at 90V for 20 mins to check for intact 28S and 18S RNA bands. Gels were imaged using a Universal Hood Gel Doc System (Bio-Rad, Hercules, CA, USA).

Real-time quantitative polymerase chain reaction (qRT-PCR)

The following primers were used for qPCR:

Gene	Forward primer	Reverse primer
PACAP	GTCTCCGTTCAAATGCCG	TGCAGCGGGTTTCCGT
PAC1	CCCTGGCATGTGGGACAA	GGCAGCTTACAAGGACCA
GAPDH	GGCCTTCCGTGTTTCCTAC	TGTCATCATACTTGGCAGGTT

Complementary DNA (cDNA) was synthesized from 500 ng of purified RNA in a 20 μ L reaction using SuperScript IV VILO Master Mix (Invitrogen, Carlsbad, CA, USA). Quantitative polymerase chain reaction (qPCR) was performed using PowerUp SYBR Green Master Mix (Applied Biosystems, Foster City, CA, USA). cDNA was diluted 10x and 7.5 ng of cDNA was used per 20 μ L qPCR reaction. The target genes and the primers used are listed below. PCR primers were used at a final concentration of 500 nM. Amplifications were performed using the following cycling protocol: UDG activation at 50°C for 2 min, Dual-Lock™ DNA polymerase hot-start at 95°C for 2 min, then 40 cycles of denaturing at 95°C for 15 min and annealing/extending at 60°C for 1 min. Reactions were performed and read using an StepOnePlus Real-Time PCR System (Applied Biosystems, Foster City, CA, USA). A melt curve was performed at the end of each assay to check for single product amplification. A standard curve made by sequential 10-fold dilution from the most concentrated standard (containing 5 μ L from all cDNA samples and diluted to a total volume of 200 μ L with nuclease-free water) was used to determine amplification efficiency. Glyceraldehyde-3-Phosphate Dehydrogenase (GAPDH) was used as the housekeeping gene for all qPCR assays.

Immunofluorescence analysis of reporter expression in brain, spinal cord, spleen and liver samples

Four weeks after systemic injection of PHP.B AAV PACAP P2A tDimer or PHP.B AAV tDimer, brains, spinal cords, spleen, and liver were collected for analysis of viral reporter expression. Tissues were fixed overnight in 4% paraformaldehyde in 1x phosphate-buffered saline (PBS). The next day they were incubated in 15% sucrose in 1x PBS 0.05% sodium azide. The following day, the samples were incubated in 30% sucrose in 1x PBS 0.05% sodium azide until the tissues sank. Samples were embedded in optimal cutting temperature (OCT) media (Sakura Finetek, Torrance, CA, USA), cryosectioned with a Leica CM1950 (Wetzlar, Germany) at 40 μm and sections were dropped into well plates containing 50% glycerol in 1x PBS 0.05%. Sections were stored at -20°C until use. For analysis, sections were rinsed 2x with 1x PBS and laid onto Fisher Finest Superfrost microscope slides (Fisher Scientific, Hampton, NH, USA). Prolong Gold Antifade Mounting media with DAPI (Invitrogen, Carlsbad, CA, USA) was applied, and a glass coverslip was sealed with nail polish.

Immunofluorescence analysis of whole mount retina and optic nerve samples

Eyes were enucleated, and retinas and optic nerves were collected²¹². To harvest the retina from the whole eye, the anterior chamber was removed, the retinal pigmental layer was peeled away, and four equidistant cuts radiating away from the optic nerve head were made to allow the retinal cup to be flattened. Whole retinas were flat mounted on nylon membranes. Optic nerve samples analyzed include the entire length of the optic nerve immediately posterior to the optic nerve head to the optic chiasm. The retinas and optic nerves were fixed in 4% paraformaldehyde in PBS overnight at 4°C . The following day, the retinas and optic nerves were rinsed twice with

1x PBS and stored in 1x PBS until the assay. For the assay, samples were blocked in 10% normal donkey serum 1% bovine serum albumin (BSA) 0.5% TritonX-100 in 1x PBS overnight at 4°C. The following day, the samples were incubated with primary antibodies in 10% normal donkey serum 1% BSA 0.5% TritonX-100 in 1x PBS overnight at 4°C. Samples were then washed with 5 x10 min 1x PBS. Then, the samples were incubated with secondary antibodies in 10% normal donkey serum 1% BSA 0.5% TritonX-100 in 1x PBS overnight at 4°C. To label nuclei, the samples were incubated with 20 mM Hoechst 3341 (Thermo Fisher Scientific, Canoga Park, CA, USA) in 1x PBS at 1:1000 for 5 minutes at room temperature (RT) in the dark. Samples were then washed 5 x 10 min with 1x PBS and mounted on microscope slides with Prolong Gold Mounting Media (Life Technologies, Carlsbad, CA, USA). Images were taken with a Zeiss LSM 800 confocal microscope (Zeiss, Oberkochen, Germany).

Immunofluorescence analysis of sectioned retina and optic nerve samples

For cryosectioned retinas and optic nerves, retinas and optic nerves were fixed overnight at in 4% paraformaldehyde in 1x PBS. The next day, retinas and optic nerves were incubated in 15% sucrose in 1x PBS 0.05% sodium azide overnight at 4°C, and the following day in 30% sucrose in 1x PBS 0.05% sodium azide at 4°C until the tissue sank. Samples were then embedded in Optimal Cutting Temperature media (Sakura Finetek, Torrance, CA, USA), cryosectioned with a Leica CM1950 (Wetzlar, Germany) at 10 µm and mounted onto Fisher Finest Superfrost microscope slides (Fisher Scientific, Hampton, NH, USA). Slides were stored at -80°C until use. For the immunofluorescence assay, tissue sections were rehydrated with 1x PBS at RT for 5 min and rinsed twice with PBS. Sections were then blocked with 10% normal goat serum (or donkey serum, depending on the assay) 1% BSA 0.05% TritonX-100 in 1x PBS for 1 hour at RT. After a

rinse with 1x PBS, sections were incubated with primary antibody diluted in 5% serum (donkey or goat (Equitech Bio, Kerville, TX, USA), depending on the assay) 1% BSA in 1x PBS overnight at 4°C. The next day, sections were washed with 3 x 10 min 1x PBS. Then, sections were incubated in secondary antibody solution diluted in 5% goat (or donkey serum, depending on the assay) 1% BSA in 1x PBS at RT for 1 hour in the dark. Hoechst 33342 (20mM at 1:1000) (Pierce, WI, USA) was applied at 1:1000 at RT for 5 min. Following 3 x 10 min washes with 1x PBS, Prolong Gold Mounting media (Invitrogen, Carlsbad, CA, USA) was applied, and a glass coverslip was sealed with nail polish.

The following is the list of antibodies used in this study along with the specific dilution used:

Primary Antibodies:

- (1:1000) Rabbit anti-Iba1 (Wako Pure Chemical Industries, Osaka, Japan)
- (1:500) Mouse anti-GFAP (Millipore, Clone GA-5, Burlington, MA, USA)
- (1:500) Rat anti-CD4 Clone RM4-5 (eBioscience, San Diego, CA, USA)
- (1:500) Goat anti-GFP (Abcam, Cambridge, UK)
- (1:1000) Mouse anti-SMI-32 (Covance/BioLegend, San Diego, CA, USA)
- (1:1000) Rabbit anti-NF200 (Abcam, Cambridge, UK)
- (1:500) Rat anti-CD45 PE (eBioscience, San Diego, CA, USA)
- (1:500) Rat anti-CD45 FITC (eBioscience, San Diego, CA, USA)

Secondary Antibodies:

- (1:500) Donkey anti-Rabbit Cy3 (Jackson Immunoresearch, West Grove, PA, USA)
- (1:500) Donkey anti-Goat Alexa Fluor 488 (Life Technologies, Carlsbad, CA, USA)
- (1:500) Goat anti-Rabbit Alexa Fluor 488 (Life Technologies, Carlsbad, CA, USA)
- (1:500) Donkey anti-Rat Cy3 (Jackson Immunoresearch, West Grove, PA, USA)
- (1:500) Donkey anti-Mouse Alexa Fluor 647 (Life Technologies, Carlsbad, CA, USA)
- (1:500) Donkey anti-Rabbit Alexa Fluor 647 (Life Technologies, Carlsbad, CA, USA)
- (1:500) Goat anti-Rat Alexa Fluor 488 (Life Technologies, Carlsbad, CA, USA)

Microscopy and image processing

Images of fluorescent cross section samples were captured using an Axio Imager 2 (Carl Zeiss, Oberkochen, Germany) while images of fluorescent whole mount samples were captured using a Zeiss LSM 800 confocal microscope (Carl Zeiss, Oberkochen, Germany) with ZEN Blue software (Carl Zeiss, Oberkochen, Germany). A 5x objective was used to capture whole retina images for axonal quantitation. A 10x objective was used to capture whole optic nerve, retina images for neuronal quantitation, and whole brain images.

Z-stack, stitched images were imported into ImageJ (National Institutes of Health, Bethesda, MD, USA) using BioFormat Importer (Open Microscopy Environment) and processed into maximum intensity projection images for analysis.

Quantification of neuron loss

To quantitate total neuron loss, flat mount retinas were labeled for RNA-binding protein with multiple splicing (RBPMS) which labels retinal ganglion neurons ²¹³. Four non-overlapping images from each retina were used to calculate measurements for each retina. To quantitate subpopulation of neurons which have been shown to be vulnerable in the glaucoma model of disease ²¹⁴, antibodies to SMI-32 were used. Measurements were made in a blinded manner.

Quantification of axonopathy

Retina. To quantitate axon loss, flat mount retinas were labeled for SMI-32 as described above. SMI-32 immunopositive axons were counted by a blinded investigator using the ImageJ (National Institute of Health, Bethesda, MD, USA) Point Tool 500 μ m from the optic nerve head.

Optic nerve. To visualize the morphology of axons associated with neurons in which virus-mediated PAC1 deletion occurred, the viral reporter, tDimer, was used. To visualize the morphology of all axons, the marker for heavy neurofilament, NF200, was used. To visualize the morphology of a subset of neurons, the native fluorescence expressed by Thy1-YFP mice was used.

Quantitation of inflammation

Antibodies against Glial fibrillary acidic protein (GFAP) were used to label astrocytes, Ionized calcium binding adaptor molecule 1 (Iba1) to label microglia and macrophages, and cluster of differentiation 45 (CD45) to label leucocytes. Cell counting was performed with the ImageJ (NIH, Bethesda, MD, USA) Cell Counter tool. Immunopositive fluorescence intensity was measured using the Histogram tool.

Statistical Analysis

Microsoft Excel (Redmond, WA, USA) were used for statistical analysis and for generating graphs. Analysis of variance (ANOVA) and Student's t-test were used to determine statistical significance. Any statistical data point 1.5 times greater than or less than the interquartile range of the data set were considered outliers and excluded from analysis.

RESULTS

Systemic delivery of PACAP

In preliminary tests, we systemically administered PHP.B AAV PACAP P2A tDimer or PHP.B AAV tDimer to pups at postnatal day 2. We observed high expression of the viral reporter

in the brain, less in the spinal cord, and none in the spleen or liver (**Figure 4-3**). In addition, by qPCR analysis we confirmed that there is approximately a 60% increase in PACAP mRNA in brains from animals injected with AAV PACAP as compared to brains injected with the control virus (**Figure 4-4**). The level of PAC1 receptor expression does not change with PACAP overexpression. This is important as downregulation of the receptor may occur when the ligand is overexpressed. Furthermore, mice which received the PACAP virus had statistically significant delayed onset of EAE symptoms as compared to mice which received the control virus although there was no change in peak disease severity (**Figure 4-5**). Despite approximately only approximately 10% of the retina being infected with systemically delivered virus (as visualized by the presence of the viral reporter) (**Figure 4-6**), in the optic nerves of EAE animals with PACAP overexpression, there were fewer CD45 immunopositively labeled cells (**Figure 4-7**). This finding indicates that PACAP reduces inflammation in the optic nerve during EAE and that not a high percentage of the retina needs to be targeted by the virus to be protective.

Distribution of viral reporter in the retina

Injection of retinas with PHP.B AAV tDimer resulted in infection of several layers of the retina, including the retinal ganglion cell layer, as indicated by the expression of the viral reporter (**Figure 4-8**). Analysis of the brain also shows that the virus does not infect cells in the brain as expression of the viral reporter in the brain is limited to regions directly innervated by neurons in the retina – the lateral geniculate nucleus and suprachiasmatic nucleus (**Figure 4-9**). These data suggest that intraocular injection of a PACAP overexpressing AAV is an effective strategy to locally target cells in the retina and could also be an effective strategy to target expression of other proteins to the retina as well.

DISCUSSION

PACAP is a promising candidate for development of therapeutics for neurodegenerative disease, but there are two major challenges to using PACAP protein as a treatment: 1) the protein is very unstable in blood and thus cannot be administered intravenously, and 2) it would require continual administration throughout the patient's life because MS is chronic. The use of an AAV vector to deliver into the CNS overcomes these two challenges and also is a solution for delivering a therapeutic through the blood brain barrier.

The preliminary results from the systemic administration of the PACAP-overexpressing virus demonstrates central nervous system homing ability and high promoter specificity as expected by using this recombinant AAV²⁷⁶ along with a neuron-specific promoter. In EAE mice, the blood brain barrier is compromised due to disease, but it is important that we also observe high viral reporter in the CNS of naïve mice. Therefore, this recombinant AAV is able to access the CNS even through a non-compromised blood brain barrier. Additionally, as the viral reporter was only localized in the brain to two regions directly innervated by fiber tracts from the retina – the lateral geniculate nucleus and suprachiasmatic nucleus, it is expected that the virus infection is localized to the eye. However, it is possible PACAP made from the transgene is secreted from these neurons into the brain. In ongoing studies, we are determining if local PACAP overexpression in the retina can protect against neuron loss, axonopathy, and inflammation in a model of optic neuritis. We expect these results to corroborate results found in the study in which we use a Cre-Lox systemic to conditionally delete PAC1 receptors in the eye (see Chapter 3).

Thus far, these studies demonstrate a proof of principle that systemic administration of a CNS-specific AAV can be used to overexpress an anti-inflammatory protein to reach a statistically

significant measurable therapeutic effect in reducing inflammation. This approach can be used to deliver other genes of interest to the CNS to treat inflammatory, neurodegenerative diseases.

ACKNOWLEDGEMENTS

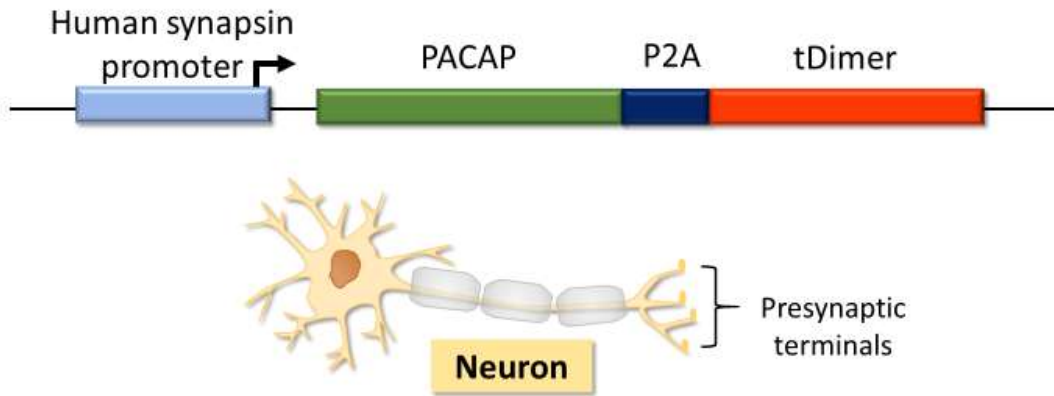
We would like to thank the National Multiple Sclerosis Society for funding this study (RG3928A2, RG-1501-02646).

We would also like to thank Dr. Benjamin Deverman (previously California Institute of Technology) for his valuable guidance in designing a construct to overexpress PACAP, for packaging our construct into AAV, and for his gift of the PACAP overexpressing virus as well as a control virus.

Microscopy and cryosectioning was performed using instruments made available through the UCLA Intellectual and Developmental Disabilities Research Center (IDDRC) Core. The UCLA IDDRC is supported by a P30 grant from the Eunice Kennedy Shriver National Institute of Child Health and Human Development (NICHD) and is an Organized Research Unit supported by the Jane and Terry Semel Institute for Neuroscience and Human Behavior.

FIGURES

pAAV Syn PACAP 2A tDimer construct



pAAV Syn PACAP P2A tDimer

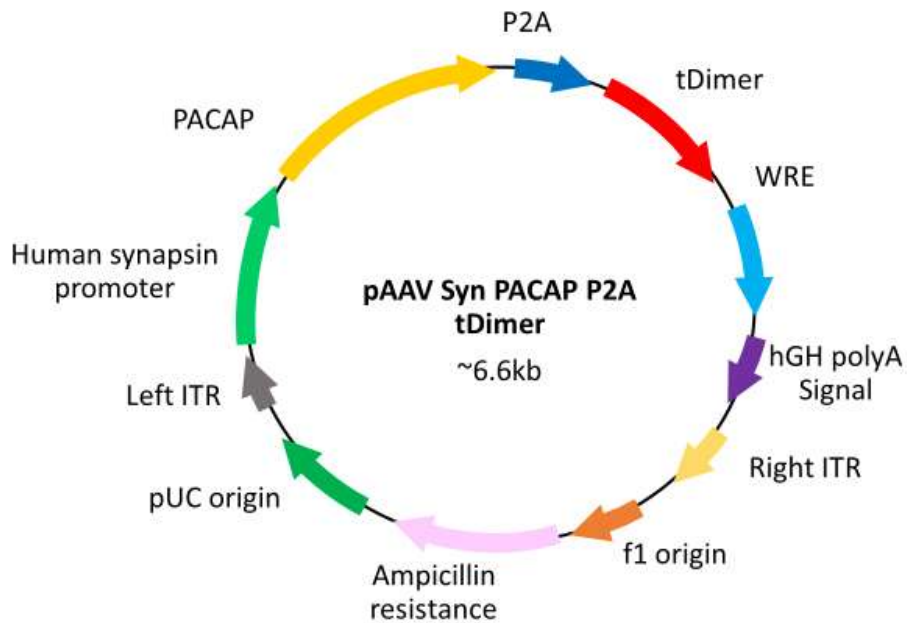


Figure 4-1. Construct to express PACAP and a red fluorescent reporter protein under the human synapsin promoter.

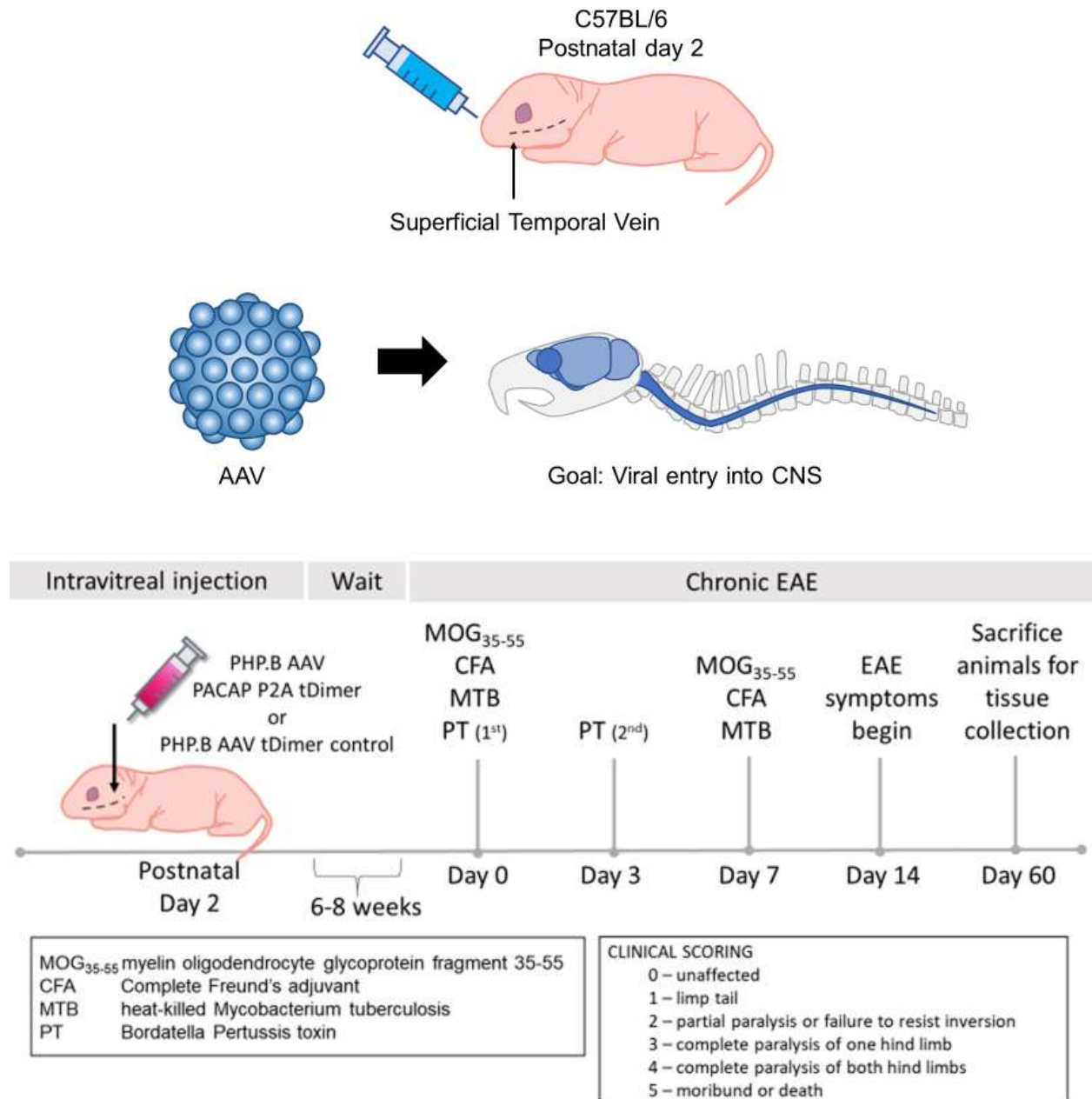


Figure 4-2. Experimental approach for systemic administration of PACAP overexpressing virus and subsequent induction of EAE. C57BL/6 animals are systemically injected via the superficial temporal vein with PHP.B AAV PACAP P2A tDimer virus or PHP.B AAV tDimer control virus. After 6-8 weeks to allow for viral vector gene expression and for the animal to mature, chronic EAE is induced. Symptoms begin around day 14 and animals are sacrificed at day 60 post EAE induction, a time point in which others have shown that long term neuronal damage has occurred with this model.

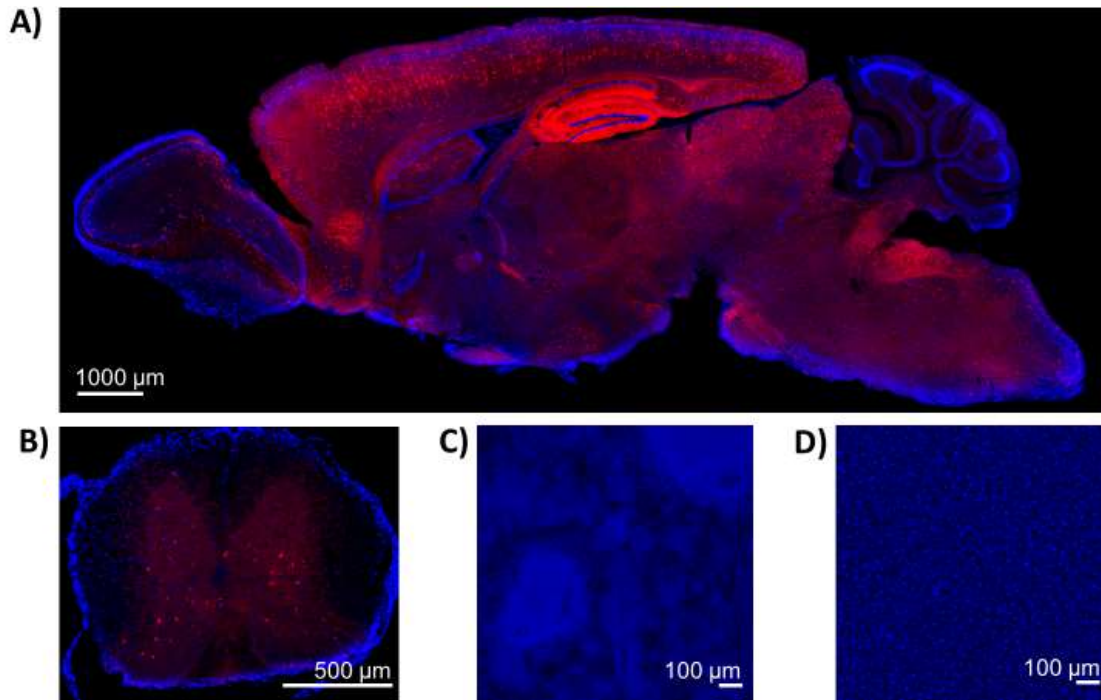


Figure 4-3. Using PHP.B AAV to express a transgene under the human synapsin promoter results highly specific expression of the viral reporter in the CNS.

Tissues from a C57BL/6 mouse systemically injected with PH.B. AAV Syn tDimer. The red fluorescent protein viral reporter is highly expressed in the brain (a) and spinal cord (b) but not detectable in the spleen (c) or liver (d). Blue – DAPI. Red – tDimer reporter native fluorescence.

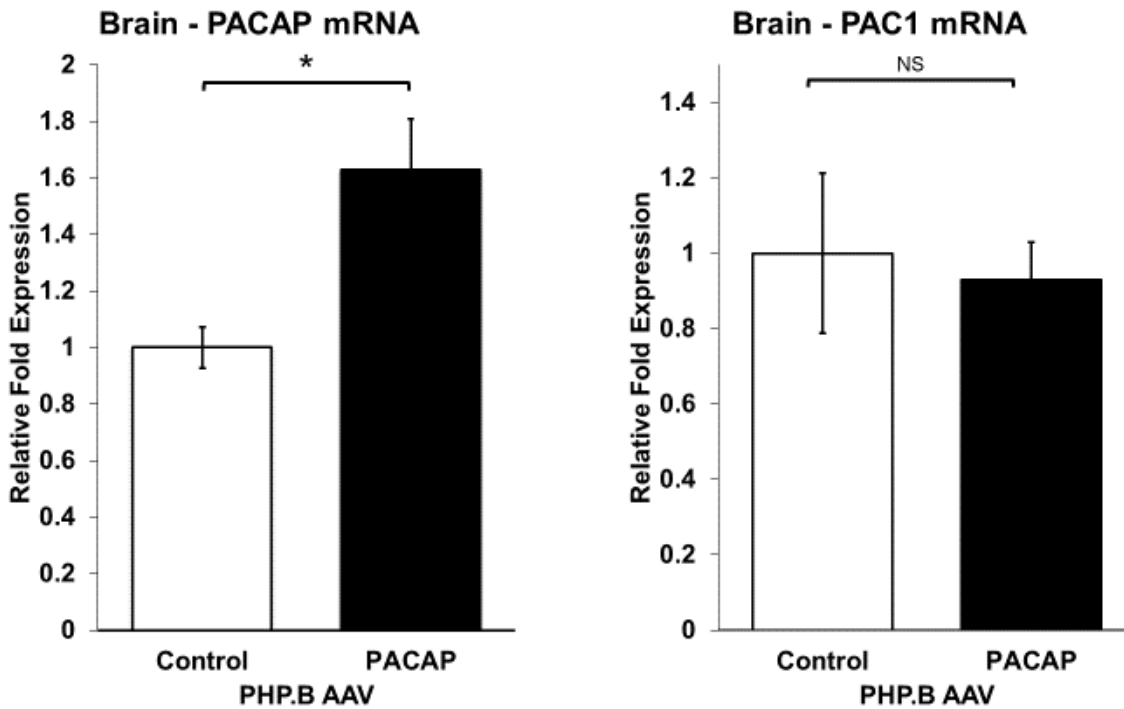


Figure 4-4. PACAP expressed is increased in the brains of animals systemically injected with the PACAP overexpressing virus while the levels of PAC1 receptor expression does not change.

cDNA was made RNA was extracted from the brains of animals systemically injected with either the PHP.B AAV PACAP P2A tDimer virus or the PHP.B AAV tDimer control virus. qPCR was used to analyze the levels of PACAP and PAC1 expressed in these brains. PACAP expression is increased by about 60% in animals injected with the PACAP overexpressing virus while the level of PAC1 does not change. Number of animals: tDimer =4, PACAP=4. Student's t-test. NS=not statistically significant. * $p < 0.05$. Error bars show SEM.

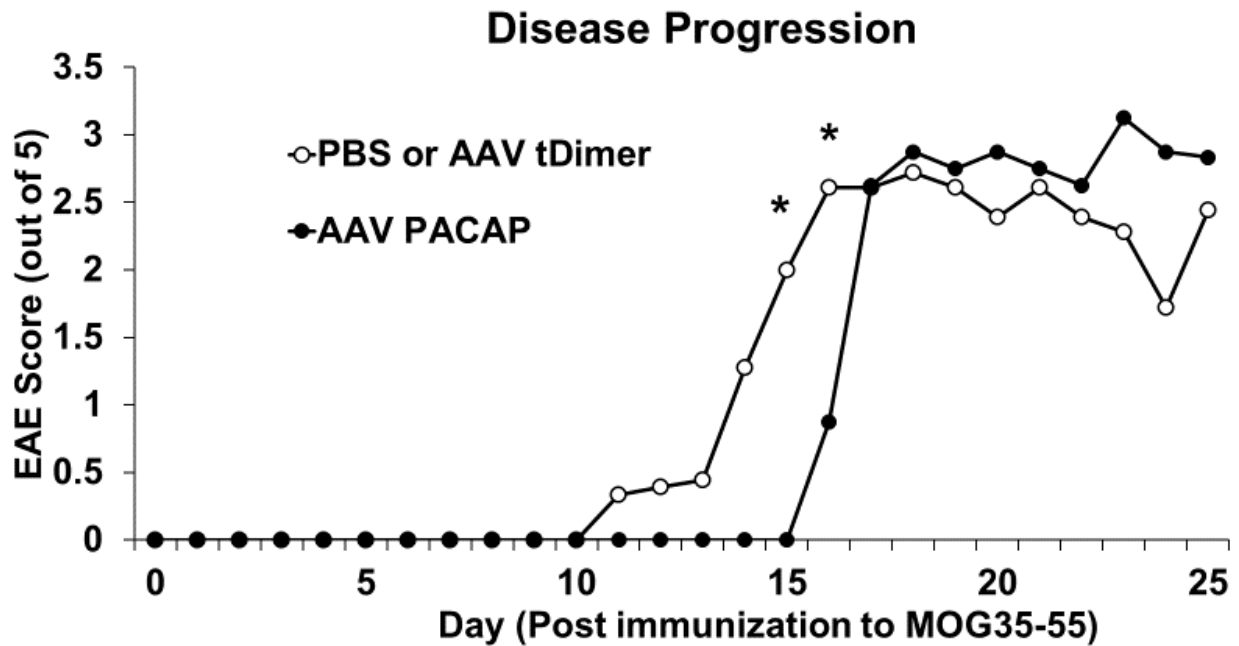


Figure 4-5. Clinical scores for animals systemically injected with PBS, AAV tDimer, and AAV PACAP, and induced with chronic EAE.

On postnatal day 2, C57BL/6 mice were systemically administered PBS, PHP.B AAV tDimer or PHP.B AAV PACAP P2A tDimer via the superficial temporal vein. After 6 weeks, chronic EAE was induced. Number of animals: PBS=5, AAV tDimer =4, PACAP=4. * $p < 0.05$.

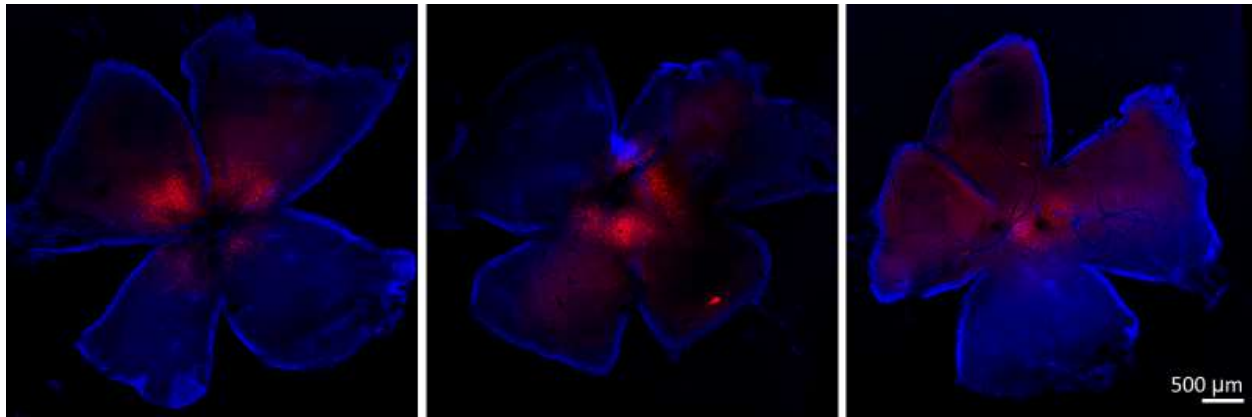


Figure 4-6. Virus reporter expression in retina of animals systemically injected with PHP.B AAV tDimer.

Mice were administered PHP.B AAV tDimer at postnatal day 2. After 4 weeks, the animals were sacrificed, and eyes were collected for analyses. Retinas were flat mounted on a nylon membrane and native virus reporter fluorescence was examined. Above are retinas taken from 3 different animals. Blue = Hoechst, red = viral reporter tDimer native fluorescence.

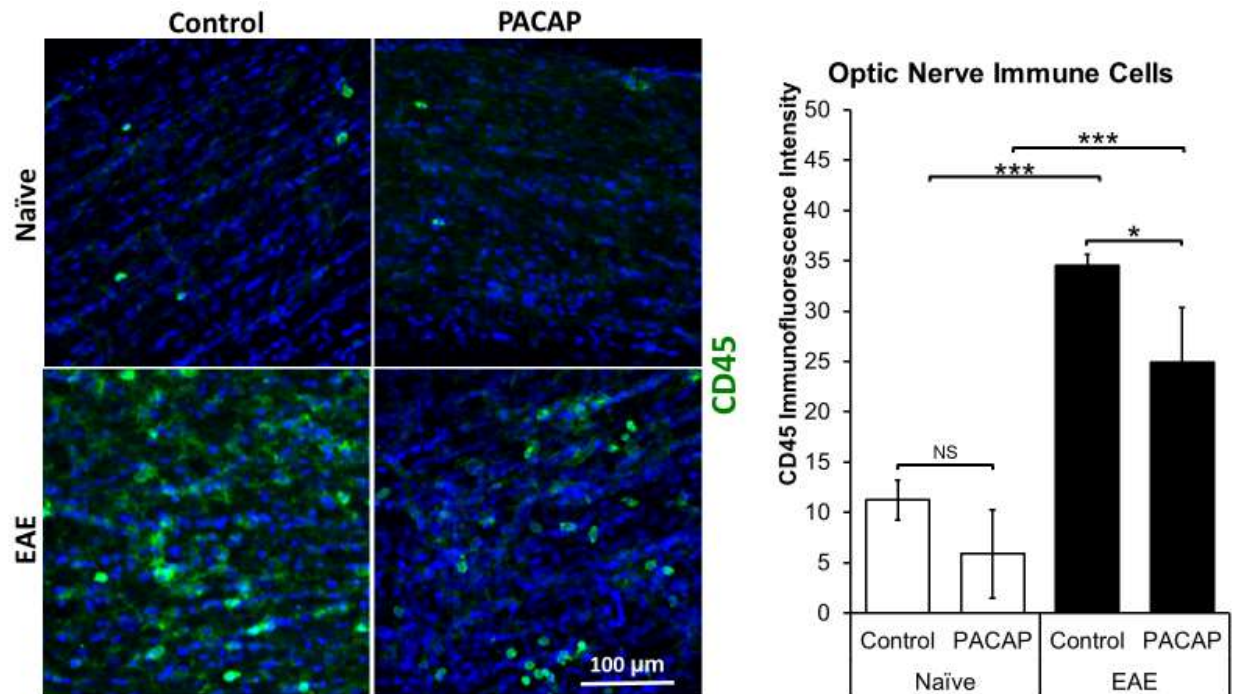


Figure 4-7. Effect of systemic administration of PHP.B AAV PACAP P2A tDimer or control virus on numbers of CD45 immunopositive cells in the optic nerve.

At postnatal day 2, pups received systemic injections of PHP.B AAV PACAP P2A tDimer or the control virus PHP.B AAV tDimer. At 6 weeks of age, chronic EAE was induced. Animals were sacrificed 60 days post EAE-induction. Optic nerves were collected and labeled for CD45, a pan immune marker (green) and nuclei (Hoescht). Number of animals: naïve control = 7, naïve PACAP =3, EAE Control = 8, EAE PACAP=3. Quantification performed blinded. Student's t-test. NS=not statistically significant. * $p < 0.05$, ** $p < 0.01$ *** $p < 0.001$. Error bars show SEM. 1 independent test.

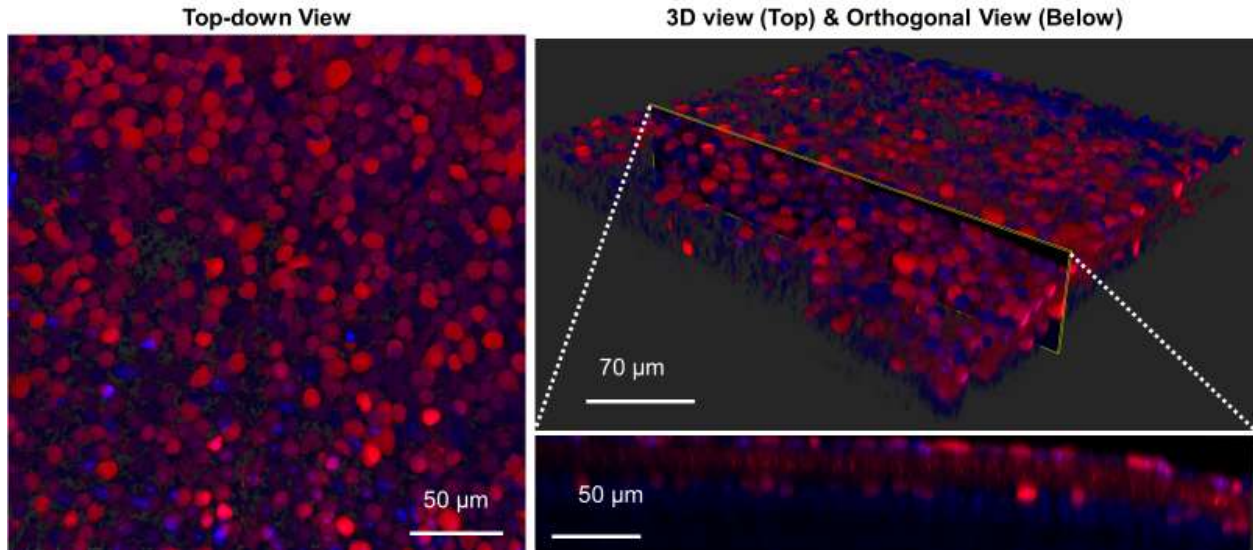


Figure 4-8. Viral reporter of intraocularly injected PHP.B AAV tDimer in retina.

The retina was harvested and flat mounted on a nylon membrane. Z-stack images were captured using a 20x objective. 3D blend mode in Imaris was used to visualize the image stack. Orthogonal view was used to visualize a YZ slice through the image stack. Blue = Hoescht, Red = native tDimer fluorescence.

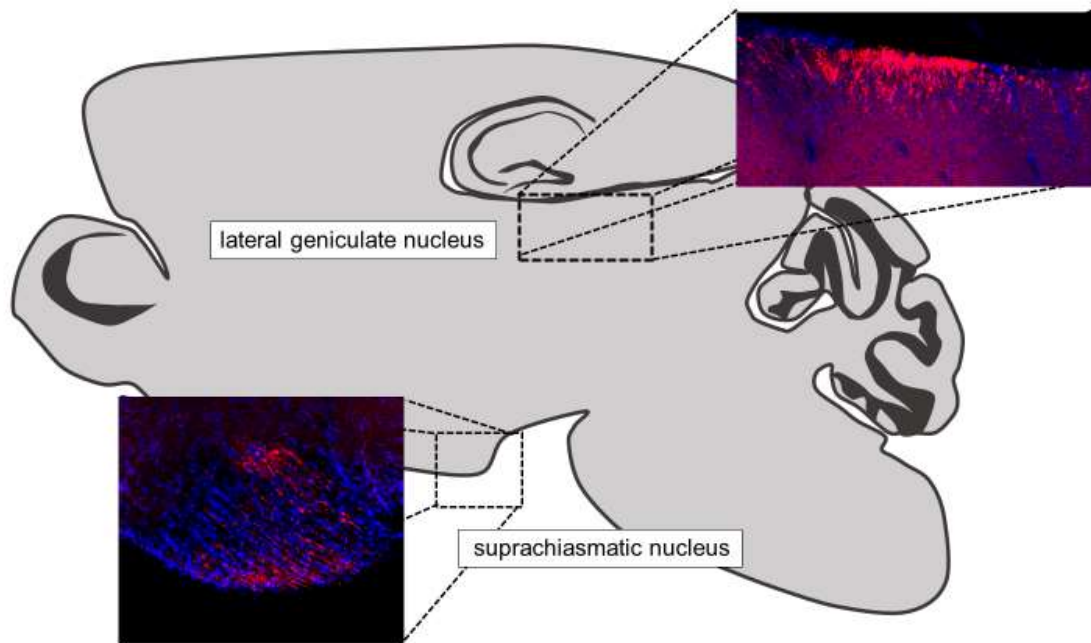


Figure 4-9. Viral reporter of intraocularly injected PHP.B AAV tDimer in the brain
At postnatal day 13, mice were intraocularly injected with PHP.B AAV tDimer. After 4 weeks, the animals were sacrificed, and brains collected to identify regions of native virus reporter expression. tDimer expression was detected in the fiber tracts of the lateral geniculate nucleus and the suprachiasmatic nucleus.

Chapter 5 – Conclusions, Limitations, and Future Studies

Pathological inflammation of the CNS is observed in many diseases, including multiple sclerosis, Alzheimer's Disease, stroke, and traumatic brain injury. These diseases are also characterized by neuron damage and loss. Inflammation and neurodegeneration in such diseases may be chronic and/or can lead to cognitive and motor impairment that severely impact daily life activities. Moreover, increasingly advanced medical technology has prolonged the average human lifespan, but with increased age comes the increased risk for developing neurodegenerative diseases. Identifying new strategies to control inflammation and protect neurons can lead to development of new treatments for neurodegenerative and inflammatory diseases. Current FDA approved drugs can reduce inflammation, but continual or residual inflammation nonetheless leads to cumulative neurodegeneration and worsening disease in patients. There is currently an unmet need for a therapeutic which can both reduce inflammation and protect against neurodegeneration.

An endogenous neuropeptide called PACAP has both neuroprotective and anti-inflammatory properties in several models of neurodegenerative diseases and is thus a candidate of interest for developing a therapeutic. In these studies, we chose to explore the role of the PAC1 receptor in the EAE model of multiple sclerosis based on previously published in our lab using PACAP and VPAC2 KO mice. Here, we investigated the abilities of PACAP action on its PAC1 receptor to reduce inflammation as well as protect against neuron loss and axonopathy. We tested two possible routes of action: 1) in which PACAP acts on PAC1 receptors expressed within a well-known neural circuit (the sympathetic nervous system) that modulates the inflammatory response, and 2) in which PACAP binds on PAC1 receptors on neural cells to protect against neurodegeneration. Then, we tested if PACAP overexpression could protect against EAE.

We first investigated PACAP's role in neuromodulation of inflammation by PAC1 receptors on catecholaminergic neurons, which includes neurons of the sympathetic nervous systems. We demonstrated time-dependent modulation of inflammation in a monophasic EAE model in which PAC1 signaling on catecholaminergic neurons surprisingly both promoted inflammatory T cell polarization and anti-inflammatory T_{reg} proliferation during disease development. The disease severity scores suggest that during disease development, PAC1 initially promotes EAE but later protects against EAE. However further work is needed to dissect the role of PAC1 on postganglionic neurons of the SNS on inflammatory responses as opposed to more general actions of PAC1 on catecholaminergic circuits. Furthermore, it is not yet known which intracellular pathways are activated by PAC1 to regulate T cell polarization or T_{reg} expansion during EAE development. Additionally, more investigation is required to better understand how PAC1's roles in these processes differ between disease development versus recovery in the monophasic EAE model and how will this impact development of a therapy. Our current findings of PAC1's role during disease development suggests that designing a therapy to optimize the benefits of PAC1's properties would ideally activate PAC1 signaling after active inflammation has already begun, thereby promoting recovery. However, specific and effective targeting of the postganglionic neurons of the SNS is challenging mainly because the size and location of these ganglia makes local targeting more or less unfeasible with current tools, and systemic administration of, for example, a small molecule PAC1 agonist could lead to widespread off-target effects due to PAC1 expression on other cell populations. More research is required to understand how to manipulate this neuromodulatory pathway. Nonetheless, the findings of this study not only identifies a mechanism by which to modulate SNS regulation of inflammation, it also identifies a possible mechanism to manipulate the SNS's other functions. This strategy to manipulate SNS

function could be applied to other diseases related to dysregulation of the SNS, including cardiovascular, metabolic, and psychiatric diseases.

We also investigated the role of PAC1 in protecting against optic neuritis by conditionally knocking out the PAC1 receptor in the retina. These findings in the model employed indicate that PAC1 is important for maintaining a subset of retinal ganglion neurons in the retina as well as the integrity of their dendrites and axons, surprisingly even in the absence of disease. Perhaps PAC1 promotes constitutive expression of key neurotrophic factors. Furthermore, PAC1 loss led to increased numbers of immune cells in the optic nerves, including microglia/macrophages, during EAE. This suggests that PAC1 signaling restricts inflammation in the optic nerve, but it is possible that these immune cells are pro-repair rather than pro-inflammatory at this time point. More work is needed to characterize these immune cells. Furthermore, it is not known how PAC1 regulates immune cells in the optic nerve. Given that PACAP has a role in promoting neuron survival, one possible mechanism that PAC1 indirectly regulates immune cells is by preventing cell death. The reduction in cellular debris during EAE would result in reduced numbers of responding microglia or macrophages, which would in turn release less pro-inflammatory chemokines to activate and recruit other immune cells. Also, it is known that neural cells do communicate with immune cells. Thus, another possible mechanism is that PAC1 signaling in neural cells plays a role in increasing or decreasing factors which promote or inhibit immune cell activation or recruitment. These findings can also be applied to other diseases of the eye, and although this study focused on the eye, these findings can also give us a glimpse into PAC1's role in inflammatory and neurodegenerative diseases of other regions of the CNS (i.e. the brain and spinal cord).

We also tested as a proof of principle whether administering PACAP could protect the CNS against EAE. We demonstrated that PACAP overexpression in the CNS using systemic administration of a CNS-trophic AAV led to delayed onset of EAE symptoms and reduced numbers of inflammatory cells in the optic nerve. These results indicate that PACAP-overexpressing can protect against optic neuritis in the context of EAE. In ongoing studies, we investigate whether local administration of this PACAP overexpressing AAV into the eye can protect against neuron loss and optic neuritis. Comparing the results from the systemic injection versus the local injection of the PACAP overexpressing virus will allow us to compare the capabilities and limitations of either system. Such findings are informative for efforts in developing methods to target therapeutics to specific regions of the CNS. Furthermore, the specific cells in the CNS infected by the virus need to be identified. Then, the cell-type specific increases in PACAP expression need to be evaluated as well as the effects of PACAP overexpression on these cells. Additionally, there needs to be a way to control the dosage of PACAP. Such methods include modifying the virus tropism further, identifying an optimal titer of the virus, using a more cell specific promoter, and adding a drug-inducible regulatory component to the expression cassette. In light of these results, developing protein or small molecule agonists of the PAC1 receptor are also of interest. Overall, the data highlights some capabilities of PACAP that could be applied to other diseases of the CNS.

In conclusion, these studies implicate PACAP and its PAC1 receptor as promising targets for developing therapeutics to manipulate the inflammatory response and to protect against neuron loss and axonopathy, particularly in the context of inflammatory neurodegenerative diseases.

REFERENCES

1. Yacoubian, T. A. Neurodegenerative Disorders. in *Drug Discovery Approaches for the Treatment of Neurodegenerative Disorders* 1–16 (Elsevier, 2017). doi:10.1016/B978-0-12-802810-0.00001-5
2. Batista, P. & Pereira, A. Quality of Life in Patients with Neurodegenerative Diseases. *J. Neurol. Neurosci.* **7**, (2016).
3. Hemmett, L., Holmes, J., Barnes, M. & Russell, N. What drives quality of life in multiple sclerosis? *QJM Int. J. Med.* **97**, 671–676 (2004).
4. Hadjimichael, O., Kerns, R. D., Rizzo, M. A., Cutter, G. & Vollmer, T. Persistent pain and uncomfortable sensations in persons with multiple sclerosis: *Pain* **127**, 35–41 (2007).
5. Ford, C. *et al.* Continuous long-term immunomodulatory therapy in relapsing multiple sclerosis: results from the 15-year analysis of the US prospective open-label study of glatiramer acetate. *Mult. Scler. Houndmills Basingstoke Engl.* **16**, 342–350 (2010).
6. Bornstein, M. B. *et al.* A pilot trial of Cop 1 in exacerbating-relapsing multiple sclerosis. *N. Engl. J. Med.* **317**, 408–414 (1987).
7. Comi, G., Filippi, M., Wolinsky, J. S. & European/Canadian Glatiramer Acetate Study Group. European/Canadian multicenter, double-blind, randomized, placebo-controlled study of the effects of glatiramer acetate on magnetic resonance imaging-measured disease activity and burden in patients with relapsing multiple sclerosis. *Ann. Neurol.* **49**, 290–297 (2001).
8. Martinelli Boneschi, F., Vacchi, L., Rovaris, M., Capra, R. & Comi, G. Mitoxantrone for multiple sclerosis. *Cochrane Database Syst. Rev.* (2013).
doi:10.1002/14651858.CD002127.pub3

9. Fox, E. J. Mechanism of action of mitoxantrone. *Neurology* **63**, S15-18 (2004).
10. Vollmer, T., Stewart, T. & Baxter, N. Mitoxantrone and cytotoxic drugs' mechanisms of action. *Neurology* **74**, S41–S46 (2010).
11. Murdoch, D. & Lyseng-Williamson, K. A. Spotlight on Subcutaneous Recombinant Interferon- β -1a (Rebif®) in Relapsing-Remitting Multiple Sclerosis. *BioDrugs* **19**, 323–325 (2005).
12. Randomised double-blind placebo-controlled study of interferon beta-1a in relapsing/remitting multiple sclerosis. PRISMS (Prevention of Relapses and Disability by Interferon beta-1a Subcutaneously in Multiple Sclerosis) Study Group. *Lancet Lond. Engl.* **352**, 1498–1504 (1998).
13. Markowitz, C. E. Interferon-beta: mechanism of action and dosing issues. *Neurology* **68**, S8-11 (2007).
14. Kieseier, B. C. The Mechanism of Action of Interferon- β in Relapsing Multiple Sclerosis. *CNS Drugs* **25**, 491–502 (2011).
15. Shirani, A. *et al.* Association Between Use of Interferon Beta and Progression of Disability in Patients With Relapsing-Remitting Multiple Sclerosis. *JAMA* **308**, (2012).
16. Kappos, L. *et al.* Factors influencing long-term outcomes in relapsing–remitting multiple sclerosis: PRISMS-15. *J. Neurol. Neurosurg. Psychiatry* **86**, 1202–1207 (2015).
17. Jacobs, L. D. *et al.* Intramuscular interferon beta-1a for disease progression in relapsing multiple sclerosis. *Ann. Neurol.* **39**, 285–294 (1996).
18. Hutchinson, M. Natalizumab: A new treatment for relapsing remitting multiple sclerosis. *Ther. Clin. Risk Manag.* **3**, 259–268 (2007).

19. Brandstadter, R. & Katz Sand, I. The use of natalizumab for multiple sclerosis. *Neuropsychiatr. Dis. Treat.* **Volume 13**, 1691–1702 (2017).
20. Shirani, A. & Stüve, O. Natalizumab for Multiple Sclerosis: A Case in Point for the Impact of Translational Neuroimmunology. *J. Immunol.* **198**, 1381–1386 (2017).
21. Singer, B. A. The role of natalizumab in the treatment of multiple sclerosis: benefits and risks. *Ther. Adv. Neurol. Disord.* **10**, 327–336 (2017).
22. Delbue, S., Comar, M. & Ferrante, P. Natalizumab treatment of multiple sclerosis: new insights. *Immunotherapy* **9**, 157–171 (2017).
23. Sanford, M. Fingolimod: A Review of Its Use in Relapsing-Remitting Multiple Sclerosis. *Drugs* **74**, 1411–1433 (2014).
24. Sanchez, T. *et al.* Phosphorylation and Action of the Immunomodulator FTY720 Inhibits Vascular Endothelial Cell Growth Factor-induced Vascular Permeability. *J. Biol. Chem.* **278**, 47281–47290 (2003).
25. Adachi, K. & Chiba, K. FTY720 story. Its discovery and the following accelerated development of sphingosine 1-phosphate receptor agonists as immunomodulators based on reverse pharmacology. *Perspect. Med. Chem.* **1**, 11–23 (2007).
26. Chun, J. & Hartung, H.-P. Mechanism of Action of Oral Fingolimod (FTY720) in Multiple Sclerosis. *Clin. Neuropharmacol.* **33**, 91–101 (2010).
27. O'Connor, P. *et al.* Randomized Trial of Oral Teriflunomide for Relapsing Multiple Sclerosis. *N. Engl. J. Med.* **365**, 1293–1303 (2011).
28. Miller, A. E. Teriflunomide in multiple sclerosis: an update. *Neurodegener. Dis. Manag.* **7**, 9–29 (2017).

29. Confavreux, C. *et al.* Oral teriflunomide for patients with relapsing multiple sclerosis (TOWER): a randomised, double-blind, placebo-controlled, phase 3 trial. *Lancet Neurol.* **13**, 247–256 (2014).
30. Oh, J. & O’Connor, P. W. Teriflunomide in the treatment of multiple sclerosis: current evidence and future prospects. *Ther. Adv. Neurol. Disord.* **7**, 239–252 (2014).
31. Linker, R. A. & Haghikia, A. Dimethyl fumarate in multiple sclerosis: latest developments, evidence and place in therapy. *Ther. Adv. Chronic Dis.* **7**, 198–207 (2016).
32. Bompreszi, R. Dimethyl fumarate in the treatment of relapsing-remitting multiple sclerosis: an overview. *Ther. Adv. Neurol. Disord.* **8**, 20–30 (2015).
33. Havrdova, E., Horakova, D. & Kovarova, I. Alemtuzumab in the treatment of multiple sclerosis: key clinical trial results and considerations for use. *Ther. Adv. Neurol. Disord.* **8**, 31–45 (2015).
34. Coles, A. J. *et al.* Alemtuzumab CARE-MS II 5-year follow-up: Efficacy and safety findings. *Neurology* **89**, 1117–1126 (2017).
35. Gallo, P., Centonze, D. & Marrosu, M. G. Alemtuzumab for multiple sclerosis: the new concept of immunomodulation. *Mult. Scler. Demyelinating Disord.* **2**, (2017).
36. Zhang, X. *et al.* Differential Reconstitution of T Cell Subsets following Immunodepleting Treatment with Alemtuzumab (Anti-CD52 Monoclonal Antibody) in Patients with Relapsing-Remitting Multiple Sclerosis. *J. Immunol.* **191**, 5867–5874 (2013).
37. Ziemssen, T. & Thomas, K. Alemtuzumab in the long-term treatment of relapsing-remitting multiple sclerosis: an update on the clinical trial evidence and data from the real world. *Ther. Adv. Neurol. Disord.* **10**, 343–359 (2017).

38. Shirley, M. Daclizumab: A Review in Relapsing Multiple Sclerosis. *Drugs* **77**, 447–458 (2017).
39. Kappos, L. *et al.* Daclizumab HYP versus Interferon Beta-1a in Relapsing Multiple Sclerosis. *N. Engl. J. Med.* **373**, 1418–1428 (2015).
40. Liu, S., Liu, X., Chen, S., Xiao, Y. & Zhuang, W. Oral versus intravenous methylprednisolone for the treatment of multiple sclerosis relapses: A meta-analysis of randomized controlled trials. *PLOS ONE* **12**, e0188644 (2017).
41. Brusafferri, F. & Candelise, L. Steroids for multiple sclerosis and optic neuritis: a meta-analysis of randomized controlled clinical trials. *J. Neurol.* **247**, 435–442 (2000).
42. Zivadinov, R. *et al.* Effects of IV methylprednisolone on brain atrophy in relapsing-remitting MS. *Neurology* **57**, 1239–1247 (2001).
43. Baranzini, S. E. & Oksenberg, J. R. The Genetics of Multiple Sclerosis: From 0 to 200 in 50 Years. *Trends Genet.* **33**, 960–970 (2017).
44. O’Gorman, C., Lucas, R. & Taylor, B. Environmental Risk Factors for Multiple Sclerosis: A Review with a Focus on Molecular Mechanisms. *Int. J. Mol. Sci.* **13**, 11718–11752 (2012).
45. Frau, J., Coghe, G., Loreface, L., Fenu, G. & Cocco, E. New horizons for multiple sclerosis therapeutics: milestones in the development of ocrelizumab. *Neuropsychiatr. Dis. Treat.* **Volume 14**, 1093–1099 (2018).
46. Mulero, P., Midaglia, L. & Montalban, X. Ocrelizumab: a new milestone in multiple sclerosis therapy. *Ther. Adv. Neurol. Disord.* **11**, 175628641877302 (2018).
47. Thompson, A. J., Toosy, A. T. & Ciccarelli, O. Pharmacological management of symptoms in multiple sclerosis: current approaches and future directions. *Lancet Neurol.* **9**, 1182–1199 (2010).

48. Voskuhl, R. R. *et al.* Estriol combined with glatiramer acetate for women with relapsing-remitting multiple sclerosis: a randomised, placebo-controlled, phase 2 trial. *Lancet Neurol.* **15**, 35–46 (2016).
49. Bose, G., Atkins, H. L., Bowman, M. & Freedman, M. S. Autologous hematopoietic stem cell transplantation improves fatigue in multiple sclerosis. *Mult. Scler. J.* 135245851880254 (2018). doi:10.1177/1352458518802544
50. Muraro, P. A. *et al.* Long-term Outcomes After Autologous Hematopoietic Stem Cell Transplantation for Multiple Sclerosis. *JAMA Neurol.* **74**, 459 (2017).
51. Mancardi, G. L. *et al.* Autologous hematopoietic stem cell transplantation in multiple sclerosis: A phase II trial. *Neurology* **84**, 981–988 (2015).
52. Genc, B., Bozan, H. R., Genc, S. & Genc, K. Stem Cell Therapy for Multiple Sclerosis. in (Springer US, 2018). doi:10.1007/5584_2018_247
53. Lublin, F. D. *et al.* Human placenta-derived cells (PDA-001) for the treatment of adults with multiple sclerosis: A randomized, placebo-controlled, multiple-dose study. *Mult. Scler. Relat. Disord.* **3**, 696–704 (2014).
54. Llufriu, S. *et al.* Randomized Placebo-Controlled Phase II Trial of Autologous Mesenchymal Stem Cells in Multiple Sclerosis. *PLoS ONE* **9**, e113936 (2014).
55. Connick, P. *et al.* Autologous mesenchymal stem cells for the treatment of secondary progressive multiple sclerosis: an open-label phase 2a proof-of-concept study. *Lancet Neurol.* **11**, 150–156 (2012).
56. Sergiyivna Sych, N. *et al.* Complex Treatment of Multiple Sclerosis Patients by Use of Fetal Stem Cells. *J. Stem Cell Res. Ther.* **07**, (2017).

57. Senders, A. *et al.* Impact of mindfulness-based stress reduction for people with multiple sclerosis at 8 weeks and 12 months: A randomized clinical trial. *Mult. Scler. J.* 135245851878665 (2018). doi:10.1177/1352458518786650
58. Gilbertson, R. M. & Klatt, M. D. Mindfulness in Motion for People with Multiple Sclerosis: A Feasibility Study. *Int. J. MS Care* **19**, 225–231 (2017).
59. Crawford, D. K. *et al.* Oestrogen receptor beta ligand: a novel treatment to enhance endogenous functional remyelination. *Brain J. Neurol.* **133**, 2999–3016 (2010).
60. Mangiardi, M. *et al.* An animal model of cortical and callosal pathology in multiple sclerosis. *Brain Pathol. Zurich Switz.* **21**, 263–278 (2011).
61. Morales, L. B. J. *et al.* Treatment with an estrogen receptor alpha ligand is neuroprotective in experimental autoimmune encephalomyelitis. *J. Neurosci. Off. J. Soc. Neurosci.* **26**, 6823–6833 (2006).
62. Constantinescu, C. S., Farooqi, N., O'Brien, K. & Gran, B. Experimental autoimmune encephalomyelitis (EAE) as a model for multiple sclerosis (MS). *Br. J. Pharmacol.* **164**, 1079–1106 (2011).
63. Greenfield, A. L. & Hauser, S. L. B-cell Therapy for Multiple Sclerosis: Entering an era: MS: Entering the Era of B-Cell Therapy. *Ann. Neurol.* **83**, 13–26 (2018).
64. Allan, S. Balancing B-cell subsets in EAE: Autoimmunity. *Nat. Rev. Immunol.* **8**, 825–825 (2008).
65. Sefia, E., Pryce, G., Meier, U.-C., Giovannoni, G. & Baker, D. Depletion of CD20 B cells fails to inhibit relapsing mouse experimental autoimmune encephalomyelitis. *Mult. Scler. Relat. Disord.* **14**, 46–50 (2017).

66. Constantinescu, C. S., Farooqi, N., O'Brien, K. & Gran, B. Experimental autoimmune encephalomyelitis (EAE) as a model for multiple sclerosis (MS). *Br. J. Pharmacol.* **164**, 1079–1106 (2011).
67. Bolton, C. The translation of drug efficacy from in vivo models to human disease with special reference to experimental autoimmune encephalomyelitis and multiple sclerosis. *Inflammopharmacology* **15**, 183–187 (2007).
68. Steinman, L. & Zamvil, S. S. Virtues and pitfalls of EAE for the development of therapies for multiple sclerosis. *Trends Immunol.* **26**, 565–571 (2005).
69. Friese, M. A. The value of animal models for drug development in multiple sclerosis. *Brain* **129**, 1940–1952 (2006).
70. Miyata, A. *et al.* Isolation of a novel 38 residue-hypothalamic polypeptide which stimulates adenylate cyclase in pituitary cells. *Biochem. Biophys. Res. Commun.* **164**, 567–574 (1989).
71. Vaudry, D. *et al.* Pituitary adenylate cyclase-activating polypeptide and its receptors: from structure to functions. *Pharmacol. Rev.* **52**, 269–324 (2000).
72. Brifault, C. *et al.* Delayed Pituitary Adenylate Cyclase–Activating Polypeptide Delivery After Brain Stroke Improves Functional Recovery by Inducing M2 Microglia/Macrophage Polarization. *Stroke* STROKEAHA.114.006864 (2014).
doi:10.1161/STROKEAHA.114.006864
73. Chen, W.-H. & Tzeng, S.-F. Pituitary adenylate cyclase-activating polypeptide prevents cell death in the spinal cord with traumatic injury. *Neurosci. Lett.* **384**, 117–121 (2005).
74. Chen, Y. *et al.* Neuroprotection by endogenous and exogenous PACAP following stroke. *Regul. Pept.* **137**, 4–19 (2006).

75. Lee, E. H. & Seo, S. R. Neuroprotective roles of pituitary adenylate cyclase-activating polypeptide in neurodegenerative diseases. *BMB Rep.* **47**, 369–375 (2014).
76. Reglodi, D., Kiss, P., Lubics, A. & Tamas, A. Review on the protective effects of PACAP in models of neurodegenerative diseases in vitro and in vivo. *Curr. Pharm. Des.* **17**, 962–972 (2011).
77. Waschek, J. VIP and PACAP: neuropeptide modulators of CNS inflammation, injury, and repair. *Br. J. Pharmacol.* **169**, 512–523 (2013).
78. Seaborn, T., Masmoudi-Kouli, O., Fournier, A., Vaudry, H. & Vaudry, D. Protective effects of pituitary adenylate cyclase-activating polypeptide (PACAP) against apoptosis. *Curr. Pharm. Des.* **17**, 204–214 (2011).
79. Dejda, A. *et al.* Inhibitory effect of PACAP on caspase activity in neuronal apoptosis: a better understanding towards therapeutic applications in neurodegenerative diseases. *J. Mol. Neurosci. MN* **36**, 26–37 (2008).
80. Laburthe, M., Couvineau, A. & Tan, V. Class II G protein-coupled receptors for VIP and PACAP: Structure, models of activation and pharmacology. *Peptides* **28**, 1631–1639 (2007).
81. Dickson, L. & Finlayson, K. VPAC and PAC receptors: From ligands to function. *Pharmacol. Ther.* **121**, 294–316 (2009).
82. Said, S. I. & Mutt, V. Polypeptide with broad biological activity: isolation from small intestine. *Science* **169**, 1217–1218 (1970).
83. Delgado, M., Pozo, D. & Ganea, D. The significance of vasoactive intestinal peptide in immunomodulation. *Pharmacol. Rev.* **56**, 249–290 (2004).

84. Shivers, B. D., Görös, T. J., Gottschall, P. E. & Arimura, A. Two High Affinity Binding Sites for Pituitary Adenylate Cyclase-Activating Polypeptide Have Different Tissue Distributions*. *Endocrinology* **128**, 3055–3065 (1991).
85. Vaudry, D. *et al.* Pituitary adenylate cyclase-activating polypeptide and its receptors: 20 years after the discovery. *Pharmacol. Rev.* **61**, 283–357 (2009).
86. Baranzini, S. E. *et al.* Genome-wide association analysis of susceptibility and clinical phenotype in multiple sclerosis. *Hum. Mol. Genet.* **18**, 767–778 (2009).
87. Cunningham, S. *et al.* The neuropeptide genes TAC1, TAC3, TAC4, VIP and PACAP(ADCYAP1), and susceptibility to multiple sclerosis. *J. Neuroimmunol.* **183**, 208–213 (2007).
88. Burton, P. R. *et al.* Association scan of 14,500 nonsynonymous SNPs in four diseases identifies autoimmunity variants. *Nat. Genet.* **39**, 1329–1337 (2007).
89. Sun, W., Hong, J., Zang, Y. C. Q., Liu, X. & Zhang, J. Z. Altered expression of vasoactive intestinal peptide receptors in T lymphocytes and aberrant Th1 immunity in multiple sclerosis. *Int. Immunol.* **18**, 1691–1700 (2006).
90. Kato, H. *et al.* Pituitary adenylate cyclase-activating polypeptide (PACAP) ameliorates experimental autoimmune encephalomyelitis by suppressing the functions of antigen presenting cells. *Mult. Scler. Houndmills Basingstoke Engl.* **10**, 651–659 (2004).
91. Tan, Y.-V. *et al.* Pituitary adenylyl cyclase-activating polypeptide is an intrinsic regulator of Treg abundance and protects against experimental autoimmune encephalomyelitis. *Proc. Natl. Acad. Sci. U. S. A.* **106**, 2012–2017 (2009).

92. Tan, Y.-V., Abad, C., Wang, Y., Lopez, R. & Waschek, J. A. Pituitary Adenylate Cyclase Activating Peptide Deficient Mice Exhibit Impaired Thymic and Extrathymic Regulatory T Cell Proliferation during EAE. *PLoS ONE* **8**, e61200 (2013).
93. Tan, Y.-V. *et al.* Pituitary adenylyl cyclase-activating polypeptide is an intrinsic regulator of Treg abundance and protects against experimental autoimmune encephalomyelitis. *Proc. Natl. Acad. Sci.* **106**, 2012–2017 (2009).
94. Tan, Y.-V., Abad, C., Wang, Y., Lopez, R. & Waschek, J. A. VPAC2 (vasoactive intestinal peptide receptor type 2) receptor deficient mice develop exacerbated experimental autoimmune encephalomyelitis with increased Th1/Th17 and reduced Th2/Treg responses. *Brain. Behav. Immun.* **44**, 167–175 (2015).
95. Abad, C. *et al.* VPAC1 receptor (Vipr1)-deficient mice exhibit ameliorated experimental autoimmune encephalomyelitis, with specific deficits in the effector stage. *J. Neuroinflammation* **13**, (2016).
96. Abad, C. *et al.* Vasoactive intestinal peptide loss leads to impaired CNS parenchymal T-cell infiltration and resistance to experimental autoimmune encephalomyelitis. *Proc. Natl. Acad. Sci.* **107**, 19555–19560 (2010).
97. Martinez, C., Delgado, M., Gomariz, R. P. & Ganea, D. Vasoactive intestinal peptide and pituitary adenylate cyclase-activating polypeptide-38 inhibit IL-10 production in murine T lymphocytes. *J. Immunol.* **156**, 4128 (1996).
98. Wang, H. Y. *et al.* Vasoactive intestinal peptide inhibits cytokine production in T lymphocytes through cAMP-dependent and cAMP-independent mechanisms. *Regul. Pept.* **84**, 55–67 (1999).

99. Fabricius, D., O'Dorisio, M. S., Blackwell, S. & Jahrsdorfer, B. Human Plasmacytoid Dendritic Cell Function: Inhibition of IFN- Secretion and Modulation of Immune Phenotype by Vasoactive Intestinal Peptide. *J. Immunol.* **177**, 5920–5927 (2006).
100. Lara-Marquez, M., O'Dorisio, M., O'Dorisio, T., Shah, M. & Karacay, B. Selective gene expression and activation-dependent regulation of vasoactive intestinal peptide receptor type 1 and type 2 in human T cells. *J. Immunol. Baltim. Md 1950* **166**, 2522–2530 (2001).
101. Beaudet, M. M., Braas, K. M. & May, V. Pituitary adenylate cyclase activating polypeptide (PACAP) expression in sympathetic preganglionic projection neurons to the superior cervical ganglion. *J. Neurobiol.* **36**, 325–336 (1998).
102. Braas, K. M. & May, V. Pituitary Adenylate Cyclase-activating Polypeptides Directly Stimulate Sympathetic Neuron Neuropeptide Y Release through PAC1 Receptor Isoform Activation of Specific Intracellular Signaling Pathways. *J. Biol. Chem.* **274**, 27702–27710 (1999).
103. Diane, A. *et al.* PACAP is essential for the adaptive thermogenic response of brown adipose tissue to cold exposure. *J. Endocrinol.* **222**, 327–339 (2014).
104. Seaborn, T., Masmoudi-Kouli, O., Fournier, A., Vaudry, H. & Vaudry, D. Protective effects of pituitary adenylate cyclase-activating polypeptide (PACAP) against apoptosis. *Curr. Pharm. Des.* **17**, 204–214 (2011).
105. Rozzi, S. J. *et al.* PACAP27 is protective against tat-induced neurotoxicity. *J. Mol. Neurosci. MN* **54**, 485–493 (2014).
106. Szabadfi, K. *et al.* Protective effects of the neuropeptide PACAP in diabetic retinopathy. *Cell Tissue Res.* **348**, 37–46 (2012).

107. Szabadfi, K. *et al.* PACAP promotes neuron survival in early experimental diabetic retinopathy. *Neurochem. Int.* **64**, 84–91 (2014).
108. Ziemssen, T. Modulating processes within the central nervous system is central to therapeutic control of multiple sclerosis. *J. Neurol.* **252**, v38–v45 (2005).
109. Bellinger, D. L. *et al.* Sympathetic modulation of immunity: Relevance to disease. *Cell. Immunol.* **252**, 27–56 (2008).
110. Kenney, M. & Ganta, C. Autonomic Nervous System and Immune System Interactions. *Compr. Physiol.* **4**, 1177–1200 (2014).
111. Elenkov, I. J., Wilder, R. L., Chrousos, G. P. & Vizi, E. S. The sympathetic nerve--an integrative interface between two supersystems: the brain and the immune system. *Pharmacol. Rev.* **52**, 595–638 (2000).
112. Dube, S. R. *et al.* Cumulative Childhood Stress and Autoimmune Diseases in Adults: *Psychosom. Med.* **71**, 243–250 (2009).
113. Elenkov, I. J. & Chrousos, G. P. Stress Hormones, Proinflammatory and Antiinflammatory Cytokines, and Autoimmunity. *Ann. N. Y. Acad. Sci.* **966**, 290–303 (2002).
114. Geenen, R. The Impact of Stressors on Health Status and Hypothalamic-Pituitary-Adrenal Axis and Autonomic Nervous System Responsiveness in Rheumatoid Arthritis. *Ann. N. Y. Acad. Sci.* **1069**, 77–97 (2006).
115. Johnson, E. O., Kostandi, M. & Moutsopoulos, H. M. Hypothalamic-Pituitary-Adrenal Axis Function in Sjogren's Syndrome: Mechanisms of Neuroendocrine and Immune System Homeostasis. *Ann. N. Y. Acad. Sci.* **1088**, 41–51 (2006).

116. Straub, R. H., Dhabhar, F. S., Bijlsma, J. W. J. & Cutolo, M. How psychological stress via hormones and nerve fibers may exacerbate rheumatoid arthritis. *Arthritis Rheum.* **52**, 16–26 (2005).
117. Abdollahpour, I., Nedjat, S., Mansournia, M. A., Eckert, S. & Weinstock-Guttman, B. Stress-full life events and multiple sclerosis: A population-based incident case-control study. *Mult. Scler. Relat. Disord.* **26**, 168–172 (2018).
118. O’Donovan, A. *et al.* Elevated Risk for Autoimmune Disorders in Iraq and Afghanistan Veterans with Posttraumatic Stress Disorder. *Biol. Psychiatry* **77**, 365–374 (2015).
119. Roberts, A. L. *et al.* Association of Trauma and Posttraumatic Stress Disorder With Incident Systemic Lupus Erythematosus in a Longitudinal Cohort of Women. *Arthritis Rheumatol.* **69**, 2162–2169 (2017).
120. Warren, S., Greenhill, S. & Warren, K. G. Emotional stress and the development of multiple sclerosis: case-control evidence of a relationship. *J. Chronic Dis.* **35**, 821–831 (1982).
121. Sternberg, Z. Promoting sympathovagal balance in multiple sclerosis; pharmacological, non-pharmacological, and surgical strategies. *Autoimmun. Rev.* **15**, 113–123 (2016).
122. Nance, D. M. & Sanders, V. M. Autonomic innervation and regulation of the immune system (1987–2007). *Brain. Behav. Immun.* **21**, 736–745 (2007).
123. Bhowmick, S. *et al.* The sympathetic nervous system modulates CD4+FoxP3+ regulatory T cells via a TGF- β -dependent mechanism. *J. Leukoc. Biol.* **86**, 1275–1283 (2009).
124. Wirth, T. *et al.* The sympathetic nervous system modulates CD4+Foxp3+ regulatory T cells via noradrenaline-dependent apoptosis in a murine model of lymphoproliferative disease. *Brain. Behav. Immun.* **38**, 100–110 (2014).

125. Nance, D. M. & Sanders, V. M. Autonomic innervation and regulation of the immune system (1987-2007). *Brain. Behav. Immun.* **21**, 736–745 (2007).
126. Sanders, V. M., Kasproicz, D. J., Swanson-Mungerson, M. A., Podojil, J. R. & Kohm, A. P. Adaptive immunity in mice lacking the beta(2)-adrenergic receptor. *Brain. Behav. Immun.* **17**, 55–67 (2003).
127. Shadiack, A. M., Sun, Y. & Zigmond, R. E. Nerve growth factor antiserum induces axotomy-like changes in neuropeptide expression in intact sympathetic and sensory neurons. *J. Neurosci. Off. J. Soc. Neurosci.* **21**, 363–371 (2001).
128. Zhu, J. & Paul, W. E. CD4 T cells: fates, functions, and faults. *Blood* **112**, 1557–1569 (2008).
129. Abdul-Majid, K.-B. *et al.* Comparing the pathogenesis of experimental autoimmune encephalomyelitis in CD4^{-/-} and CD8^{-/-} DBA/1 mice defines qualitative roles of different T cell subsets. *J. Neuroimmunol.* **141**, 10–19 (2003).
130. Sonobe, Y. *et al.* Chronological changes of CD4(+) and CD8(+) T cell subsets in the experimental autoimmune encephalomyelitis, a mouse model of multiple sclerosis. *Tohoku J. Exp. Med.* **213**, 329–339 (2007).
131. Petermann, F. & Korn, T. Cytokines and effector T cell subsets causing autoimmune CNS disease. *FEBS Lett.* **585**, 3747–3757 (2011).
132. Fletcher, J. M., Lalor, S. J., Sweeney, C. M., Tubridy, N. & Mills, K. H. G. T cells in multiple sclerosis and experimental autoimmune encephalomyelitis. *Clin. Exp. Immunol.* **162**, 1–11 (2010).
133. Gocke, A. R. *et al.* T-bet Regulates the Fate of Th1 and Th17 Lymphocytes in Autoimmunity. *J. Immunol.* **178**, 1341–1348 (2007).

134. Fernando, V. *et al.* Regulation of an Autoimmune Model for Multiple Sclerosis in Th2-Biased GATA3 Transgenic Mice. *Int. J. Mol. Sci.* **15**, 1700–1718 (2014).
135. Cua, D. J., Groux, H., Hinton, D. R., Stohlman, S. A. & Coffman, R. L. Transgenic interleukin 10 prevents induction of experimental autoimmune encephalomyelitis. *J. Exp. Med.* **189**, 1005–1010 (1999).
136. Croxford, J. L., Feldmann, M., Chernajovsky, Y. & Baker, D. Different therapeutic outcomes in experimental allergic encephalomyelitis dependent upon the mode of delivery of IL-10: a comparison of the effects of protein, adenoviral or retroviral IL-10 delivery into the central nervous system. *J. Immunol. Baltim. Md 1950* **166**, 4124–4130 (2001).
137. Jäger, A., Dardalhon, V., Sobel, R. A., Bettelli, E. & Kuchroo, V. K. Th1, Th17, and Th9 effector cells induce experimental autoimmune encephalomyelitis with different pathological phenotypes. *J. Immunol. Baltim. Md 1950* **183**, 7169–7177 (2009).
138. Bettelli, E. *et al.* Loss of T-bet, but not STAT1, prevents the development of experimental autoimmune encephalomyelitis. *J. Exp. Med.* **200**, 79–87 (2004).
139. Hilliard, B. & Chen, Y. H. Immunomodulation of EAE: Altered Peptide Ligands, Tolerance, and Th1/Th2. in *Experimental Models of Multiple Sclerosis* (eds. Lavi, E. & Constantinescu, C. S.) 451–470 (Springer US, 2005).
140. Domingues, H. S., Mues, M., Lassmann, H., Wekerle, H. & Krishnamoorthy, G. Functional and Pathogenic Differences of Th1 and Th17 Cells in Experimental Autoimmune Encephalomyelitis. *PLoS ONE* **5**, e15531 (2010).
141. Pedotti, R. *et al.* Allergy and multiple sclerosis: a population-based case-control study. *Mult. Scler.* **15**, 899–906 (2009).

142. Tremlett, H. L., Evans, J., Wiles, C. M. & Luscombe, D. K. Asthma and multiple sclerosis: an inverse association in a case-control general practice population. *QJM Mon. J. Assoc. Physicians* **95**, 753–756 (2002).
143. Stohlman, S. A., Pei, L., Cua, D. J., Li, Z. & Hinton, D. R. Activation of regulatory cells suppresses experimental allergic encephalomyelitis via secretion of IL-10. *J. Immunol. Baltim. Md 1950* **163**, 6338–6344 (1999).
144. Sakaguchi, S., Sakaguchi, N., Asano, M., Itoh, M. & Toda, M. Immunologic self-tolerance maintained by activated T cells expressing IL-2 receptor alpha-chains (CD25). Breakdown of a single mechanism of self-tolerance causes various autoimmune diseases. *J. Immunol.* **155**, 1151 (1995).
145. Asano, M. Autoimmune disease as a consequence of developmental abnormality of a T cell subpopulation. *J. Exp. Med.* **184**, 387–396 (1996).
146. Bennett, C. L. *et al.* The immune dysregulation, polyendocrinopathy, enteropathy, X-linked syndrome (IPEX) is caused by mutations of FOXP3. *Nat. Genet.* **27**, 20–21 (2001).
147. Brunkow, M. E. *et al.* Disruption of a new forkhead/winged-helix protein, scurf, results in the fatal lymphoproliferative disorder of the scurfy mouse. *Nat. Genet.* **27**, 68–73 (2001).
148. Itoh, M. *et al.* Thymus and autoimmunity: production of CD25+CD4+ naturally anergic and suppressive T cells as a key function of the thymus in maintaining immunologic self-tolerance. *J. Immunol. Baltim. Md 1950* **162**, 5317–5326 (1999).
149. Sakaguchi, S., Yamaguchi, T., Nomura, T. & Ono, M. Regulatory T Cells and Immune Tolerance. *Cell* **133**, 775–787 (2008).
150. Piccirillo, C. A. & Thornton, A. M. Cornerstone of peripheral tolerance: naturally occurring CD4+CD25+ regulatory T cells. *Trends Immunol.* **25**, 374–380 (2004).

151. Kim, J. M., Rasmussen, J. P. & Rudensky, A. Y. Regulatory T cells prevent catastrophic autoimmunity throughout the lifespan of mice. *Nat. Immunol.* **8**, 191–197 (2007).
152. Abad, C. *et al.* Vasoactive intestinal peptide loss leads to impaired CNS parenchymal T-cell infiltration and resistance to experimental autoimmune encephalomyelitis. *Proc. Natl. Acad. Sci.* **107**, 19555–19560 (2010).
153. Tan, Y.-V. *et al.* Pituitary adenylyl cyclase-activating polypeptide is an intrinsic regulator of Treg abundance and protects against experimental autoimmune encephalomyelitis. *Proc. Natl. Acad. Sci. U. S. A.* **106**, 2012–2017 (2009).
154. Miyata, A. *et al.* Isolation of a novel 38 residue-hypothalamic polypeptide which stimulates adenylate cyclase in pituitary cells. *Biochem. Biophys. Res. Commun.* **164**, 567–574 (1989).
155. Waschek, J. VIP and PACAP: neuropeptide modulators of CNS inflammation, injury, and repair: VIP and PACAP in neural injury. *Br. J. Pharmacol.* **169**, 512–523 (2013).
156. Pettersson, L. M. E., Heine, T., Verge, V. M. K., Sundler, F. & Danielsen, N. PACAP mRNA is expressed in rat spinal cord neurons. *J. Comp. Neurol.* **471**, 85–96 (2004).
157. DiCicco-Bloom, E. *et al.* Autocrine Expression and Ontogenetic Functions of the PACAP Ligand/Receptor System during Sympathetic Development. *Dev. Biol.* **219**, 197–213 (2000).
158. Lu, N., Zhou, R. & DiCicco-Bloom, E. Opposing mitogenic regulation by PACAP in sympathetic and cerebral cortical precursors correlates with differential expression of PACAP receptor (PAC1-R) isoforms. *J. Neurosci. Res.* **53**, 651–662 (1998).
159. Stubbusch, J. *et al.* Generation of the tamoxifen-inducible DBH-Cre transgenic mouse line DBH-CT. *Genes. N. Y. N 2000* **49**, 935–941 (2011).

160. Jamen, F. *et al.* PAC1 receptor-deficient mice display impaired insulinotropic response to glucose and reduced glucose tolerance. *J. Clin. Invest.* **105**, 1307–1315 (2000).
161. Otto, C. Pulmonary Hypertension and Right Heart Failure in Pituitary Adenylate Cyclase-Activating Polypeptide Type I Receptor-Deficient Mice. *Circulation* **110**, 3245–3251 (2004).
162. Olivas, A. *et al.* Myocardial Infarction Causes Transient Cholinergic Transdifferentiation of Cardiac Sympathetic Nerves via gp130. *J. Neurosci. Off. J. Soc. Neurosci.* **36**, 479–488 (2016).
163. Tsarovina, K. *et al.* The Gata3 transcription factor is required for the survival of embryonic and adult sympathetic neurons. *J. Neurosci. Off. J. Soc. Neurosci.* **30**, 10833–10843 (2010).
164. Damsker, J. M., Hansen, A. M. & Caspi, R. R. Th1 and Th17 cells. *Ann. N. Y. Acad. Sci.* **1183**, 211–221 (2010).
165. Lafaille, J. J. The role of helper T cell subsets in autoimmune diseases. *Cytokine Growth Factor Rev.* **9**, 139–151 (1998).
166. Simmons, S. B., Pierson, E. R., Lee, S. Y. & Goverman, J. M. Modeling the heterogeneity of multiple sclerosis in animals. *Trends Immunol.* **34**, 410–422 (2013).
167. Delgado, M. VIP/PACAP preferentially attract Th2 effectors through differential regulation of chemokine production by dendritic cells. *FASEB J.* (2004). doi:10.1096/fj.04-1548fje
168. Korn, T. *et al.* IL-6 controls Th17 immunity in vivo by inhibiting the conversion of conventional T cells into Foxp3+ regulatory T cells. *Proc. Natl. Acad. Sci.* **105**, 18460–18465 (2008).

169. Okuda, Y. *et al.* IL-6 plays a crucial role in the induction phase of myelin oligodendrocyte glycoprotein 35-55 induced experimental autoimmune encephalomyelitis. *J. Neuroimmunol.* **101**, 188–196 (1999).
170. Samoilova, E. B., Horton, J. L., Hilliard, B., Liu, T. S. & Chen, Y. IL-6-deficient mice are resistant to experimental autoimmune encephalomyelitis: roles of IL-6 in the activation and differentiation of autoreactive T cells. *J. Immunol. Baltim. Md 1950* **161**, 6480–6486 (1998).
171. Gijbels, K., Brocke, S., Abrams, J. S. & Steinman, L. Administration of neutralizing antibodies to interleukin-6 (IL-6) reduces experimental autoimmune encephalomyelitis and is associated with elevated levels of IL-6 bioactivity in central nervous system and circulation. *Mol. Med. Camb. Mass* **1**, 795–805 (1995).
172. Zhang, X. *et al.* IL-10 is involved in the suppression of experimental autoimmune encephalomyelitis by CD25+CD4+ regulatory T cells. *Int. Immunol.* **16**, 249–256 (2004).
173. Khan, R. S. *et al.* SIRT1 activating compounds reduce oxidative stress and prevent cell death in neuronal cells. *Front. Cell. Neurosci.* **6**, (2012).
174. Nimmagadda, V. K. *et al.* Overexpression of SIRT1 Protein in Neurons Protects against Experimental Autoimmune Encephalomyelitis through Activation of Multiple SIRT1 Targets. *J. Immunol.* (2013). doi:10.4049/jimmunol.1202584
175. Lim, H. W. *et al.* SIRT1 deacetylates ROR γ t and enhances Th17 cell generation. *J. Exp. Med.* **212**, 607–617 (2015).
176. Kwon, H.-S. *et al.* Three Novel Acetylation Sites in the Foxp3 Transcription Factor Regulate the Suppressive Activity of Regulatory T Cells. *J. Immunol.* **188**, 2712–2721 (2012).

177. van Loosdregt, J. *et al.* Regulation of Treg functionality by acetylation-mediated Foxp3 protein stabilization. *Blood* **115**, 965–974 (2010).
178. Veldhoen, M., Hocking, R. J., Flavell, R. A. & Stockinger, B. Signals mediated by transforming growth factor- β initiate autoimmune encephalomyelitis, but chronic inflammation is needed to sustain disease. *Nat. Immunol.* **7**, 1151–1156 (2006).
179. Lin, J. T., Martin, S. L., Xia, L. & Gorham, J. D. TGF- β 1 uses distinct mechanisms to inhibit IFN- γ expression in CD4⁺ T cells at priming and at recall: differential involvement of Stat4 and T-bet. *J. Immunol. Baltim. Md 1950* **174**, 5950–5958 (2005).
180. McGeachy, M. J. *et al.* TGF- β and IL-6 drive the production of IL-17 and IL-10 by T cells and restrain TH-17 cell-mediated pathology. *Nat. Immunol.* **8**, 1390–1397 (2007).
181. Zhang. Alteration of T helper cell subsets in the optic nerve of experimental autoimmune encephalomyelitis. *Int. J. Mol. Med.* **25**, (2010).
182. Kohm, A. P., Carpentier, P. A. & Miller, S. D. Regulation of experimental autoimmune encephalomyelitis (EAE) by CD4⁺CD25⁺ regulatory T cells. *Novartis Found. Symp.* **252**, 45–52; discussion 52-54, 106–114 (2003).
183. Korn, T. *et al.* Myelin-specific regulatory T cells accumulate in the CNS but fail to control autoimmune inflammation. *Nat. Med.* **13**, 423–431 (2007).
184. Härle, P., Möbius, D., Carr, D. J. J., Schölmerich, J. & Straub, R. H. An opposing time-dependent immune-modulating effect of the sympathetic nervous system conferred by altering the cytokine profile in the local lymph nodes and spleen of mice with type II collagen-induced arthritis. *Arthritis Rheum.* **52**, 1305–1313 (2005).

185. Ebbinghaus, M., Gajda, M., Boettger, M. K., Schaible, H.-G. & Bräuer, R. The anti-inflammatory effects of sympathectomy in murine antigen-induced arthritis are associated with a reduction of Th1 and Th17 responses. *Ann. Rheum. Dis.* **71**, 253–261 (2012).
186. Balcer, L. J. Optic Neuritis. *N. Engl. J. Med.* **354**, 1273–1280 (2006).
187. Graham, S. L. & Klistorner, A. Afferent visual pathways in multiple sclerosis: a review. *Clin. Experiment. Ophthalmol.* n/a-n/a (2016). doi:10.1111/ceo.12751
188. Rizzo, J. F. & Lessell, S. Risk of developing multiplesclerosis after uncomplicated optic neuritis: A long-term prospective study. *Neurology* **38**, 185–185 (1988).
189. Multiple Sclerosis Risk After Optic Neuritis: Final Optic Neuritis Treatment Trial Follow-up. *Arch. Neurol.* **65**, (2008).
190. Trip, S. A. *et al.* Retinal nerve fiber layer axonal loss and visual dysfunction in optic neuritis. *Ann. Neurol.* **58**, 383–391 (2005).
191. Costello, F. *et al.* Quantifying axonal loss after optic neuritis with optical coherence tomography. *Ann. Neurol.* **59**, 963–969 (2006).
192. Beck, R. W. *et al.* Visual function more than 10 years after optic neuritis: experience of the optic neuritis treatment trial. *Am. J. Ophthalmol.* **137**, 77–83 (2004).
193. Walter, S. D. *et al.* Ganglion cell loss in relation to visual disability in multiple sclerosis. *Ophthalmology* **119**, 1250–1257 (2012).
194. Arnold, A. C. Evolving management of optic neuritis and multiple sclerosis. *Am. J. Ophthalmol.* **139**, 1101–1108 (2005).
195. Atkins, E. J., Biousse, V. & Newman, N. J. The natural history of optic neuritis. *Rev. Neurol. Dis.* **3**, 45–56 (2006).

196. Kale, N. Optic neuritis as an early sign of multiple sclerosis. *Eye Brain* **Volume 8**, 195–202 (2016).
197. Beck, R. W. *et al.* A Randomized, Controlled Trial of Corticosteroids in the Treatment of Acute Optic Neuritis. *N. Engl. J. Med.* **326**, 581–588 (1992).
198. PLOS ONE: VIP Deficient Mice Exhibit Resistance to Lipopolysaccharide Induced Endotoxemia with an Intrinsic Defect in Proinflammatory Cellular Responses. Available at: <http://journals.plos.org/plosone/article?id=10.1371/journal.pone.0036922>. (Accessed: 4th November 2016)
199. Hannibal, J. & Fahrenkrug, J. Target areas innervated by PACAP-immunoreactive retinal ganglion cells. *Cell Tissue Res.* **316**, 99–113 (2004).
200. Nakamachi, T., Matkovits, A., Seki, T. & Shioda, S. Distribution and protective function of pituitary adenylate cyclase-activating polypeptide in the retina. *Neuroendocr. Sci.* **3**, 145 (2012).
201. Seki, T. *et al.* Gene Expression for PACAP Receptor mRNA in the Rat Retina by in Situ Hybridization and in Situ RT-PCR. *Ann. N. Y. Acad. Sci.* **921**, 366–369 (2000).
202. Seki, T. *et al.* Distribution and ultrastructural localization of a receptor for pituitary adenylate cyclase activating polypeptide and its mRNA in the rat retina. *Neurosci. Lett.* **238**, 127–130 (1997).
203. Dénes, V., Czotter, N., Lakk, M., Berta, G. & Gábel, R. PAC1-expressing structures of neural retina alter their PAC1 isoform splicing during postnatal development. *Cell Tissue Res.* **355**, 279–288 (2014).

204. Ye, D. *et al.* Spatiotemporal Expression Changes of PACAP and Its Receptors in Retinal Ganglion Cells After Optic Nerve Crush. *J. Mol. Neurosci.* (2018). doi:10.1007/s12031-018-1203-2
205. Atlasz, T. *et al.* Pituitary adenylate cyclase activating polypeptide in the retina: focus on the retinoprotective effects. *Ann. N. Y. Acad. Sci.* **1200**, 128–139 (2010).
206. Endo, K. *et al.* Neuroprotective effect of PACAP against NMDA-induced retinal damage in the mouse. *J. Mol. Neurosci. MN* **43**, 22–29 (2011).
207. Szabadfi, K. *et al.* Mice deficient in pituitary adenylate cyclase activating polypeptide (PACAP) are more susceptible to retinal ischemic injury in vivo. *Neurotox. Res.* **21**, 41–48 (2012).
208. Horstmann, L. *et al.* Inflammatory demyelination induces glia alterations and ganglion cell loss in the retina of an experimental autoimmune encephalomyelitis model. *J. Neuroinflammation* **10**, 120 (2013).
209. Manogaran, P. *et al.* Exploring experimental autoimmune optic neuritis using multimodal imaging. *NeuroImage* **175**, 327–339 (2018).
210. Shindler, K. S., Ventura, E., Dutt, M. & Rostami, A. Inflammatory demyelination induces axonal injury and retinal ganglion cell apoptosis in experimental optic neuritis. *Exp. Eye Res.* **87**, 208–213 (2008).
211. Quinn, T. A., Dutt, M. & Shindler, K. S. Optic Neuritis and Retinal Ganglion Cell Loss in a Chronic Murine Model of Multiple Sclerosis. *Front. Neurol.* **2**, (2011).
212. Ivanova, E., Toychiev, A. H., Yee, C. W. & Sagdullaev, B. T. Optimized Protocol for Retinal Wholemount Preparation for Imaging and Immunohistochemistry. *J. Vis. Exp.* (2013). doi:10.3791/51018

213. Rodriguez, A. R., de Sevilla Müller, L. P. & Brecha, N. C. The RNA binding protein RBPMS is a selective marker of ganglion cells in the mammalian retina. *J. Comp. Neurol.* **522**, 1411–1443 (2014).
214. Jakobs, T. C., Libby, R. T., Ben, Y., John, S. W. M. & Masland, R. H. Retinal ganglion cell degeneration is topological but not cell type specific in DBA/2J mice. *J. Cell Biol.* **171**, 313–325 (2005).
215. Wassle, H., Peichl, L. & Boycott, B. B. Morphology and Topography of on- and off-Alpha Cells in the Cat Retina. *Proc. R. Soc. B Biol. Sci.* **212**, 157–175 (1981).
216. Peichl, L., Ott, H. & Boycott, B. B. Alpha ganglion cells in mammalian retinae. *Proc. R. Soc. Lond. B Biol. Sci.* **231**, 169–197 (1987).
217. Lin, B., Wang, S. W. & Masland, R. H. Retinal Ganglion Cell Type, Size, and Spacing Can Be Specified Independent of Homotypic Dendritic Contacts. *Neuron* **43**, 475–485 (2004).
218. Deutsch, P. J. & Sun, Y. The 38-amino acid form of pituitary adenylate cyclase-activating polypeptide stimulates dual signaling cascades in PC12 cells and promotes neurite outgrowth. *J. Biol. Chem.* **267**, 5108–5113 (1992).
219. Armstrong, B. D. *et al.* Impaired nerve regeneration and enhanced neuroinflammatory response in mice lacking pituitary adenylyl cyclase activating peptide. *Neuroscience* **151**, 63–73 (2008).
220. Gonzalez, B. ., Basille, M., Vaudry, D., Fournier, A. & Vaudry, H. Pituitary adenylate cyclase-activating polypeptide promotes cell survival and neurite outgrowth in rat cerebellar neuroblasts. *Neuroscience* **78**, 419–430 (1997).

221. Hernandez, A., Kimball, B., Romanchuk, G. & Mulholland, M. W. Pituitary adenylate cyclase-activating peptide stimulates neurite growth in PC12 cells. *Peptides* **16**, 927–932 (1995).
222. Manecka, D.-L., Mahmood, S. F., Grumolato, L., Lihrmann, I. & Anouar, Y. Pituitary Adenylate Cyclase-activating Polypeptide (PACAP) Promotes Both Survival and Neuritogenesis in PC12 Cells through Activation of Nuclear Factor κ B (NF- κ B) Pathway: INVOLVEMENT OF EXTRACELLULAR SIGNAL-REGULATED KINASE (ERK), CALCIUM, AND c-REL. *J. Biol. Chem.* **288**, 14936–14948 (2013).
223. Nakajima, E., Walkup, R. D., Fujii, A., Shearer, T. R. & Azuma, M. Pituitary adenylate cyclase-activating peptide induces neurite outgrowth in cultured monkey trigeminal ganglion cells: involvement of receptor PAC1. *Mol. Vis.* **19**, 174–183 (2013).
224. Ogata, K. *et al.* PACAP Enhances Axon Outgrowth in Cultured Hippocampal Neurons to a Comparable Extent as BDNF. *PLOS ONE* **10**, e0120526 (2015).
225. Kambe, Y. & Miyata, A. Role of mitochondrial activation in PACAP dependent neurite outgrowth. *J. Mol. Neurosci. MN* **48**, 550–557 (2012).
226. Horstmann, L. *et al.* Microglia response in retina and optic nerve in chronic experimental autoimmune encephalomyelitis. *J. Neuroimmunol.* **298**, 32–41 (2016).
227. Fairless, R. *et al.* Preclinical Retinal Neurodegeneration in a Model of Multiple Sclerosis. *J. Neurosci.* **32**, 5585–5597 (2012).
228. Martinez, C. *et al.* Anti-inflammatory role in septic shock of pituitary adenylate cyclase-activating polypeptide receptor. *Proc. Natl. Acad. Sci.* **99**, 1053–1058 (2002).
229. Suzuki, R. *et al.* Expression of the receptor for pituitary adenylate cyclase-activating polypeptide (PAC1-R) in reactive astrocytes. *Brain Res. Mol. Brain Res.* **115**, 10–20 (2003).

230. Aihara, M., Ishii, S., Kume, K. & Shimizu, T. Interaction between neurone and microglia mediated by platelet-activating factor. *Genes Cells Devoted Mol. Cell. Mech.* **5**, 397–406 (2000).
231. Dobbertin, A., Schmid, P., Gelman, M., Glowinski, J. & Mallat, M. Neurons promote macrophage proliferation by producing transforming growth factor-beta2. *J. Neurosci. Off. J. Soc. Neurosci.* **17**, 5305–5315 (1997).
232. Gomes, F. C. A., Spohr, T. C. L. S., Martinez, R. & Moura Neto, V. Cross-talk between neurons and glia: highlights on soluble factors. *Braz. J. Med. Biol. Res.* **34**, 611–620 (2001).
233. de Haas, A. H., van Weering, H. R. J., de Jong, E. K., Boddeke, H. W. G. M. & Biber, K. P. H. Neuronal Chemokines: Versatile Messengers In Central Nervous System Cell Interaction. *Mol. Neurobiol.* **36**, 137–151 (2007).
234. Harrison, J. K. *et al.* Role for neuronally derived fractalkine in mediating interactions between neurons and CX3CR1-expressing microglia. *Proc. Natl. Acad. Sci.* **95**, 10896–10901 (1998).
235. Mott, R. T. *et al.* Neuronal expression of CD22: Novel mechanism for inhibiting microglial proinflammatory cytokine production. *Glia* **46**, 369–379 (2004).
236. Dohi, K. *et al.* Pituitary adenylate cyclase-activating polypeptide (PACAP) prevents hippocampal neurons from apoptosis by inhibiting JNK/SAPK and p38 signal transduction pathways. *Regul. Pept.* **109**, 83–88 (2002).
237. Shioda, S. *et al.* PACAP protects hippocampal neurons against apoptosis: involvement of JNK/SAPK signaling pathway. *Ann. N. Y. Acad. Sci.* **865**, 111–117 (1998).

238. Vaudry, D. *et al.* The neuroprotective effect of pituitary adenylate cyclase-activating polypeptide on cerebellar granule cells is mediated through inhibition of the CED3-related cysteine protease caspase-3/ CPP32. *Proc. Natl. Acad. Sci. U. S. A.* **97**, 13390–13395 (2000).
239. Lee, E. H. & Seo, S. R. Neuroprotective roles of pituitary adenylate cyclase-activating polypeptide in neurodegenerative diseases. *BMB Rep.* **47**, 369–375 (2014).
240. Reglodi, D., Vaczy, A., Rubio-Beltran, E. & MaassenVanDenBrink, A. Protective effects of PACAP in ischemia. *J. Headache Pain* **19**, (2018).
241. Rat, D. *et al.* Neuropeptide pituitary adenylate cyclase-activating polypeptide (PACAP) slows down Alzheimer's disease-like pathology in amyloid precursor protein-transgenic mice. *FASEB J.* **25**, 3208–3218 (2011).
242. Han, P. *et al.* Pituitary adenylate cyclase-activating polypeptide is reduced in Alzheimer disease. *Neurology* **82**, 1724–1728 (2014).
243. Han, P. C. *et al.* Pituitary adenylate cyclase-activating polypeptide (PACAP) protects against beta-amyloid toxicity and potentiates mitochondrial function. *Alzheimers Dement.* **9**, P355 (2013).
244. Chen, R. P. From Nose to Brain: The Promise of Peptide Therapy for Alzheimer's Disease and Other Neurodegenerative Diseases. *J. Alzheimer's Dis. Park.* **07**, (2017).
245. Lamine-Ajili, A. *et al.* Effect of the pituitary adenylate cyclase-activating polypeptide on the autophagic activation observed in in vitro and in vivo models of Parkinson's disease. *Biochim. Biophys. Acta* (2016). doi:10.1016/j.bbadis.2016.01.005
246. Tsuchida, M. *et al.* PACAP stimulates functional recovery after spinal cord injury through axonal regeneration. *J. Mol. Neurosci. MN* **54**, 380–387 (2014).

247. Tamas, A. *et al.* Effect of PACAP in Central and Peripheral Nerve Injuries. *Int. J. Mol. Sci.* **13**, 8430–8448 (2012).
248. Yamamoto, K. *et al.* Overexpression of PACAP in Transgenic Mouse Pancreatic -Cells Enhances Insulin Secretion and Ameliorates Streptozotocin-induced Diabetes. *Diabetes* **52**, 1155–1162 (2003).
249. Marzagalli, R., Scuderi, S., Drago, F., Waschek, J. A. & Castorina, A. Emerging Role of PACAP as a New Potential Therapeutic Target in Major Diabetes Complications. *Int. J. Endocrinol.* **2015**, 1–11 (2015).
250. Szabadfi, K. *et al.* PACAP promotes neuron survival in early experimental diabetic retinopathy. *Neurochem. Int.* **64**, 84–91 (2014).
251. Nakamachi, T. *et al.* PACAP suppresses dry eye signs by stimulating tear secretion. *Nat. Commun.* **7**, 12034 (2016).
252. Wu, L., Wang, J., Chen, X. & Hong, A. Expression, identification and biological effects of the novel recombination protein, PACAP38-NtA, with high bioactivity. *Int. J. Mol. Med.* **35**, 376–382 (2015).
253. Bourgault, S. *et al.* Novel stable PACAP analogs with potent activity towards the PAC1 receptor. *Peptides* **29**, 919–932 (2008).
254. Colella, P., Ronzitti, G. & Mingozi, F. Emerging Issues in AAV-Mediated In Vivo Gene Therapy. *Mol. Ther. - Methods Clin. Dev.* **8**, 87–104 (2018).
255. Zaiss, A.-K. *et al.* Differential Activation of Innate Immune Responses by Adenovirus and Adeno-Associated Virus Vectors. *J. Virol.* **76**, 4580–4590 (2002).

256. Hu, C., Busuttil, R. W. & Lipshutz, G. S. RH10 provides superior transgene expression in mice when compared with natural AAV serotypes for neonatal gene therapy. *J. Gene Med.* **12**, 766–778 (2010).
257. Flotte, T. R. & Berns, K. I. Adeno-Associated Virus: A Ubiquitous Commensal of Mammals. *Hum. Gene Ther.* **16**, 401–407 (2005).
258. Gonçalves, M. A. F. V. Adeno-associated virus: from defective virus to effective vector. *Viol. J.* **2**, 43 (2005).
259. Chirmule, N. *et al.* Immune responses to adenovirus and adeno-associated virus in humans. *Gene Ther.* **6**, 1574–1583 (1999).
260. Anand, V. *et al.* A Deviant Immune Response to Viral Proteins and Transgene Product Is Generated on Subretinal Administration of Adenovirus and Adeno-associated Virus. *Mol. Ther.* **5**, 125–132 (2002).
261. Mastakov, M. Y. *et al.* Immunological Aspects of Recombinant Adeno-Associated Virus Delivery to the Mammalian Brain. *J. Virol.* **76**, 8446–8454 (2002).
262. Chirmule, N. *et al.* Humoral Immunity to Adeno-Associated Virus Type 2 Vectors following Administration to Murine and Nonhuman Primate Muscle. *J. Virol.* **74**, 2420–2425 (2000).
263. Brockstedt, D. G. *et al.* Induction of Immunity to Antigens Expressed by Recombinant Adeno-Associated Virus Depends on the Route of Administration. *Clin. Immunol.* **92**, 67–75 (1999).
264. Wang, L., Figueredo, J., Calcedo, R., Lin, J. & Wilson, J. M. Cross-Presentation of Adeno-Associated Virus Serotype 2 Capsids Activates Cytotoxic T Cells But Does Not Render Hepatocytes Effective Cytolytic Targets. *Hum. Gene Ther.* **18**, 185–194 (2007).

265. Samulski, R. J. *et al.* Targeted integration of adeno-associated virus (AAV) into human chromosome 19. *EMBO J.* **10**, 3941–3950 (1991).
266. Henckaerts, E. *et al.* Site-specific integration of adeno-associated virus involves partial duplication of the target locus. *Proc. Natl. Acad. Sci.* **106**, 7571–7576 (2009).
267. Janovitz, T., Oliveira, T., Sadelain, M., Falck-Pedersen, E. & Imperiale, M. J. Highly Divergent Integration Profile of Adeno-Associated Virus Serotype 5 Revealed by High-Throughput Sequencing. *J. Virol.* **88**, 2481–2488 (2014).
268. Dong, B., Nakai, H. & Xiao, W. Characterization of Genome Integrity for Oversized Recombinant AAV Vector. *Mol. Ther.* **18**, 87–92 (2010).
269. Wu, Z., Yang, H. & Colosi, P. Effect of Genome Size on AAV Vector Packaging. *Mol. Ther.* **18**, 80–86 (2010).
270. Yi, Y., Jong Noh, M. & Hee Lee, K. Current Advances in Retroviral Gene Therapy. *Curr. Gene Ther.* **11**, 218–228 (2011).
271. Hacein-Bey-Abina, S. *et al.* Insertional oncogenesis in 4 patients after retrovirus-mediated gene therapy of SCID-X1. *J. Clin. Invest.* **118**, 3132–3142 (2008).
272. Howe, S. J. *et al.* Insertional mutagenesis combined with acquired somatic mutations causes leukemogenesis following gene therapy of SCID-X1 patients. *J. Clin. Invest.* **118**, 3143–3150 (2008).
273. Fu, X. *et al.* Clinical applications of retinal gene therapies. *Precis. Clin. Med.* **1**, 5–20 (2018).
274. Heier, J. S. *et al.* Intravitreal injection of AAV2-sFLT01 in patients with advanced neovascular age-related macular degeneration: a phase 1, open-label trial. *The Lancet* **390**, 50–61 (2017).

275. Kim, J. H. *et al.* High Cleavage Efficiency of a 2A Peptide Derived from Porcine Teschovirus-1 in Human Cell Lines, Zebrafish and Mice. *PLoS ONE* **6**, e18556 (2011).
276. Deverman, B. E. *et al.* Cre-dependent selection yields AAV variants for widespread gene transfer to the adult brain. *Nat. Biotechnol.* **34**, 204–209 (2016).